Role of Retrosplenial Cortex in Context Discrimination and the Underlying Neuronal Coding in Mouse (*Mus musculus*)

Thesis

for the degree of

doctor rerum naturalum (Dr. rer. nat.)

approved by the Faculty of Natural Sciences of Otto von Guericke University Magdeburg

by M.Sc., Weilun Sun, born on 31.08.1988 in Jilin, China

Examiner: Prof. Dr. Alexander Dityatev

PD Dr. Carsten T. Wotjak

submitted on: 20.11.2019 defended on: 02.06.2020

ABSTRACT

An organism's ability to successfully navigate, assign value to behaviourally relevant locations, and later recall these critical environmental features, depends on a complex network involving interacting brain regions. The retrosplenial cortex (RSC) has emerged as a key region in this network as it densely interconnects with the hippocampal formation (HF), anterior thalamic nuclei (ATN), parahippocampal formation, and visual and entorhinal cortices (Kobayashi and Amaral, 2007; van Groen and Wyss, 1992a; Vann et al., 2009; Vogt and Paxinos, 2014).

Although anatomical and behavioural studies strongly support the contribution of the RSC to integrative functions, it is elusive how it is implemented at the cellular level. Previous studies of single-cell activity in mammalian RSC have revealed that specific populations of RSC neurons encode spatial information (Alexander and Nitz, 2015; Czajkowski et al., 2014; Mao et al., 2018), demonstrate properties of head direction (HD) cells (Chen et al., 1994b; Jacob et al., 2016) or place cells (Mao et al., 2017), and can encode reward locations (Vedder et al., 2017) as well as reward history (Hattori et al., 2019). However, these studies were focused on specific cognitive dimensions and did not investigate the cellular basis of multidimensional integration in the RSC.

In this thesis, I examined the role of the RSC in learning and memory processes using a context discrimination task established in a virtual reality (VR) environment where mice were trained to associate a water reward with a specific position in a particular context. Contextual discrimination was impaired when the RSC was chemogenetically perturbed during initial acquisition and reversal learning but not during recent memory recall. Using two-photon calcium imaging, I observed a large population of neurons that encoded information representing a specific context, the associated reward-value, and its visual features, namely, the pattern of dark-light transitions. Also, many RSC neurons encoded the speed and spatial position of the mouse in a context-dependent manner. Predominantly, the same RSC neurons simultaneously encoded context, position, and speed, and the proportion of such multidimensional encoding neurons increased after reversal learning.

Taken together, the results in this thesis provide direct evidence that the RSC is essential for the formation of contextual memory but not necessary for the recall of the recent memory and suggest that RSC implements multidimensional encoding at the single-cell level, and this mechanism is involved in context value updating during reversal learning.

ZUSAMMENFASSUNG

Die Fähigkeit eines Organismus, erfolgreich zu navigieren, verhaltensrelevanten Orten einen Wert beizumessen und diese wichtigen Umweltmerkmale wieder abzurufen, basiert auf einem komplexen Netzwerk interaktiver Gehirnregionen. Der retrospleniale Cortex (RSC) hat sich dabei als Schlüsselregion in diesem Netzwerk herausgestellt, da er sehr stark mit der hippocampalen Formation (HF), den anterioren Thalamuskernen (ATK), der parahippocampalen Formation sowie dem visuellen und entorhinalen Cortex verschaltet ist (Kobayashi and Amaral, 2007; van Groen and Wyss, 1992a; Vann et al., 2009; Vogt and Paxinos, 2014).

Obwohl Anatomie- und Verhaltensstudien die Rolle des RSC bei den integrativen Funktionen stark unterstützen, ist noch unklar, inwieweit dies auf zellulärer Ebene zutrifft. Frühere Studien zur Einzelzellaktivität im RSC von Säugetieren haben gezeigt, dass spezifische Populationen an RSC-Neuronen räumliche Informationen kodieren (Alexander and Nitz, 2015; Czajkowski et al., 2014; Mao et al., 2018), Eigenschaften von Kopfrichtungszellen (Chen et al., 1994b; Jacob et al., 2016) oder Ortszellen (Mao et al., 2017) zeigen und Belohnungsorte (Vedder et al., 2017) sowie Belohnungshistorien (Hattori et al., 2019) kodieren können. Allerdings konzentrierten sich diese Studien auf spezifische kognitive Dimensionen und die zelluläre Grundlage der multidimensionalen Integration im RSC wurde nicht untersucht.

In meiner Doktorarbeit habe ich die Rolle des RSC bei Lern- und Gedächtnisprozessen mittels einer Kontextunterscheidungsaufgabe in einer virtuellen Umgebung untersucht, bei der die Mäuse lernten, eine Belohnung mit einem bestimmten Ort in einem bestimmten Kontext in Verbindung zu bringen. Die Kontextunterscheidung war beeinträchtigt, wenn der RSC während des Ersterwerbs und beim Umlernen chemogenetisch gestört wurde, aber nicht während des Abrufs von Erinnerungen aus dem Kurzzeitgedächntis. Mit Hilfe der Zwei-Photonen-Fluoreszenzmikroskopie Kalziumbildgebung konnte ich eine große Neuronenpopulation beobachten, die Informationen mit einem spezifischen Kontext, den zugehörigen Belohnungswert und seine visuellen Merkmale, nämlich die Muster aus Dunkel-Hell-Übergängen, kodierten. Außerdem kodierten viele RSC-Neuronen die Geschwindigkeit und die räumliche Position der Maus kontextabhängig. Die gleichen RSC-Neuronen kodierten gleichzeitig Kontext, Position und Geschwindigkeit und der Anteil an diesen multidimensional kodierenden Neuronen nahm nach dem Umlernen zu.

Zusammengefasst belegen die Ergebnisse in dieser Doktorarbeit, dass der RSC für die Bildung des kontextuellen Gedächtnisses aber nicht für den Abruf aus dem Neugedächtnis notwendig ist. Ferner legen die Ergebnisse nahe, dass der RSC auf Einzelzellebene multidimensional kodiert und dass dieser Mechanismus an der Aktualisierung des Kontextwertes während des Umlernens beteiligt ist.

LIST OF ABBREVIATIONS

AAV	Adeno-associated virus
AD	Alzheimer's disease
AMPA	α-amino-3-hydroxy-5-methyl-4-isoxazolepropionic acid
ANOVA	Analysis of variances
ATN	Anterior thalamic nuclei
CA1	*Cornus ammonis* 1
CA3	*Cornus ammonis 3*
CMI	Context modulation index
CNO	Clozapine-N-oxide
CNQX	6-cyano-7-nitroquinoxaline-2,3-dione
CREB	cAMP response element-binding protein
DMN	Default mode network
DREADDs	Designer Receptors Exclusively Activated by Designer Drugs
fMRI	Functional magnetic resonance imaging
HD	Head direction
HF	Hippocampal formation
IEG	Immediate early gene
ITI	Inner-trial interval
LTD	Long-term depression
MCI	Mild cognitive impairment
MEC	Medial entorhinal cortex
M2	Secondary motor cortex
NMDAR	N-methyl-D-aspartate receptor
PB	Phosphate buffer
PBS	Phosphate buffered saline
PET	Positron emission tomography
PFA	Paraformaldehyde

POR	Postrhinal cortex
Rdg	Retrosplenial dysgranular cortex
Rga	Retrosplenial granular cortex a
Rgb	Retrosplenial granular cortex b
ROI	Region of interest
RT	Room temperature
RSC	Retrosplenial cortex
SEM	Standard error of mean
VR	Virtual reality

TABLE OF CONTENTS

ABSTRACT i
ZUSAMMENFASSUNG ii
LIST OF ABBREVIATIONS iv
TABLE OF CONTENTS vi
1. INTRODUCTION 1
1.1. The importance of the retrosplenial cortex 1
1.2. Anatomy of the retrosplenial cortex 2
1.2.1. Location of the retrosplenial cortex 2
1.2.2. Subregions of the retrosplenial cortex 4
1.3. Connectivity of the retrosplenial cortex 5
1.3.1. Connectivity with the hippocampal formation 6
1.3.2. Connectivity with the thalamic regions 7
1.3.3. Connectivity with visual regions 8
1.3.4. Connectivity with other brain regions 9
1.4. The role of the retrosplenial cortex 10
1.4.1. Human lesion studies 11
1.4.2. Human imaging studies 12
1.4.3. Animal lesion or inactivation studies 13
1.4.4. Animal disconnection studies 19
1.4.5. Animal single-neuron studies 20
1.5. Clinical relevance of the retrosplenial cortex 27
2. OBJECTIVES 29
3. MATERIALS AND METHODS 30
3.1. Animals 30
3.2. Surgical procedures 31
3.3. Virtual reality setup 32
3.4. Behavioural training 34
3.5. In vivo two-photon calcium imaging 37
3.6. Histology 38
3.7. Data analysis 40
3.7.1. Two-photon calcium imaging 40

3.7.2. Position and speed decoding 42
3.7.3. Place cell analysis 44
3.7.4. Context decoding 45
3.7.5. Visual encoding cell analysis 45
3.7.6. Statistics 46
4. RESULTS 47
4.1. Context discrimination in a virtual environment 47
4.2. The role of the RSC in context discrimination acquisition 51
4.3. Decoding of contextual information 57
4.4. Decoding of spatial information 66
4.5. Decoding of speed information 70
4.6. Multidimensional encoding nature of RSC neurons 74
5. DISCUSSION 76
5.1. A novel virtual context discrimination paradigm 77
5.2. The RSC supports acquisition rather than recall of recent contextual memories 78
5.3. Information processed in the RSC 81
5.4. Multidimensional encoding neurons in the RSC 84
5.5. Limitations and outlook 86
6. CONCLUSIONS 88
7. REFERENCES 89

1. INTRODUCTION

1.1. The importance of the retrosplenial cortex

Cognitive functions, such as learning and memory, rely on complex networks involving a range of interconnected brain regions. The hippocampus is one of the most well-studied brain regions and known to play a vital role in a number of essential cognitive functions including spatial navigation, learning, and memory (O'Keefe and Dostrovsky, 1971; Squire, 1992; Tulving and Markowitsch, 1998; Zola-Morgan and Squire, 1990). In addition to the hippocampus, it has been shown that several cortical regions are also importantly engaged in such cognitive functions. Among these cortices, the retrosplenial cortex (RSC) has arisen as a critical region that actively participates in navigation, orientation, spatial memory, and contextual memory that support how an organism successfully interacts with its environment.

The RSC is a midline association region in the posterior cortical network, densely connects with a variety of brain regions including hippocampal formation, anterior thalamic nuclei, parahippocampal formation, and sensorial and entorhinal cortices (Kobayashi and Amaral, 2007; Van Groen and Wyss, 1990, 1992a, 2003; Vann et al., 2009; Vogt and Paxinos, 2014). Notably, the RSC reciprocally connects with the hippocampus, including direct inputs from dorsal hippocampal CA1 (Sugar et al., 2011), and considerable evidence has indicated the functional similarities between the hippocampus and the RSC.

This connectivity pattern suggests that RSC is in a special location to integrate both spatial and contextual information from the environment. Indeed, the RSC has been shown to be essential in diverse cognitive functions, including spatial navigation, spatial learning, and memory, contextual memory, as well as in visualizations of future actions and scene processing in humans (Mitchell et al., 2018; Vann et al., 2009). Recent rodent studies have demonstrated the contributions of the RSC to similar cognitive functions as observed in human studies (Aggleton, 2010; Cowansage et al., 2014; Harker and Whishaw, 2002; Keene and Bucci, 2008a, b, 2009; Vann and Aggleton, 2002; Wang et al., 2019).

Although many studies have indicated the involvement of the RSC in diverse cognitive functions, the exact roles of the RSC remain elusive. Moreover, the RSC has clinical relevance, as it is involved in a variety of neurological disorders, including mild cognitive impairment (MCI), vascular dementia, and Alzheimer's disease (AD). Notably, the dysfunction of the RSC

is consistently observed in the early stages of AD (Huang et al., 2002; Nestor et al., 2003; Pengas et al., 2010).

Therefore, investigations on the roles of the RSC and how it plays such roles will not only help us to understand the fundamental processes underlying multiple cognitive functions but, very importantly, may provide fundamental knowledge for further clinical research aiming to develop early detection and diagnose, as well as novel therapies for memory disorders.

1.2. Anatomy of the retrosplenial cortex

1.2.1. Location of the retrosplenial cortex

Located as a midline assemble part in the posterior cortical network, the RSC situates at the junction between many limbic and cortical areas. In primates, much of the RSC is buried deeply from the brain surface (Vann et al., 2009). The cingulate cortex in primates can be separated into two parts, the anterior and posterior part, and RSC occupies the most caudoventral part of the posterior cingulate cortex (Sugar et al., 2011), which composes Brodmann areas 29 and 30. RSC is along with areas 23 and 31 in the posterior cingulate area and divided by area 23 from the precuneate area (see Figure 1.1).

Conversely, there are no correspondent parts to areas 23 and 31 in rodent, and the RSC, composing the entire post-cingulate cortex, is positioned more dorsally, and reaches the brain surface (Sugar et al., 2011; Vogt and Peters, 1981). The size of the RSC varies a lot across different species. Notably, the RSC in rat and mouse occupies approximately half of the cerebrum (Vann et al., 2009)(see Figures 1.1 and 1.2). Moreover, RSC situates at the intermediate layer within the default mode network (DMN), an interconnected system of brain regions (Buckner et al., 2008; Greicius et al., 2009).

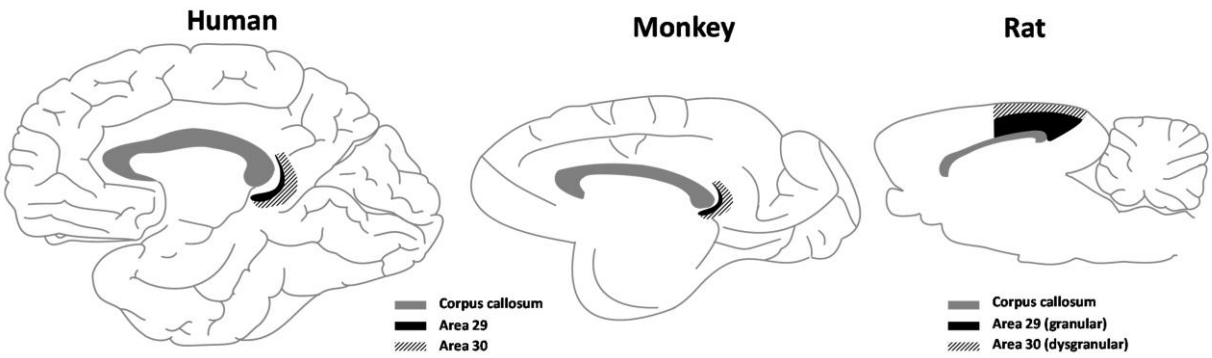

Figure 1.1 | Locations of the RSC in humans, monkeys, and rats.

Schematic of the RSC (areas 29 and 30) in humans, rhesus monkeys, and rats, as seen in the midsagittal section. Source: The figure is from "figshare" made by Jeffery (2017), available at https://figshare.com/articles/RSC_Human_monkey_rat_tif/5414179/1.

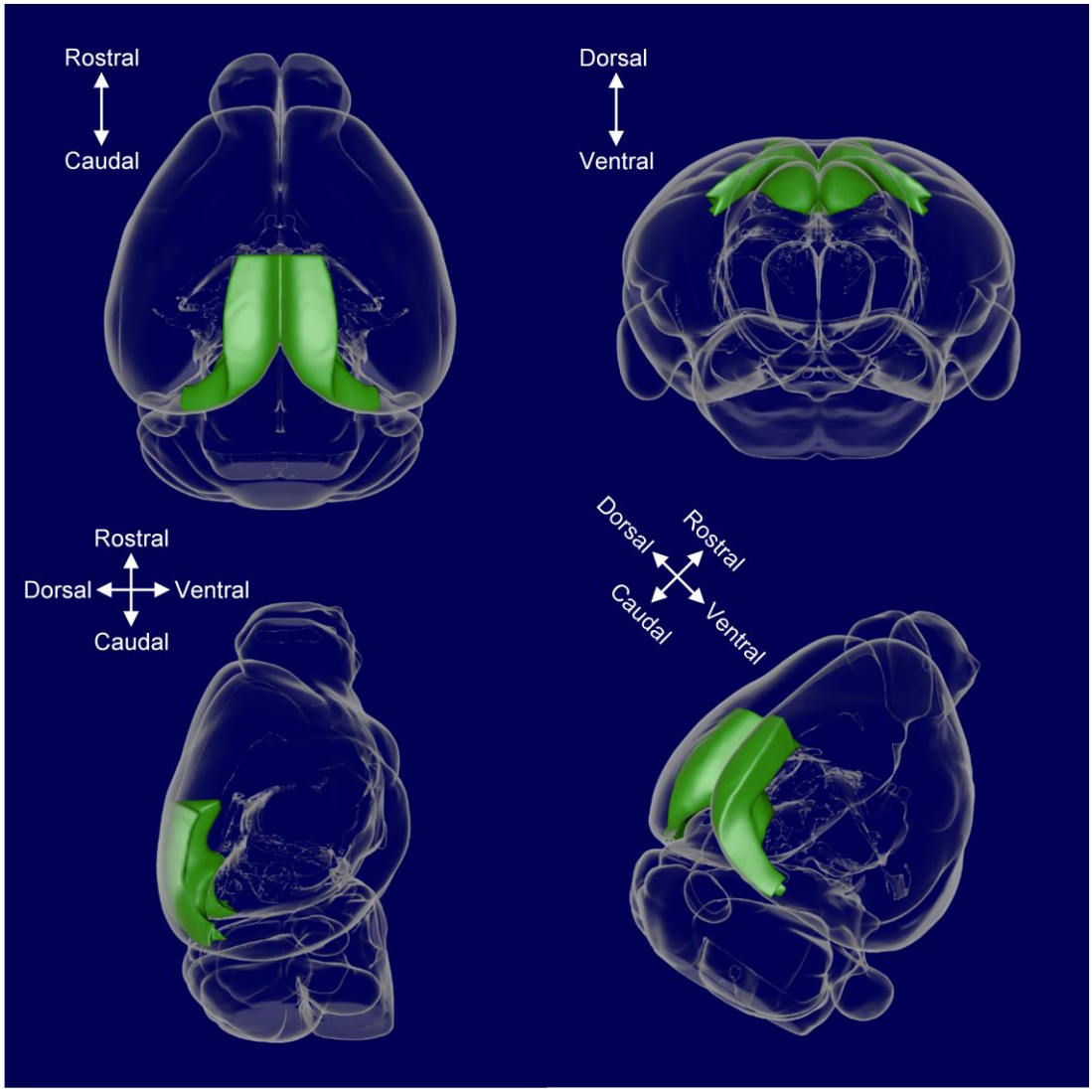

Figure 1.2 | Location of the RSC in the mouse brain.

The diagrams illustrate the location and shape of the RSC in the mouse brain. The region marked by green indicates the RSC in the mouse brain. Images were acquired and adapted using "3D brain composer" from "The Scalable Brain Atlas" (Bakker et al., 2015) based on templates from the "Allen Brain Reference Atlases" and the version is Allen Mouse Common Coordinate Framework v.3. https://scalablebrainatlas.incf.org/composer/?template=ABA_v3

1.2.2. Subregions of the retrosplenial cortex

The RSC, in general, is separated into two subregions, which are dysgranular RSC (Rdg, also called agranular RSC), referring to Brodmann area 30 and granular RSC, referring to Brodmann area 29, in both primates and rodents. In this thesis, the region of interest for two-photon calcium imaging was focused on Rdg. The granular RSC in rat and mouse is often further subdivided into either two or three subregions: granular a, and granular b; or granular a, granular b, and granular c, depending on the authority (Vann et al., 2009). In this thesis, I refer to regions and subregions based on the descriptions by Van Groen and Wyss (Van Groen and Wyss, 1990, 1992a, 2003) — that is, dysgranular (Rdg), granular a (Rga), and granular b (Rgb) regions (see Figure 1.3) — in line with many previous connectivity studies and selective lesion studies addressing the functional differences between different subdivisions of the RSC (Vann et al., 2009). The functional differences between RSC subregions will be described in section 1.4.3.

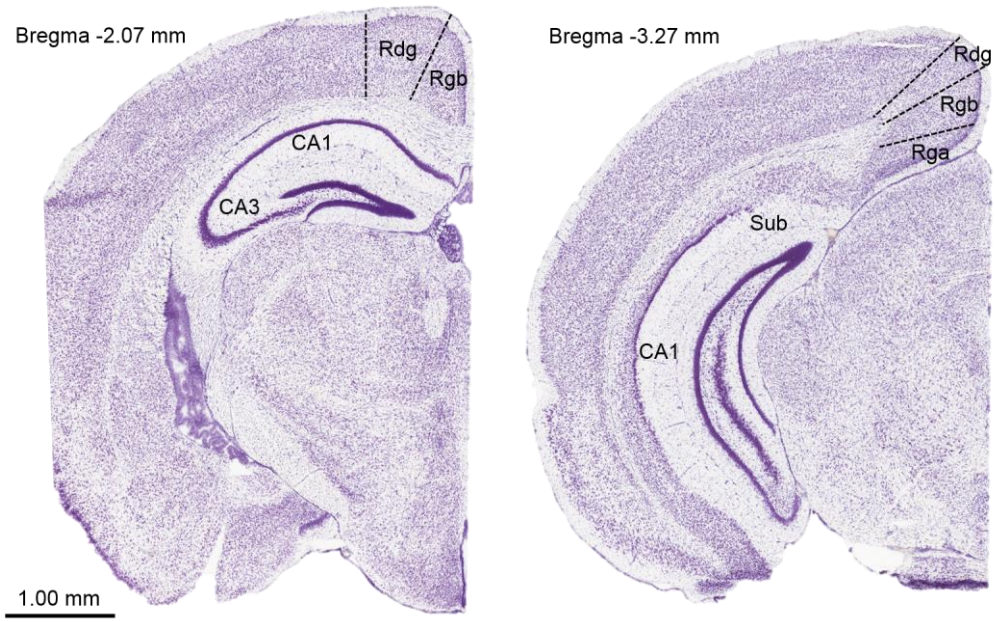

Figure 1.3 | Subregions of the RSC in the mouse brain.
Coronal view of the RSC in Nissl-stained sections showing the subregions of the RSC. Rdg, dysgranular RSC; Rga, retrosplenial granular a; Rgb, retrosplenial granular b; CA1, *Cornu Ammonis* area 1; CA3, *Cornu Ammonis* area 3; Sub, subiculum. RSC subregions are separated based on the descriptions by Van Groen and Wyss (Van Groen and Wyss, 1990, 1992a, 2003). Adapted based on the templates from © 2004 Allen Institute for Brain Science. Allen Mouse Brain Atlas. Available from: brain-map.org/api/index.html.

1.3. Connectivity of the retrosplenial cortex

The RSC densely interconnects with a wide range of brain regions, including the HF, thalamus, visual area, and other brain regions (see Figure 1.4), and importantly, many of these are reciprocal connections. Studies in macaque monkeys by axonal tracing demonstrated reciprocal connections between the RSC and the HF, the parahippocampal area, and thalamic nuclei. Similarly, the RSC in rodents is highly connected with the ATN, the lateral dorsal thalamic nucleus, and the HF. (Kobayashi and Amaral, 2007; Van Groen and Wyss, 1990, 1992a, 2003; Vann et al., 2009; Vogt and Paxinos, 2014). Due to its unique location, the RSC also connects with other brain areas. The connections may serve as the foundation for the RSC functions.

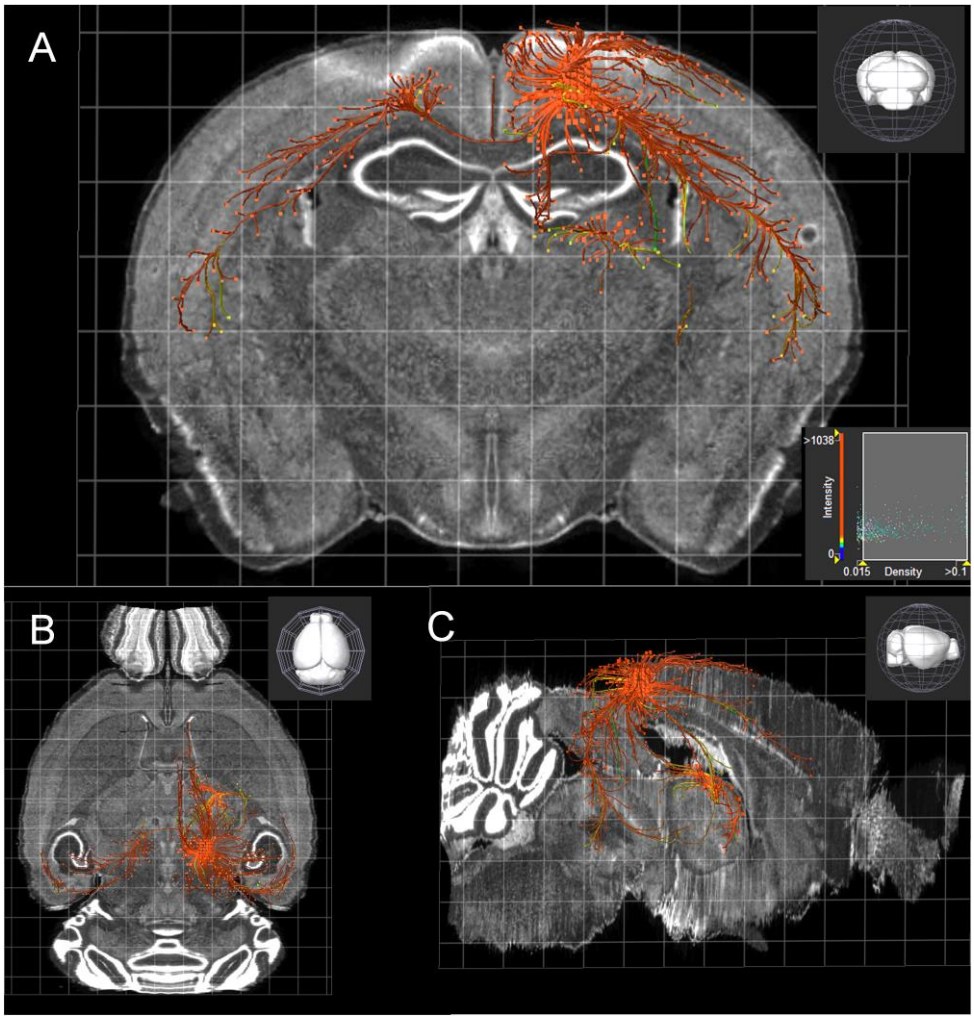

Figure 1.4 | Connections between the RSC and other brain regions.

The diagrams illustrate the projections from the RSC to other brain regions, including the HF, thalamus, visual area, and other brain regions from different views. A. Coronal view. B. Horizontal view. C. Sagittal view. Red indicates the projections originating from the RSC.

Images are adapted from Allen Mouse Brain Atlas: Mouse connectivity. Available from: brain-map.org/api/index.html.

1.3.1. Connectivity with the hippocampal formation

Hippocampal formation reciprocally connects with a wide range of higher-order association cortices representing all sensory domains, and notably, the RSC is situated at the crossroads of this network and reciprocally connects with the HF. The reciprocal connectivity is established through projections between subdivisions of RSC and HF. Subdivisions of the HF, including hippocampus proper, subiculum, presubiculum, parasubiculum, as well as postsubiculum have been shown to share connectivity with the RSC (Agster and Burwell, 2009; Finch et al., 1984; Haugland et al., 2019; Honda et al., 2011; Honda and Ishizuka, 2015).

The RSC receives unidirectional projections from the CA1 area (Cenquizca and Swanson, 2007; Mitchell et al., 2018; Miyashita and Rockland, 2007) (see Figure 1.5) and the subiculum (Honda and Ishizuka, 2015; Wyass and Van Groen, 1992). This important connection may explain the fact that the RSC plays a vital role in spatial function and neurons in the RSC encode spatial information, including place cell-like properties (see section 1.4 for functional implications). Notably, the HF projects more densely to the granular RSC (Rga and Rgb), whereas sparsely to the dysgranular RSC (Rdg) (Wyass and Van Groen, 1992). Therefore, the granular regions of the RSC are more closely connected with the HF (Pothuizen et al., 2009). More detailed, the projections that target at the Rgb originates mainly in the CA1 area, dorsal (septal) subiculum, and postsubiculum, which contains HD cells. Subregions of the RSC receiving inputs from various areas of the HP may lead to the functional differences in subregions of the RSC. In fact, a previous study has shown that selective lesion in Rgb rather than Rga impairs spatial learning and memory in rats (see section 1.4.3), which may conversely reflect the diverse anatomical connections between RSC subregions at functional level.

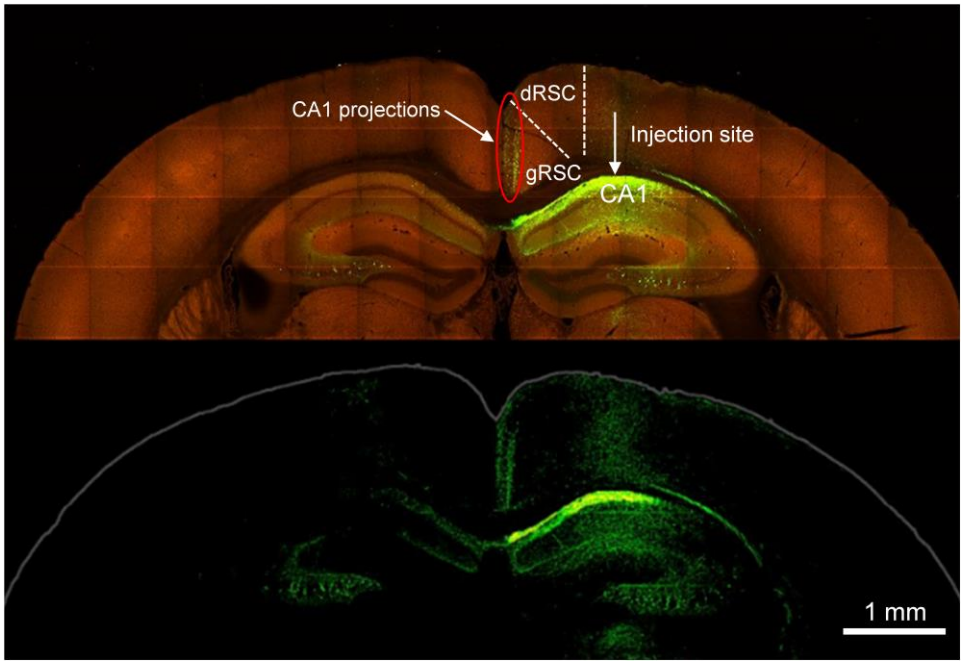

Figure 1.5 | Direct projections from the CA 1 area to the RSC.
The diagram illustrates direct projections from the CA1 field to the granular RSC. Tracer was injected in the CA1 area and projected from the CA1 area directly to the RSC, especially the granular RSC. dRSC, dysgranular retrosplenial cortex; gRSC, granular retrosplenial cortex; CA1, *Cornu Ammonis* area 1. Images and adapted from Allen Brain Atlas: Mouse connectivity. Available from: brain-map.org/api/index.html.

1.3.2. Connectivity with the thalamic regions

In addition to the connections with the HF, the RSC is densely connected with the thalamic regions, which are known to contain HD cells (Clark et al., 2012; Taube, 1995). Moreover, they are connected reciprocally. Specifically, the RSC share connectivity with anterior and lateral-dorsal thalamic nuclei (Kobayashi and Amaral, 2007; Van Groen and Wyss, 1992b; Vogt et al., 1987), which are important for spatial information (O'Mara, 2013; Todd and Bucci, 2015). Accordingly, this connection may facilitate the RSC to transform spatial information. The RSC predominantly connects to the ATN among other thalamic regions.

The projections from the granular RSC and the Rdg have variable densities of terminal areas in the ATN (Aggleton et al., 2014). Conversely, the projections from the ATN to the RSC have been reported previously (Van Groen and Wyss, 1992b; Van Groen and Wyss, 1995) and provided valuable information about the thalamo-retrosplenial projection network (Vogt and

Paxinos, 2014), which may assist the function of origination. HD cells have been found in the RSC, though with a small proportion, and the RSC is suggested to be important for orientating using environmental cues. See section 1.4 for details of the role of the RSC in orientation.

1.3.3. Connectivity with visual regions

Among various connections with other brain regions, the RSC reciprocally connects with the visual cortex (Todd and Bucci, 2015). Direct projections to the RSC have been found from V2 and V4 of the occipital lobes and the lateroposterior thalamic nuclei, and the claustrum provide visual information (Vogt and Miller, 1983).

It is noteworthy that the Rdg receives information from the visual cortex (area 17) (Clark et al., 2018; Donnelly et al., 1983; Thompson and Robertson, 1987; Van Groen and Wyss, 1992b). Consequently, it is suggested by the anatomical data that the Rdg is a potential hub integrating information from visual and limbic regions (van Groen and Wyss, 1992a). This is one of the reasons why the field of view for two-photon imaging was selected in Rdg in this study.

Such dense connections between the RSC and visual areas suggest functional correlations. Indeed, a recent study (Murakami et al., 2015) has shown visually evoked activity selectively in the RSC among non-visual areas (see Figure 1.6). The authors found that the RSC significantly responded to the visual stimuli (drifting gratings) similar to the visual area, and further cellular imaging revealed that some neurons in the RSC responded sharply selective for orientation and direction, which is typically observed in the visual area. These results may be due to the connectivity between the RSC and visual regions. The results from this thesis that RSC neurons encode visual features also support this connection at the functional level.

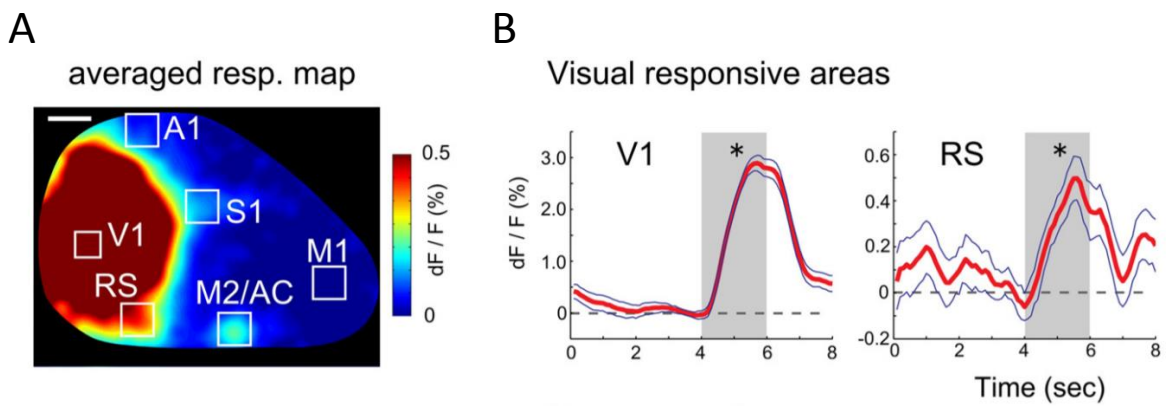

Figure 1.6 | Visually evoked responses in the RSC.

A. Averaged response map to visual stimulation in an entire mouse hemisphere. The retrosplenial cortex (indicated as "RS" in the figure) responds significantly to the visual stimulation (gratings) like the response in V1. **B.** Representative average time courses of visually responsive in V1 and retrosplenial cortex (RS). Red line: Averaged dF/F; Dashed line: calcium baseline; Grey: visual stimulation period. Adapted from (Murakami et al., 2015).

1.3.4. Connectivity with other brain regions

In addition to the major connections with the HF, ATN, and visual areas, the RSC is also reciprocally connected with parts of the prefrontal cortex, which could supply critical pathways between the HF and cortical areas that are engaged in executive functions such as working memory. The RSC has a function in spatial working memory (Keene and Bucci, 2009), which may be explained by the connection with the prefrontal cortex. The medial entorhinal cortex (MEC), which is the central conjunction between the hippocampus and neocortex, also projects to the RSC, though sparsely. The MEC contributes to memories, especially spatial memories, and hence, the connectivity with the MEC suggests the function of the RSC in spatial memories.

Additionally, reciprocal connections between the RSC and M 2 in mice were illustrated (Yamawaki et al., 2016). This connection may link to the important result found in this thesis that RSC neurons encode speed-related information (see section 4.5).

The unique location of the RSC, well situated centrally between the limbic areas and the cortical areas, determines the vast and diverse connections between the RSC and other important brain regions, and hence, suggest a variety of cognitive functions, including navigation and memory, that the RSC may be involved (see section 1.4).

Besides, there are also preferences regarding the connections between subdivisions of the RSC. For example, the granular RSC preferentially connects with the limbic regions, whereas the Rdg connects more with cortical regions (Miller et al., 2014). The functions of the RSC and the functional differences between the subdivisions of the RSC will be described in section 1.4.

In summary, the RSC is connected with the HF, thalamus, multiple cortical areas, including visual areas, prefrontal cortex, parietal cortex, and posterior secondary motor cortex (see Figure 1.7).

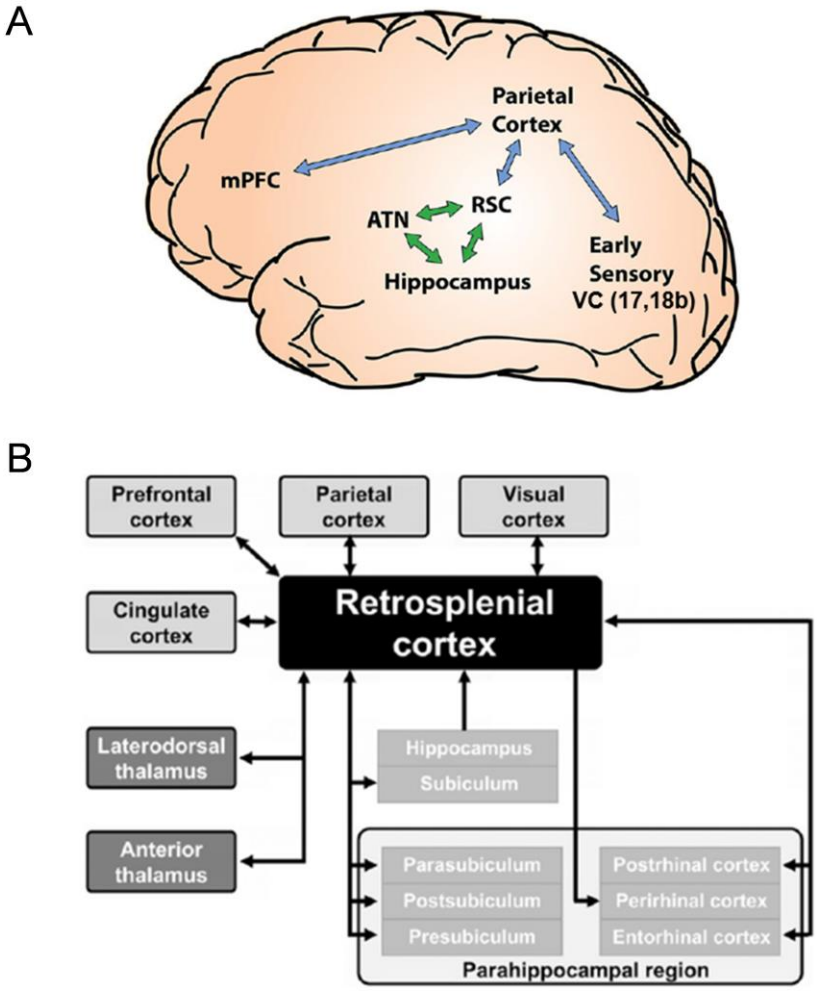

Figure 1.7 | Connectivity of the RSC.

A. The RSC is in the middle of sensory cortical areas (indicated by blue) and limbic areas (indicated by green). **B**. A schematic diagram showing the gross connectivity of the RSC. Adapted from (Miller et al., 2014) and (Mitchell et al., 2018).

1.4. The role of the retrosplenial cortex

Due to its unique location and various interconnection with an array of brain regions known to be essential for multiple cognitive functions, including navigation, spatial learning and memory, context memory, and episodic memory, RSC has been implicated in a variety of cognitive functions. Here, I will introduce the potential roles of the RSC based on evidence provided by previous human and animal studies.

1.4.1. Human lesion studies

Although bilateral lesions have been rarely observed in humans and the locations of the lesions in humans are not as precise as those in experimental animals, few previous human lesion studies provide valuable information that can help us understand the roles of the RSC. Most of the studies involved RSC lesions have suggested a function of the RSC in spatial navigation and spatial memory.

Humans and animals need landmark-based piloting strategies to navigate (Epstein and Vass, 2013). Several case reports have revealed the impairments in orientation/localization, forming and recalling long-term spatial memory, and route-planning (Epstein and Vass, 2013) in the presence of RSC lesions. For instance, people with RSC lesions were not able to find the path despite they could recognize the landmarks in the familiar neighborhoods and kept familiarity sense in the presence of lesions in the right RSC. Besides, most of the patients were not able to draw maps to show the environment nor describe routes between locations in detail, indicating the deficits in spatial memory. Additionally, damage to the RSC also prevented the patients to acquire new routes, indicating that RSC damage can impair spatial learning as well (Ino et al., 2007; Maeshima et al., 2001; Maguire, 2001; Osawa et al., 2008). Such topographical disorientation was also observed in patients with RSC lesions occurred in the left hemisphere (Ino et al., 2007; Maeshima et al., 2001; Osawa et al., 2008).

It is known that hippocampal lesions also impair the ability to navigate in environments but, different from RSC lesions, usually, they preserve the orientating ability in familiar surroundings (Maguire et al., 2006; Spiers and Maguire, 2007; Vann et al., 2009). These features could be partially explained by the fact that some RSC neurons have the properties of HD cells, which will be discussed in section 1.4.5.

Notably, the onset of such spatial impairment following RSC lesions is usually quite dramatic. (Ino et al., 2007). However, such deficits generally resolved in a few months after onset (Alsaadi et al., 2000; Maguire, 2001; Takahashi et al., 1997), possibly due to the compensation of remaining RSC tissue and/or the undamaged hemisphere. In addition to spatial deficits, verbal encoding deficits were also observed in a patient with RSC damage (McDonald et al., 2001).

Taken these reported spatial deficits in patients with damage to RSC together with the connectivity of the RSC, it has been proposed that the RSC has a ‘translational’ function, transforming allocentric information into egocentric information and vice versa (Burgess et al.,

2001; Byrne et al., 2007; Epstein, 2008; Maeshima et al., 2001; Vann et al., 2009). This translational function is further supported by evidence from animal studies, which will be described in section 1.4.3 and 1.4.4. However, one important role of the RSC in contextual memory, which is the focus of this thesis, is missing from previous human lesion studies, and I will discuss this function in section 1.4.3 based on animal lesion studies.

1.4.2. Human imaging studies

As described above, previous lesion studies in humans have revealed the role of the RSC in spatial cognition. However, the RSC lesions in humans are quite limited and impossible to control. Human neuroimaging methods have been extensively used to explore brain functions in a wide range of brain regions, including the RSC, and previous human neuroimaging studies have found the involvement of the RSC in multiple cognitive functions.

Functional magnetic resonance imaging (fMRI), which is extensively applied now, can show the activity in the RSC during/after a variety of tasks or processes, has been successfully used to investigate the role of RSC in cognitive functions.

It has been demonstrated by human imaging that the RSC is engaged in contextual associations

(Bar and Aminoff, 2003; Kveraga et al., 2011). In addition, most neuroimaging studies in humans have shown consistent activation of the RSC in spatial tasks, including mental navigation, passive viewing of navigationally relevant visual cues, and interactive navigation in the VR environments (Epstein, 2008; Vann et al., 2009) or tasks involved with orientation using visual cues in the environment (Mitchell et al., 2018).

Combining fMRI and VR, an earlier study (Iaria et al., 2007) found the RSC was involved in both the development and the usage of the cognitive map, indicating that the RSC contributes to topographical orientation by renewing the position while the reference alters (see Figure 1.8).

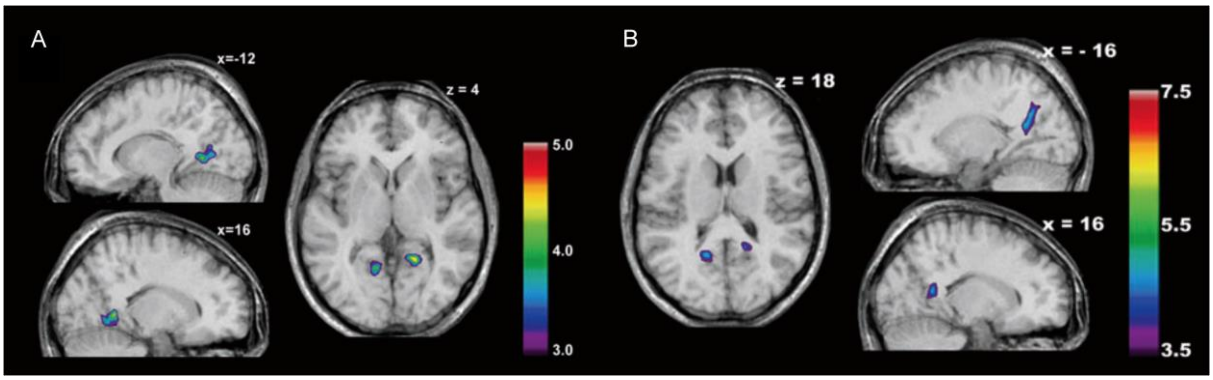

Figure 1.8 | Brain activity while forming and using the cognitive map.
A. RSC is active during the development of the cognitive map. B. RSC is also active during the usage of the cognitive map. Adapted from (Iaria et al., 2007).

Notably, the RSC shows a stronger response to the familiar than to the novel environment (Epstein, 2008; Epstein et al., 2007a; Epstein et al., 2007b; Sugiura et al., 2005), which also suggests the role of the RSC in contextual memory. For example, in a recent study (Epstein et al., 2007b), it was shown that the activity of the RSC had preferences for the recalled information, and the RSC responded more to the familiar than to the novel surroundings displayed by images.

Moreover, it has been shown that RSC is selectively engaged in the encoding of stable, permanent landmarks (Auger et al., 2012; Auger et al., 2015; Marchette et al., 2014; Troiani et al., 2014). In a recent study (Auger et al., 2015), it had been revealed the RSC preferably encoded permanent information. Moreover, such preference of permanence was also observed in verbal tasks that were beyond the spatial domain (Auger and Maguire, 2018).

HD coding was observed previously in retrosplenial complex (Baumann and Mattingley, 2010; Marchette et al., 2014). A recent study (Shine et al., 2016) found evidence for global heading representation in the RSC and thalamus, both of which contain HD cells, which will be discussed in section 1.4.5. These findings may partially explain the fact that the damage to RSC mostly leads to a deficit in orientation.

1.4.3. Animal lesion or inactivation studies

As described in the above chapter, it is challenging to study the role of the RSC in humans using lesion studies because the lesions that happened in humans are quite limited and not controlled.

However, in rodents, researchers can make bilateral and well-controlled lesions in the RSC and then test the functions of the RSC in different behavioural tests. Moreover, the lesions in rodents can be made in different stages to address the roles and functions of the RSC at different stages of learning and memory.

Navigation and spatial memory

A number of previous animal lesions studies have shown a role of the RSC in spatial learning and memory especially when visual information is involved, path integration, segregation of spatial information, HD orientation, and spatial working memory (Aggleton, 2010; Cain et al., 2006; Cooper et al., 2001; Haijima and Ichitani, 2008; Harker and Whishaw, 2002; Hindley et al., 2014a; Lukoyanov et al., 2005; Nelson et al., 2015; Parron and Save, 2004; Sutherland et al., 1988; Vann and Aggleton, 2002; Vann et al., 2009).

For instance, a previous study (Hindley et al., 2014a) showed the roles of the RSC in spatial learning and memory using a series of different spatial tasks and suggested that the RSC is crucial for effectively using distal visual information to deal with spatial tasks and further highlight the concept that the RSC facilitates the integration of different visuospatial information.

Path integration relies on egocentric information to recognize positions in the environment. In an early study (Cooper and Mizumori, 1999), they evaluated the spatial memory performance and the contribution of the RSC in active navigation in light and dark conditions by transient inactivation of the RSC. They revealed that RSC inactivation impaired behavioural performance selectively in darkness and the results supported the idea that the RSC may provide mnemonic associations of visual information and other non-visual information in the environment, and therefore the RSC plays a vital role in navigation in the darkness. Similar results suggesting a role of the RSC in integration visuospatial information were found in a later study with RSC lesions (Elduayen and Save, 2014). A further study (Cooper et al., 2001) used spatial memory tasks and found that RSC inactivation in rats impaired the spatial memory, and inactivation of the RSC decreased the accuracy during navigation in the darkness.

As described in sections 1.4.1 and 1.4.2, it has been suggested by lesion studies in human beings that the RSC is important for determining the direction and originating. In line with human studies, studies in rodents also found that lesions in the RSC impair the ability to use direction

cues for alternation (Pothuizen et al., 2008), especially when conflict cues were presented or in darkness (Nelson et al., 2015). Moreover, it has been revealed that neurotoxic or electrolytic lesions of the RSC in rats significantly impaired the representation of head cells in the anterodorsal thalamus. Specifically, RSC lesions reduced the preferred firing direction stability of head cells in the anterodorsal thalamus, even with an apparent visual cue (Clark et al., 2010). This study indicates that the RSC contributes landmark information processing for precise HD cell orientation and may further explain the deficit of directional sense in humans with damage to the RSC.

Also, the RSC has a function in spatial working memory, especially when the difficulty of the task increases (Keene and Bucci, 2009) and in the segregation of spatial information (Wesierska et al., 2009).

These previous studies, predominantly using lesions in the RSC of rodents, have demonstrated one of the most critical roles of the RSC, which is in spatial cognition. These results are in line with the suggestion from the anatomical data described in section 1.3. Moreover, the notion that the RSC is highly involved in spatial cognition encouraged me to design the paradigm used in this thesis, in which not only context discrimination but also spatial information is involved.

Contextual memory

Contextual learning and memory rely on a complex network involving a range of brain regions. It is well known that the hippocampus is vital for contextual learning, and memory, and it has been further shown that the hippocampus contributes to contextual learning and memory in a parameter-dependent manner. For instance, lesions in the hippocampus of rats generated both anterograde and retrograde context amnesia with ‘weak’ training procedures but only produced retrograde context amnesia when rats were trained with more trials and/or stronger footshocks. Previous studies already showed that RSC lesions in rats impaired contextual memory with weak training (Wiltgen et al., 2006). A very recent work (Fournier et al., 2019) showed that, unlike the hippocampus, the RSC lesions produced both retrograde and anterograde context amnesia when rats underwent strong training procedures in fear conditioning paradigms. These results suggest that unlike the hippocampus, the RSC is necessary for contextual memory, and other regions cannot compensate for the role.

Several lines of studies have shown an essential role of the RSC in contextual learning and memory. For instance, Keene and Bucci performed a standard signed fear conditioning task using rats with the RSC electrolytically damaged and found that lesions in the RSC impaired the response of contextual fear conditioning but not cue-specific fear conditioning and thus suggested that the RSC plays a role in the processing of contextual information (Keene and Bucci, 2008a). Furthermore, in another study (Keene and Bucci, 2008b), they applied fiber-sparing neurotoxic damage to RSC and further addressed the contributions of the RSC in contextual fear memory using both signed and unsigned fear conditioning tasks. Similarly, in both signed and unsigned fear conditioning tasks, neurotoxic lesions of the RSC in rats impaired the contextual memory and further suggest that the RSC contributes to contextual learning and memory.

Therefore, it is generally accepted that the RSC had a vital function in contextual memory. Further studies have revealed that the RSC plays a time-dependent role in cue-specific memory. In one previous study, Jiang and colleagues (Jiang et al., 2018) found fear expression to a visual stimulus was impaired when lesions were made in the RSC 28 days after fear conditioning, whereas no impairment was observed when the lesions happened one day after conditioning. These results suggest that RSC plays an essential part in the retrieval of remote cued fear memories. This notion is supported by another study (Todd et al., 2016), which showed that either neurotoxic or electrolytic lesions, which were made several weeks after conditioning, impaired a previously acquired remote auditory fear memory. In addition to the permanent lesion experiments, they also temporarily inactivated the RSC during the testing session using a chemogenetic approach and observed that the remote memory retrieval for an auditory signal was impaired. These results, coupled with the results described above, suggest that the RSC plays an essential role in the retrieval of remote memories.

Unlike lesion studies that cause severe damage to the region of the interest in the brain, chemogenetic approaches can be used to transiently silence neurons and thus to address the involvement of a specific brain region in a particular phase of the cognitive function. Chemogenetic technologies have been developed as valuable tools to control neuronal signal transduction, cellular signaling, and behaviour, and importantly, it can link the behavioural outputs with neural circuits (Dar et al., 2012; Roth, 2016; Whissell et al., 2016). Among these chemogenetically engineered proteins, Designer Receptors Exclusively Activated by Designer Drugs (DREADDs) is the most popularly used by neuroscientists (Roth, 2016) and is also the one I used in this study. DREADDs can be used to activate or inactivate targeted populations

of neurons, depending on the expression of the receptor and timing of designer drug application. DREADDs receptors can be introduced in a particular brain region via different gene transfer strategies, and in this study, the gene delivery of inhibitory receptor hM4Di was done using by AAV. The receptor is only activated after the application of CNO and thus provides the ability to apply temporally-controlled and repeatable interventions (Smith et al., 2016). This is one of the most significant advantages of DREADDs compared to the lesion approach used for investigating the role of the RSC, which generates permanent damage and loses the potential to study the contribution in different phases.

The formation of associations between sensory information in the world is a critical aspect of contextual memory. In one previous study (Robinson et al., 2014), the authors trained control rats and rats expressing inhibitory receptors in a sensory preconditioning paradigm and found that chemogenetic inactivation of neurons in the RSC in the phase of preconditioning impaired the formation of an association between sensory cues and abolished the effect of the sensory preconditioning which suggests that the RSC may play a part in episodic memory formation by providing links between essential sensory information during the learning process.

These previous studies conducted permanent lesions or temporal inactivations in the rodent RSC and revealed the involvement of the RSC in contextual learning and memory. However, the role of the RSC at different stages of contextual learning and memory and the neuronal dynamics underlying such functions remain unclear. For instance, if the RSC required for the acquisition of contextual memory or the memory recall or both needs to be addressed. Afterward, if the RSC contributes to the function of contextual memory, then how this is achieved at the cellular level also requires investigation. These open questions will be addressed in this thesis, see results in section 4.

Object recognition and recency memory

The RSC and hippocampus are anatomically connected, and both of them play a role in learning and memory. A previous study (Haijima and Ichitani, 2012) addressed the effects of excitotoxic lesions in the RSC and hippocampus on the performance of rats in the spontaneous object recognition task. They observed that hippocampus-lesioned rats showed deficits independent of the retention interval during the test sessions of the object recognition. On the other hand, RSC-lesioned rats also had an impairment, which was, however, retention interval dependent

with an impairment only occurring for the longer interval. Besides, both lesions had no effects on short term recognition memory independently of delay length. These results indicate that the RSC and hippocampus contribute to long term object recognition memory with different roles.

Additionally, a recent study (Powell et al., 2017) found RSC-lesioned rats showed a deficit in discriminating the temporal order of the objects and thus suggested a role of the RSC in recency memory, which may be explained by the connections with hippocampal formation and medial frontal cortex.

Selective lesions in subregions of the RSC

Some studies failed to find comparable impairments after RSC lesions, and this may be due to the size or location of the lesions since the RSC is a relatively large region. To address this question, two studies (Vann and Aggleton, 2004; Vann et al., 2003) tested different sized lesions in the RSC and specific location of the lesion in the RSC in tasks involved spatial working memory and heading direction, and found that rats with 'standard' lesion made in caudal RSC showed mild impairment, but the performance of the rats with 'complete' lesion in the RSC was more disrupted.

Most of the lesion studies in rodents do not separate the subregions of the RSC but perform extensive lesions in the entire RSC. Few studies, however, investigate the effect of selective lesions. For instance, a previous study (Vann and Aggleton, 2005) showed that rats with selective dysgranular RSC lesions relied less on distal visual information but relied more on a turning strategy to resolve the task involved working memory in the radial-arm maze, which may be explained by the anatomical facts that visual inputs primarily target the dysgranular RSC when arriving the RSC. Besides, RSC has also been suggested to contribute to the integration of different types of information (Hindley et al., 2014b), the results in this thesis further support this, see section 4.

In addition to the lesion studies, (Pothuizen et al., 2009) provided direct evidence for the differences between the granular RSC and Rdg: the granular RSC engages in navigation and spatial learning depending on both external and internal cues, whereas the Rdg contributes more selectively during tasks involved distal visual cues.

In addition to the selective lesion in the dysgranular RSC, one early study (van Groen et al., 2004) found that lesions (ibotenic acid) in Rgb showed small but significant impairment in a

water maze spatial task, but no impairment was observed in the rats with Rga lesions. The results indicate the Rgb may have a small, independent contribution to spatial learning and memory and thus highlight the complicated and exceptional contribution of each subregion of the RSC to behaviour. Taken these results, along with the previous studies together, it is suggested that the dysgranular and granular RSC subregions work closely to support spatial learning.

1.4.4. Animal disconnection studies

The hippocampus and the ATN have been studied and shown the functional connection with the RSC. For instance, it has been shown that lesions (either excitotoxin or radiofrequency) in the ATN prevented IEG activation in selective regions of the RSC in rats despite that no cytoarchitectonic changes were observed (Jenkins et al., 2004) and a lamina selective loss of long-term depression (LTD) in RSC slices was found several months after ATN lesions (Garden et al., 2009). Collectively, these data indicate that tight interconnection between the RSC and the ATN.

In addition, radio-frequency lesions in the hippocampus produced a pronounced loss of IEG (Fos and Zif268) in the RSC without cytoarchitectonic changes detected. (Albasser et al., 2007). Unlike the effect of the ATN, lesion describes above, the loss of IEG following hippocampal lesion was found in both granular and dysgranular RSC without selective laminae dependence. These findings provide evidence of functional connection and interdependency between the RSC and hippocampus.

On the other hand, the dysfunction of the RSC may also affect the regions that are interconnected with it. For instance, the hippocampal place-field location was changed by temporary RSC inactivation, and the place coding was changed irrelevant to behavioural impairments. The findings support the notion that the RSC has an impact on the hippocampus and suggests that the RSC facilitates accurate path integration by providing mnemonic spatial information for updating location information in the hippocampus and thus the RSC and hippocampus work together to mediate navigation (Cooper and Mizumori, 2001). These disconnection studies further highlight the importance of the connections between the RSC and other brain regions, as described in section 1.3.

1.4.5. Animal single-neuron studies

Lesion studies in animals provide a wide range of valuable knowledge about the role and contribution of the RSC during a variety of critical cognitive tasks. On the other hand, single-neuron studies such as in vivo electrophysiology and imaging studies can record the activity of the RSC neurons while the animals perform cognitive tasks and, therefore, can be used to explore the properties and more specific functions of the RSC. Multiple single-neuron studies have been done to explore the properties of the RSC.

Spatial location information processed in the RSC

An accurate sense of location is the key to successful navigation and spatial cognition. Based on anatomical and functional connection and also the fact that the RSC received direct inputs from CA1, one may expect to see similar properties of cells in these two regions.

A recent study (Mao et al., 2017) using in vivo cellular calcium imaging combined with a head-restrained locomotion setup revealed a population of neurons in the RSC whose ensemble neuronal activity showed highly similar properties to the place cells in hippocampal CA1 recorded within the same task. These cells predominantly located in superficial layers of the RSC. Similar to classic place cells in CA1, these neurons activate in sequences during running on the treadmill and showed an orthogonal, sparse code correlated with the position. Additionally, the activity of such RSC place cell-like neurons showed partial remapping pattern after manipulation to environmental cues like light condition, which resembles the place cells observed in CA1 during the same task, and such these RSC neurons are robust to environmental manipulation. The findings from this study showed the critical notion that the RSC contains neurons that encode place cell-like activity, and the results are also valuable to help understand that how RSC neurons encode navigational and spatial information and, therefore, may facilitate the RSC on its contribution to navigation and memory (see Figure 1.9).

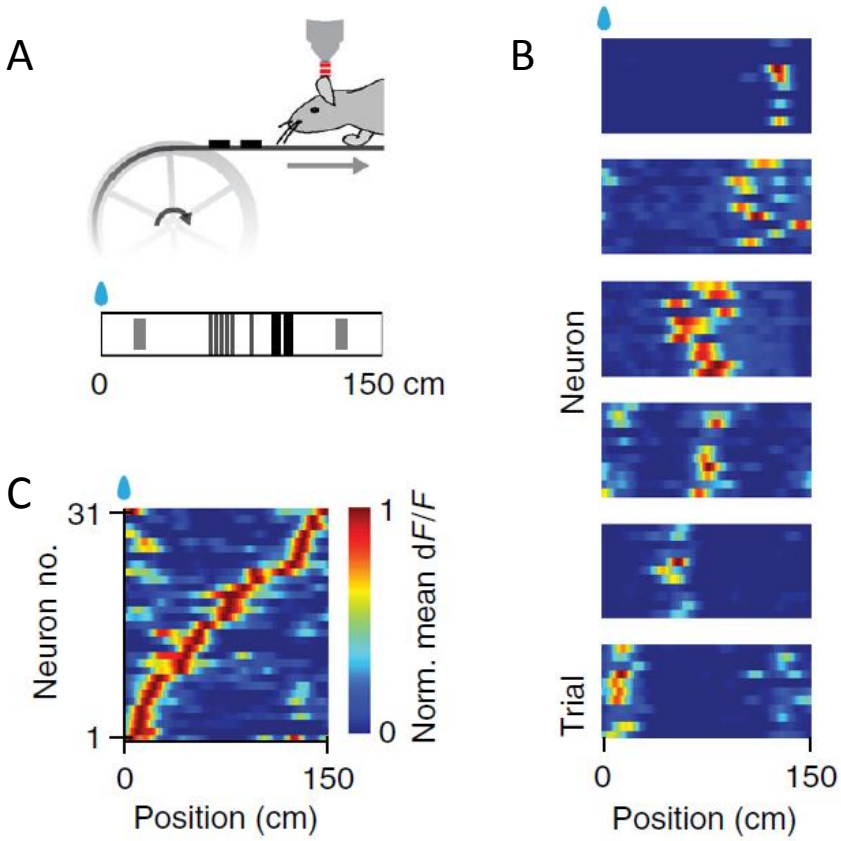

Figure 1.9 | Sparse orthogonal population encoding of spatial position in the RSC.
A. Two-photon imaging was performed in the RSC in a head-mixed mouse running on a treadmill. **B**. The normalized activity of the RSC neurons with place cell-like pattern. **C**. The normalized activity of 31 RSC neurons with place cell-like properties as a function of position on the treadmill. Adapted from (Mao et al., 2017).

Other single-neuron studies have also shown that the RSC processes location-related information. For instance, one precious study (Alexander and Nitz, 2015) suggested that the RSC acts as a mediator between different brain regions providing different forms of spatial information and such support the notion that the RSC integrates different information and has a 'translation' function between allocentric and egocentric information.

It is believed that RSC neurons concurrently encode location within routes and other spatial information. In order to examine the contribution of the RSC in sub-route encoding, a recent study (Alexander and Nitz, 2017) recorded single neurons in the RSC, while rats were trained to travel a route that has recurrent properties at different scales. They found a unique activation of RSC neurons, which is periodic and repetitive across the segments of the route that have the same shape. In the meanwhile, more RSC neurons generated single-cycle periodic activity over

the entire route, and such further encoded sub-route locations relative to the entire route. Furthermore, these RSC neurons concurrently generate a unique metric for distance from each specific location to all others. Taken together, the results suggest a role of the RSC in the extraction of path sub-spaces within a complicated route, the encoding of distances traveled.

To further explore the specific role of the RSC in spatial cognition, another study (Vedder et al., 2017) applied single-cell electrophysiological recording in granular b of the RSC while rats performed a reward indicated T-maze task in which the location of the reward was indicated. The identified that neurons in the RSC encoded the flashing light cue rapidly, and additionally, they also encoded the reward and the location of it. Furthermore, distinct patterns of activity were observed along the right and left trajectories to the reward. These results provide direct neurophysiological evidence of goal-directed navigation encoding in the RSC. Coupled with RSC lesion studies in human beings and animals, the loss of such goal-directed navigation encoding signals in the RSC may underlie spatial impairments in subjects with damage to the RSC.

Spatial memory information processed in the RSC

Along with location-related information, the RSC has also been revealed to contribute to spatial memory. For instance, a previous study (Czajkowski et al., 2014) using in vivo two-photon c-fos imaging to monitor neuronal activity during the spatial learning process in a Morris water maze task to investigate whether the RSC encodes and/or keeps spatial information. They found a consistent pattern of neuron activation during spatial learning, which is in line with the hypothesis that an experienced memory trace is established during spatial learning in the RSC. Also, they reported several other vital findings that further support the hypothesis. First, transient inactivation of the RSC by infusion of CNQX (6-cyano-7-nitroquinoxaline-2,3-dione), a reversible AMPA receptor antagonist which stops neurotransmission, impairs the performance of the mice in a spatial learning paradigm. Second, by using the HSV-CREB virus to increase the expression of CREB selectively in the RSC neurons, they observed improvements in spatial memory. Moreover, in the following experiment, when they inactivated the viral-CREB expressing neurons, the enhancement of the spatial memory was prevented. All these findings together suggest that the RSC plays a role in the formation and storage of spatial memory trace.

Another study (Milczarek et al., 2018) using two-photon-based c-fos imaging to monitor activity patterns of thousands of neurons in the dysgranular RSC during the mice were trained in a task involved spatial memory. They found a context-specific pattern of neuronal responses gradually emerged with learning, and such unique patters were re-instated during memory retrieval. Furthermore, more stable engrams accompanying with better memory, that can be used to predict the level of forgetting. The importance of this work is the evidence that the contribution of the RSC in spatial memory storage at neuronal ensembles level and demonstrating the interdependence of the RSC memory engram formation and spatial memory consolidation.

Besides, to address the relationships between the neuronal activity in the RSC and spatial memory, a recent study (Miller et al., 2019) recorded neuronal activity in the RSC while the rats were trained to perform a continuous T-maze alternation task. The authors revealed that the spatial position was represented by the activity pattern of a population of RSC neurons while the rats learned during the task, and RSC activity can be used for predicting upcoming turn decisions. Furthermore, while the rats became experts in the task, the RSC firing patterns started to simulate the location of the goal while the rats arrived near the choice position. Finally, they also conducted lesions in the RSC and found an impairment in the performance of alternation after learning. In summary, these results showed that the RSC encoded space and future goal location with learning.

Head direction information processed in the RSC

Navigation relies on the perception of location and directional heading information, and it is known that HD cells, which are preferably activated when the subject faces a specific direction, compute the sense of direction (Taube, 2007). As described in human lesion studies and animal lesion studies, damage to the RSC severely impairs the ability to sense the direction and further orientate correctly. Therefore, one may expect to see head cells in the RSC and indeed, this is the case.

Chen and colleagues (Chen et al., 1994a; Chen et al., 1994b) recorded single neurons in the RSC during rats performing a spatial working memory paradigm on a radial arm maze within a cue-controlled experimental room. They identified around 8.5% of recorded neurons in the RSC to be HD cells. Interestingly, most of the HD cells in the RSC were not modulated by the

behaviour. This study suggests an association between head directionality and movement that is used to transform the egocentric information to an allocentric directional representation.

A subsequent study (Cho and Sharp, 2001) also found HD cells in both granular and dysgranular RSC with similar firing patterns to those seen in other regions, and these HD cells can be used to anticipate a specific direction. Moreover, they found another type of cell that had a complicated pattern of spatial activity in which these cells fired the most for certain combinations of HD, position, and locomotion that indicated that these cells might become active when the animal approaches a specific position with a specific movement. Taken these facts that the neurons in the RSC contain movement and spatial-related information and because the RSC closely connects with the motor cortex, it is suggested that the RSC may contribute to path integration or navigational motor planning.

A recent study further investigated the HD signal in the RSC (Jacob et al., 2016). First, in this study, the authors also found around 9% of recorded RSC neurons to be HD cells. Furthermore, in addition to the conventional head cells, they found that around 11% of neurons have bidirectional firing tuning curves. Such bidirectional cells are exclusively identified in the dysgranular, whereas the classic HD cells were found in both granular and dysgranular RSC. Additionally, such bidirectional direction cells were not found in the other two HD cell regions, the anterior thalamus, and postsubiculum. All the data together indicate that local cues dominate the activity of neurons even when these environmental cues conflict with the global HD and thus suggests a mechanism for an association or dissociation environmental cues from the global HD in the dysgranular RSC exclusively.

Speed-related information processed in the RSC

Along with the well-studied properties like position-related information, and HD information, it has also been suggested by previous studies that the RSC processes information related to the locomotion speed. Although this property that speed-related information is processed in the RSC is not directly studied, results from a few previous studies have suggested this feature. For instance, an early study (Cho and Sharp, 2001) using single-cell electrophysiological recording found that the activity of some cells in the RSC correlated with the spatial-movement variables that were examined and suggested the RSC contains movement-related signals. Another recent study (Chinzorig et al., 2019) also found the activity of some neurons in the RSC correlated with the speed of the rat running on the treadmill indecently on the directions. Based on these

suggestions, it is worthy of investigating the correlation between the activity of the neurons in the RSC and the running speed deeply.

Contextual information processed in the RSC

A previous study (Smith et al., 2012) aimed to test whether the hippocampus mainly encodes context while the RSC encodes behaviourally significant cues. To address this question, they recorded the neuronal activity in both the hippocampus and the RSC simultaneously during the rats learned to perform behavioural context discrimination. They revealed that both RSC neurons and neurons in the hippocampus produced highly context-specific activity during context discrimination learning progress. Interestingly, neurons in the hippocampus showed context-specific encoding to multiple events and stimuli in the task, whereas neurons in the RSC only produced context-specific responses to the position of the reward, which acted as the identifying cue of the context. These results confirm the contributions of the hippocampus and the RSC in context discrimination and further suggest that these two regions have different but complementary functions in mediating context memories.

Moreover, a later study (Cowansage et al., 2014) further found that optogenetic stimulation of the neurons evoked with contextual learning in the RSC was able to generate retrieval of fear memory. Also, unlike the retrieval of natural contextual fear memory, the memory artificially reactivated by an optogenetic approach was not impaired by hippocampal inactivation. These findings support the notion that RSC can subserve recently learned behaviour independent of the hippocampus.

Decision making is a complex process which is often depending on the value formed from previous experience. To study which areas contribute to the value coding and the plasticity of it, in a recent study (Hattori et al., 2019), the authors used a value-based decision task to train the mice and performed cellular imaging of neural activity in multiple areas, including anterior-lateral motor cortex, posterior premotor cortex, posterior parietal cortex, the RSC, primary somatosensory cortex, and primary visual cortex. They found that the RSC uniquely encoded value-and history-related information consistently, and such RSC history-related encoding improved with learning. Finally, after the inactivation of the RSC, the reward-history-related behavioural strategy was impaired. This study indicates that the RSC consistently encodes value-based information and flexibly adjusts the history encoding to maintain adaptive behaviours.

Besides, it has also been shown that the RSC contributes to systems consolidation of contextual memory. A recent study (de Sousa et al., 2019) used artificial high-frequency (100 Hz) optogenetic approach to selectively stimulate neuronal ensembles that were activated during context fear conditioning and representing the fear memory (engram neurons) in the RSC 24 hours after learning to generate a recent memory. Interestingly, this recent memory contains the properties commonly seen in consolidated remote memory, including contextual generalization, the involvement of cortical regions during memory recall, and less dependence on the hippocampus. Furthermore, this phenomenon was only observed if memory engrams were reactivated during light anesthesia or sleep. Taken these results together, it is suggested that RSC engram neurons reactivation during post-learning can induce systems consolidation and formation of remote memories, and this process can be most efficient by reactivation during the unconscious condition.

Visual information processed in the RSC

As described in section 1.3.3, the RSC receives direct visual input from visual areas and therefore suggests that the neurons in the RSC may contain visual information. Indeed, a previous study (Murakami et al., 2015) showed the RSC was actively responsive to low-temporal and high-spatial frequency visual stimulations. Furthermore, two-photon cellular imaging revealed that some neurons, though a minority, showed visual responses highly selective for direction and orientation of the gratings, similar to those observed in the visual cortex. This study provided direct evidence that the RSC processes visual information in a minor proportion of neurons.

In summary, based on the rich connections with a variety of brain regions, and the previous studies from humans and animals, including lesion studies and single-neuron studies, the RSC had been implicated to a range of cognitive functions, including spatial navigation and memory especially with visual information involved, path integration, HD orientation, contextual learning and memory, object-based information, and the ‘translation’ function between egocentric and allocentric information (see Figure 1.10).

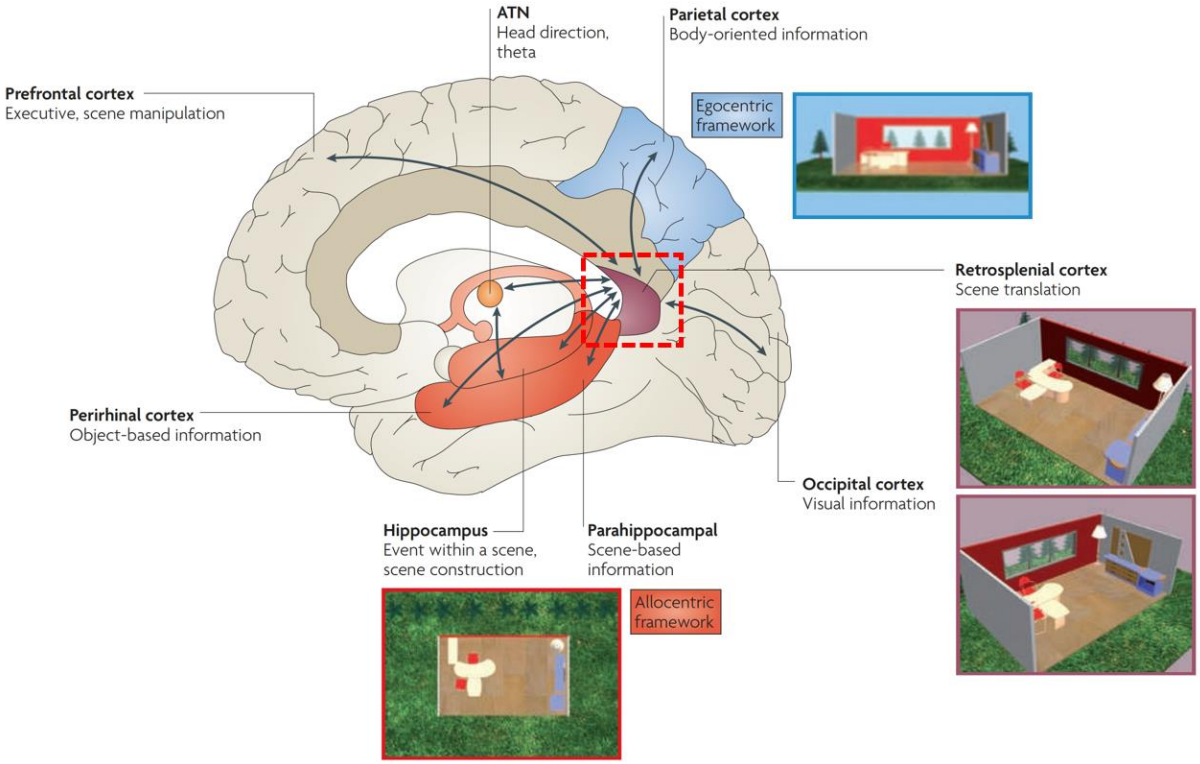

Figure 1.10 | The primary connections and functions of the RSC.
Cognitive functions rely on the integration and manipulation of diverse types of information. Due to the rich connections with a variety of brain regions, including the hippocampus, ATN, prefrontal cortex, visual areas and many other regions, the RSC is uniquely situated to play a translational role between egocentric and allocentric frameworks as well as other functions such as navigation, orientation, contextual memory, and working memory. Adapted from (Vann et al., 2009).

1.5. Clinical relevance of the retrosplenial cortex

As described in the above sections, the RSC is involved in a wide range of cognitive functions, especially in spatial learning and memory, and contextual memory, which is known to be impaired in multiple neurological diseases. Therefore, RSC pathology is suggested to related to a battery of neurological diseases.

Indeed, from previous reports, we know that the RSC pathology is implicated in neurological diseases, such as: autistic spectrum disorders (Starck et al., 2013; Weng et al., 2010), vascular dementia (Martinez-Bisbal et al., 2004), depression (Ries et al., 2009), post-traumatic stress disorder (Liberzon et al., 1999; Piefke et al., 2007), epilepsy (Archer et al., 2003), fibromyalgia

(Wik et al., 2006), bipolar disorder (Nugent et al., 2006), Korsakoff's syndrome (Aupée et al., 2001; Reed et al., 2003) and schizophrenia (Bluhm et al., 2009; Laurens et al., 2005; Mitelman et al., 2005; Newell et al., 2005). However, most of these are case reports, and some of them did not have specific isolation of the RSC but just referred to pathology in the posterior cingulate cortex.

On the other hand, RSC dysfunction, both atrophic (Pengas et al., 2010; Tan et al., 2013) and metabolic (Chetelat et al., 2008; Hashimoto and Nakano, 2014; Lee et al., 2014; Minoshima et al., 1997; Nestor et al., 2003) have been consistently implicated in AD, especially at the very early stage of the disease, usually referred as prodromal phase of AD, known as mild cognitive impairment (MCI).

For instance, in a previous study (Pengas et al., 2010), twenty-four patients with MCI, who all eventually progressed to meet the criteria of AD, were imaged with volumetric MRI. They found significant atrophy in the RSC (areas 29/30), which was comparable to that observed in the hippocampus, which showed that RSC atrophy shows up at the very early clinical stage of AD. Another early study (Nestor et al., 2003) has shown consistent hypometabolism in the RSC (areas 29/30) at prodromal Alzheimer's disease stage.

It is also found that changes in the retrosplenial regions could be used to predict the progress of AD from the MCI stage (Huang et al., 2002; Johnson et al., 1998). Therefore, more knowledge of the RSC is quite valuable to help us open avenues for potential clinical diagnoses, especially for the earlier detection of AD.

2. OBJECTIVES

As described in the above sections, anatomical and behavioural studies in both humans and animals have revealed a variety of roles of the RSC and strongly suggest an integrative role for the RSC. However, how the integration is implemented at the cellular level is still unclear. The integration may be achieved through interaction between subpopulations of neurons that encode a single stimulus dimension/parameter, or by neurons encoding multiple dimensions, or through mixed mono- and multidimensional encoding.

The previous studies of single-cell activity in mammalian RSC have revealed that specific subpopulations of RSC neurons can encode spatial information (Alexander and Nitz, 2015; Czajkowski et al., 2014; Mao et al., 2018), possess properties of HD cells (Chen et al., 1994b; Jacob et al., 2016) or place cells (Mao et al., 2017), and can encode reward locations (Vedder et al., 2017) as well as reward history (Hattori et al., 2019). However, these studies were focused on specific cognitive dimensions and did not study the cellular basis of multidimensional integration in the RSC.

The specific objectives of this thesis are the following:

- Establish a methodology to combine cellular *in vivo* two-photon imaging with a context discrimination paradigm created in VR.

- Validate the context discrimination diagram during learning and reversal learning using naïve and control mice.

- Examine the specific role of the RSC in various stages of learning and memory using a chemogenetic approach (DREADDs).

- Characterize the neuronal activity of the RSC underlying the formation and updating of context-reward value associations.

- Compare contributions of mono- and multidimensional neurons to the encoding of information following learning and/or reversal learning, as a measure of cognitive flexibility

3. MATERIALS AND METHODS

3.1. Animals

In order to perform *in vivo* two-photon calcium imaging, C57BL/6J-Tg (Thy1-GCaMP6f) GP5.5Dkim/J (Jackson Laboratory, USA; RRID: IMSR_JAX: 024276) transgenic mice were used for all experiments (male; 5- to 6-month-old at the time of surgery). These transgenic mice express GCaMP6f (green fluorescent calcium indicator) in subsets of excitatory neurons in the brain and are suitable for imaging to monitor the neuronal activity at the single-neuron level. These mice were made by the Genetically-Encoded Neuronal Indicator and Effector (GENIE) Project at the HHMI's Janelia Farm Research Campus and donated to The Jackson Laboratory by Douglas Kim (Chen et al., 2013).

All mice were cared and treated strictly following the ethical animal research standards defined by the Directive of the European Communities Parliament and Council on the protection of animals used for scientific purposes (2010/63/EU) and were approved by the Ethical Committee on Animal Health and Care of Saxony-Anhalt state, Germany (license number: 42502-2-1346). Mice were group-housed until surgery under a fixed 12-h light/dark reversed cycle (light is on at 21:00 and off at 9:00) with food and water available *ad libitum*.

In total, eighteen mice were used for this project. For the first baseline experiment, six mice were used, which did not receive any adeno-associated virus (AAV) injection. For the next control experiment, five mice were injected with a control virus AAV8/hSyn-mCherry (AV6443, UNC GTC Vector Core, USA; RRID: Addgene_114472; titer: 4.6 x 10^{12} vg/mL), which drives mCherry expression. For the last inactivation experiment, a chemogenetic approach was used to inactivate the RSC in seven mice. Therefore, AAV8/hSyn-hM4Di-mCherry (AV5630D, UNC GTC Vector Core, USA; RRID: Addgene_50475; titer: 7.4 x 10^{12} vg/mL) was injected into the RSC followed by Clozapine-N-oxide (CNO)-induced neuronal inhibition at specific periods during the experiment. In control experiments, mice expressing mCherry received CNO at the same time points as hM4Di plus mCherry expressing mice.

3.2. Surgical procedures

Surgical procedures were modified from previous studies (Holtmaat et al., 2009; Pakan et al., 2016; Sun et al., 2019). Anesthesia was induced with 4% isoflurane (Baxter, Germany) before the mouse was fixed in the stereotaxic apparatus (SR-6M, Narishige Scientific Instrument Lab, Japan) and adjusted to 1.5-2% during surgery with 0.4 L/min O_2. Ophthalmic ointment was applied to the eyes for protection (Bepanthen, Bayer, Germany), and to decrease cortical stress response and avoid cerebral edema, dexamethasone (2 mg/kg body weight; Mephamesone, Mepha Pharma, Switzerland) was subcutaneously injected, and carprofen (5 mg/kg body weight; Rimadyl, Pfizer, USA) was intraperitoneally injected to reduce inflammation. The mouse was put on a controlled heating pad, and the temperature was maintained at 37 °C (ATC1000, World Precision Instruments, USA) (Figure 3.1A). The scalp was shaved and cleaned with 70% ethanol followed by an incision, and the surface of the skull was cleaned with 10% povidone-iodine (Dynarex, USA) and 3% hydrogen peroxide solution (Sigma-Aldrich, Germany).

A craniotomy (Figure 3.1D) over the retrosplenial cortex (4 mm in diameter, centered over the midline and -2.0 mm from Bregma) was performed with a high-speed dental drill (Eickemeyer, Germany). To avoid heat-induced damage, the drilling procedure was stopped periodically, and sterile cold saline was applied on the skull during the interval. AAVs were bilaterally injected into the RSC (ML, ± 0.4 mm; AP, -2.0 mm from Bregma) using a 10 μL NanoFil syringe with a 35-gauge beveled needle, attached to an Ultra Micro Pump (UMP3) with Micro 4 MicroSyringe Pump Controller (World Precision Instruments, USA) at a speed of 100 nL/min at two different depths (~ 200 and 700 μm; 500 nL per site)(Drexel et al., 2017; Wang et al., 2019). After each injection, the needle was kept in place for five minutes before it was slowly withdrawn (Figure 3.1B).

A 5-mm in diameter circular glass coverslip (Thermo Fisher Scientific, Germany) was then used to cover the craniotomy sealed by cyanoacrylic glue. A custom-built 3D printed metal head-plate (Figure 3.1C; i.materialise, Belgium) was implanted on the exposed skull with cyanoacrylic glue and dental acrylic (Paladur, Heraeus Kulzer, Germany). After recovery from anesthesia, mice were returned back to homecage, and training began one week after surgery. Mice were treated once per day with carprofen to prevent inflammation and reduce pain (5 mg/kg body weight, i.p.) for the first three days following surgery.

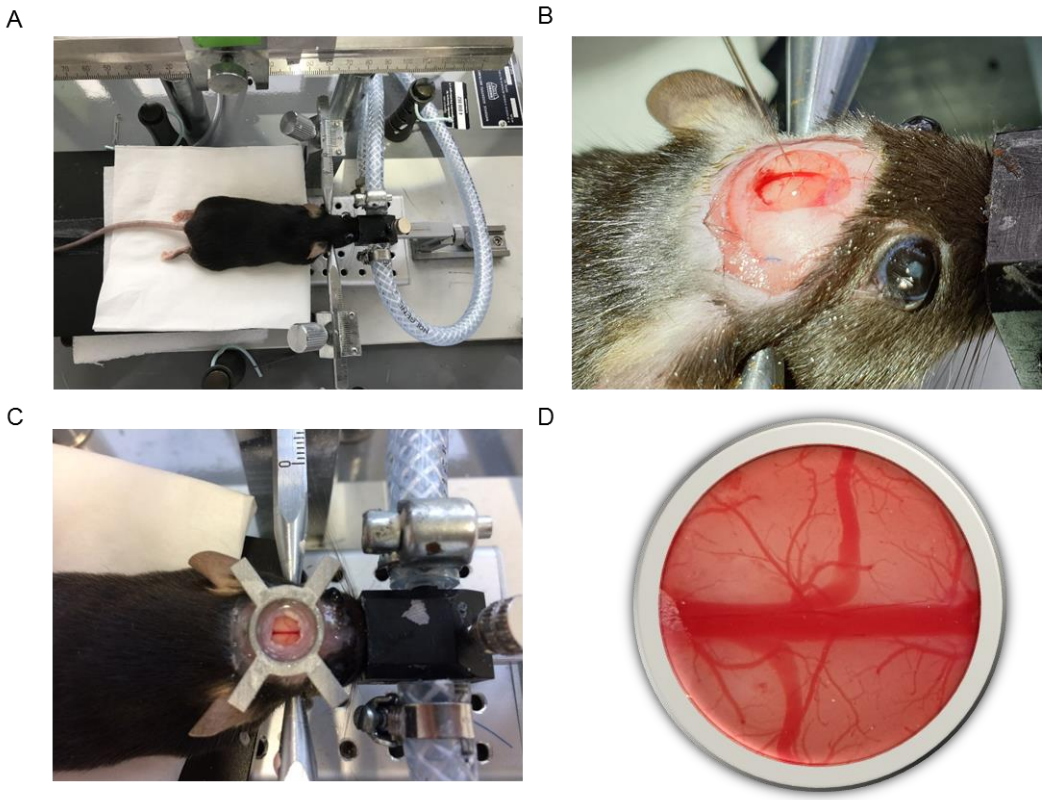

Figure 3.1 | Surgical procedures.

A. Surgery was performed with mouse fixed in the stereotaxic apparatus and anesthetized by 1.5-2% isoflurane with 0.4 L/min O_2. B. A 4-mm diameter craniotomy over the RSC was carefully made using a high-speed dental drill, and AAVs were bilaterally injected into the RSC using a 10 µl NanoFil syringe with a 35-gauge beveled needle at a speed of 100 nl/min at two different depths (~ 200 and 700 µm; 500 nl per site). The needle was kept in position for 5 min before it was withdrawn after each injection. C. The craniotomy was then covered with a circular glass coverslip (5 mm in diameter) and sealed with cyanoacrylic glue. A custom-built 3D printed metal head-plate was then implanted on the exposed skull with cyanoacrylic glue and dental acrylic. D. Representative image of the cranial window for *in vivo* two-photon imaging.

3.3. Virtual reality setup

The VR system and environment were modified from previous studies (Fuhrmann et al., 2015; Hainmueller and Bartos, 2018; Harvey et al., 2012). Experiments were performed using a JetBall-TFT VR system (PhenoSys, Berlin, Germany), which consisted of a TFT surround

monitor system (6 monitors) (Figure 3.2C) covering ~270° of the horizontal visual field of the mouse and an air-cushioned spherical treadmill (Figure 3.2A) with two XY-motion sensors that translate the movements of the sphere into VR coordinates (Figure 1b), with a gain of 1 (physical distance to VR distance). The VR system recorded the XY-coordinates at a 100 Hz sampling rate via two optoelectronic XY-sensors with direct USB connection, and mean running speed was calculated from recorded data using custom-written code (MATLAB, MathWorks, MA, USA).

A retractable reward spout, equipped with a licking sensor and connected to a peristaltic pump, was put into position when animals arrived at a specified VR location for every trial (regardless of whether a reward was dispensed or not) and was retracted either 1.5 seconds after the dispensing of the reward or after 1.5 seconds if no reward was given. A 4 µL droplet (10% sucrose in water) was dispensed on reward trials if the animal licked at the pre-defined reward position (Figure 3.2B).

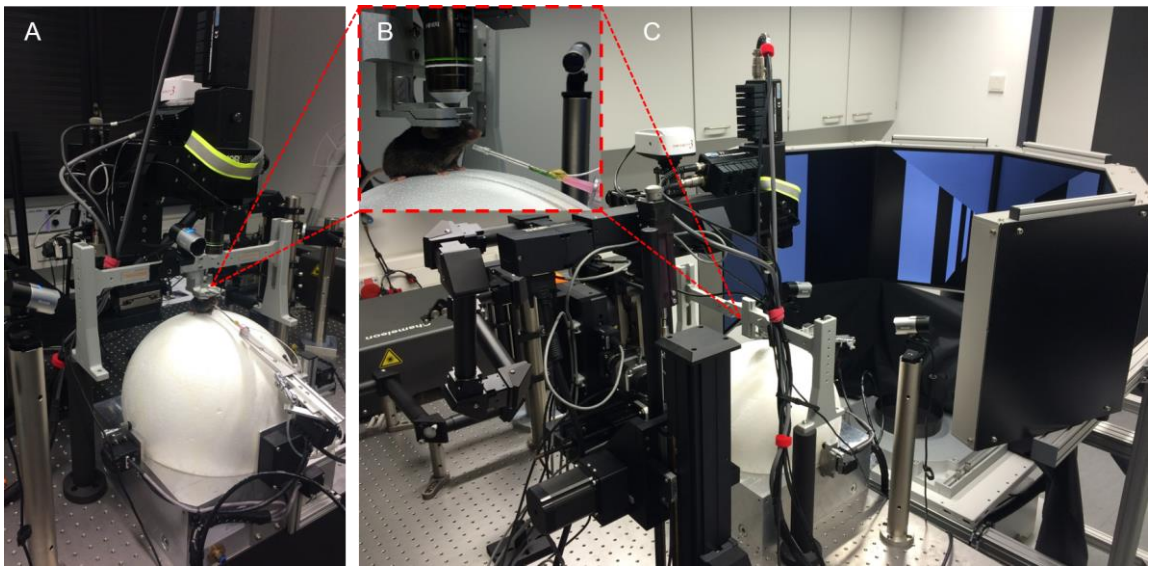

Figure 3.2 | Virtual reality setup.

A. The mouse was head-fixed and was able to run on an air-cushioned spherical treadmill with two XY-motion sensors that translate the movements of the sphere into VR coordinates. **B**. A retractable reward spout, equipped with a licking sensor and connected to a peristaltic pump, was put into position when animals arrived at a specified VR location for every trial (regardless of whether a reward was dispensed or not) and was retracted either 1.5 seconds after the dispensing of the reward or after 1.5 seconds if no reward was given. **C**. JetBall-TFT system which consists of a TFT surround monitor system (6 monitors) covering ~270° of the horizontal visual field of the mouse and an air-cushioned spherical treadmill.

PhenoSys software was used to establish and perform the presentation of the VR environment and record the related behavioural data (PhenoSys, Berlin, Germany). Three linear virtual corridors were used in this study (context 1, context 2, and context 3), which each consisted of different visual stimuli along the virtual corridor walls (Figure 3.3). The total length of each corridor was 200 cm, and the potential reward position was located at 180 cm from the starting point. After the reward spout retracted for each trial, the screens turned to black for 3 seconds as an inter-trial interval (ITI), and the animal was 'teleported' back to the starting point of the linear track for the next trial. The interval of 10 cm before the reward position (i.e., 170-180 cm) was defined as the anticipation zone.

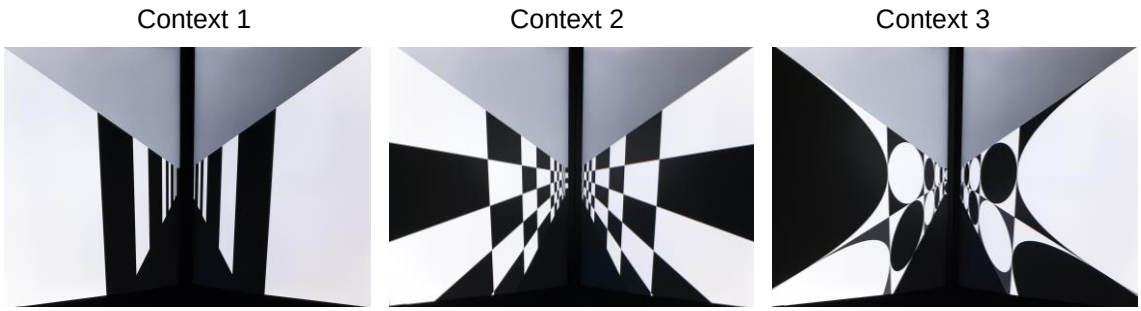

Figure 3.3 | Three linear corridors established in virtual reality.
Snapshots of the three contexts used in the study for the mice to discriminate, two monitors in the middle were shown here.

3.4. Behavioural training

The experimental schematic is shown in Figure 3.4A. After surgical procedures, mice were housed individually with food and water available *ad libitum*, and seven days were given for recovery. The initial habituation to the recording environment and pre-training for reliable running performance began one week after surgery. Mice were head-fixed at the same height as the center of the TFT monitors and able to move freely for 1 hour/day on the spherical treadmill (30 cm diameter; Phenosys, Berlin, Germany) in darkness without any virtual environment presented (Figure 3.4B). Mice were water-restricted (1.5 ml of water/day) from the first day of pre-training to the end of the experiment and weighed daily to ensure they were ≥ ~85% of their pre-water-restriction weight. During pre-training sessions, water was given via the reward spout, so the mice associated licking the spout to receiving a water reward. After 14 days of pre-training (~3 weeks after cranial window surgery and AAV injection), mice showed

fast, straight, and constant running on the spherical treadmill, and the experimental protocol and imaging began.

The experimental design and timelines are shown in Figures 3.4C-F. In the first set of experiments (baseline and control), on the first imaging day (day 1; baseline recording), each of the three virtual corridors was presented for 20 trials in a random sequence without any reward (reward spout was not extended). During subsequent learning sessions (day 2-3), contexts 1 and 2 were randomly presented for 40 trials each, and the reward spout was extended for each context, but the water reward was given only during context 1 trials at the fixed reward position (180 cm). The following day was a test session (day 4), in which all three contexts were presented for 15 trials each, and water reward was given only in context 1, as during the previous learning sessions.

After this initial learning phase (day 2-4), reversal learning sessions were performed (day 5-6), in which context 1 and 2 were randomly presented again, but the rewarded context was reversed from context 1 to context 2; this was followed by a reversal test session (day 7) where all three contexts were presented, and the water reward was still given for context 2 trials only (Figure 3.4D). For the control experiments, CNO (10 mg/kg, 0.1 ml/10 g, body weight) was applied (i.p.) 15 min prior to the virtual environment presentation on each day except for the baseline day (day 1) (Figure 3.4E).

For the inactivation experiments (DREADDs), the experimental timeline was derived from the same scheme, but with modifications to dissect the role of the RSC in acquisition versus recall of memories (Figure 3.4F). Here, initial learning sessions were first performed in the presence of CNO (day 2-4), then behaviour was tested (day 5). The next learning sessions were done in the absence of CNO (day 6-7), and mice were tested again without (day 8) and with (day 9) CNO to examine the effect of neuronal inhibition during memory formation processes. This procedure was then repeated during reversal learning (learning day 10-12 with CNO; testing day 13; learning day 14-15 without CNO; testing day 16 with and day 17 without CNO) to determine the effects on recall of formed memories. For the days without CNO application, the same volume of 0.9 % NaCl was injected (i.p.) as control.

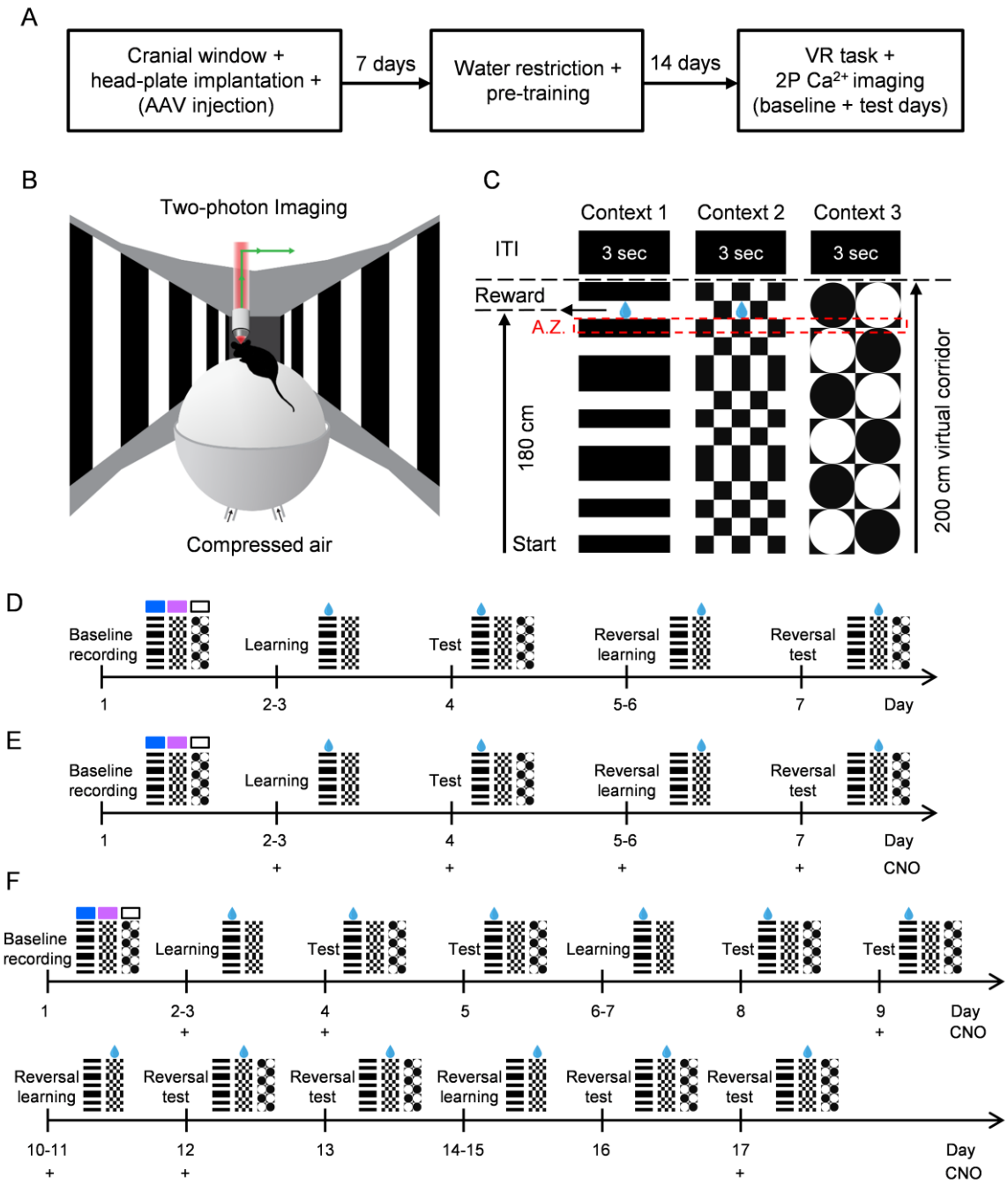

Figure 3.4 | Experimental scheme.

A. Experimental timeline for chronic cellular calcium imaging of the RSC. **B**. Scheme of the VR system for awake-behaving two-photon imaging. Mice were head-fixed above an air-cushioned spherical treadmill driving the virtual environment through a rotary encoder. The environment was displayed on a TFT surround monitor system (6 monitors) covering ~270° of the horizontal visual field of the mouse. **C**. Illustrations of the three contexts used. Three 200-cm virtual corridors were created with different visual patterns on the virtual corridor walls as different contexts, and a sucrose water reward (blue drop) was given at a fixed reward position

(180 cm) either in context 1 or in context 2. Screens were turned to black for 3sec as the inter-trial interval (ITI). 10 cm before the reward position (180 cm) was defined as the anticipation zone (A.Z.), indicated in red. **D**. Timeline for baseline experiments. Visual patterns indicate contexts 1-3 (C1-3), and the blue drop indicates the water reward. **E**. Timeline for control experiments. CNO application is indicated by "+". **F**. Timeline for DREADDs experimental group.

3.5. In vivo two-photon calcium imaging

Two-photon calcium imaging was performed using a resonant scanning two-photon microscopy (B-scope; Thorlabs, USA), and a Ti: Sapphire pulsing laser (Chameleon Ultra II, Coherent, USA) tuned to 920 nm. GCaMP6f fluorescence emission was isolated by a band-pass filter (525/50, Semrock, USA) and detected by a GaAsP photomultiplier tube (Hamamatsu, Germany). Images were acquired through a 20x water immersion objective (1.00 N.A.; Olympus, Japan) with a frame rate of 14.7 Hz (real-time averaging by 4) for bidirectional scanning at a resolution of 256 x 256 pixels (300 x 300 µm field of view) and controlled by ThorImageLS imaging software (version 2.4). In order to prevent light leakage from the VR displays into the microscope, a custom-made black foam ring was used between the microscope objective and the head-plate. Imaging and behavioural data were synchronized by custom-written code (MATLAB, MathWorks, MA, USA). Images were collected at a single L2/3 focal plane per animal at cortical depths between 120 and 180 µm, and the same RSC region was imaged across multiple days (Figure 3.5).

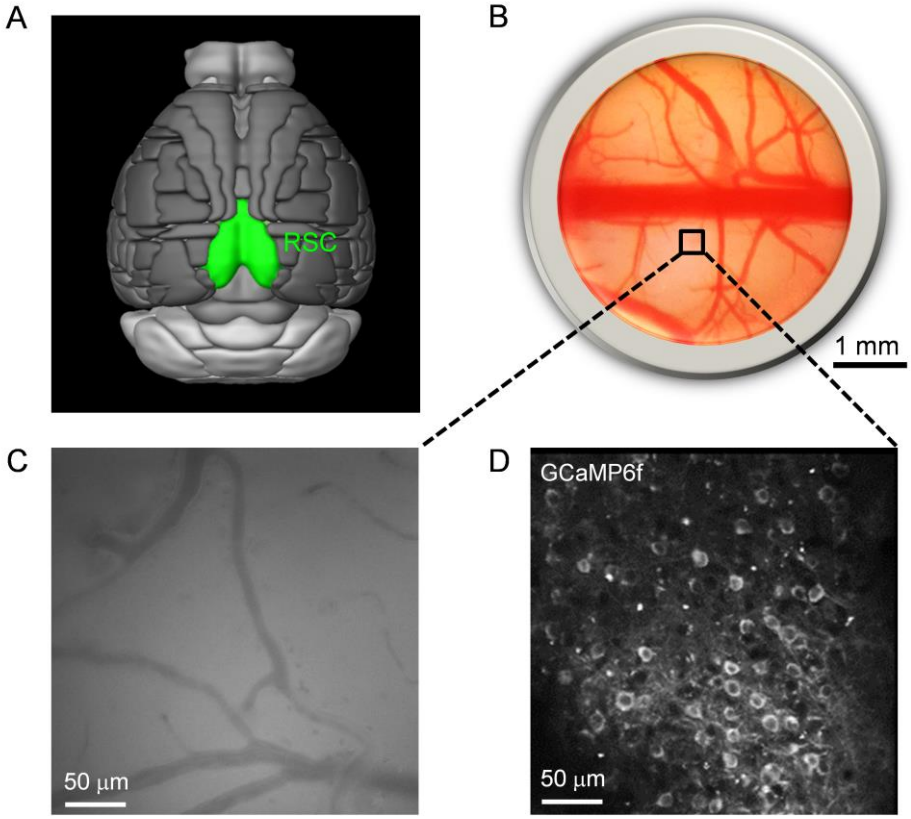

Figure 3.5 | In vivo two-photon calcium imaging.

A. Schematic showing the site for imaging highlighted in green (RSC) based on the Allen Institute's 3D mouse brain atlas. **B.** The cranial window for imaging and exemplary field of view for imaging. Two-photon imaging was performed in the dysgranular RSC. **C.** Snapshot of the brain surface in the imaging field of view. **D.** Exemplary image of GCaMP6f-expressing neurons in layer 2/3 of the RSC in Thy1-GCaMP6f transgenic mouse. Images were collected at a single L2/3 focal plane per animal at cortical depths between 120 and 180 µm, and the same RSC region was imaged across multiple days.

3.6. Histology

Procedures for histology were performed based on previously used protocols (Kaushik et al., 2018; Matuszko et al., 2017). After all the behavioural and imaging experiments were completed, each mouse was deeply anesthetized with isoflurane (Baxter, Germany) in a chamber and then transcardially perfused first with 0.1 M phosphate buffer saline (PBS, pH 7.4) for 10 min at the speed corresponding to 2-3 times quantify of its body weight by the 10-min-

perfusion, followed by 4% phosphate-buffered paraformaldehyde (PFA) for 10 min at the same speed.

After perfusion was finished, the brain was carefully removed from the mouse and postfixed for 24 h in 4% PFA at 4°C. The brain was then transferred to a 30% sucrose solution until the solution had infiltrated into the whole brain (~48 h) in order to cryoprotect the tissue. Afterward, the brain was frozen in 100% 2- methylbutan (kept at -80ºC) and stored at -80ºC until sanctioning.

Forty micrometer-thick coronal sections were cut using a cryostat (Leica CM1950, Germany). Floating sections were kept in cryoprotection solution (one part of ethylene glycol (Carl Roth, 6881), one part of glycerine (Carl Roth, 3783), and two parts of 1x PBS (Life Technologies, 10010056), pH 7.4). For staining, sections were first washed in phosphate buffer (PB; 3x 10 min, at room temperature (RT) with gentle shaking) and then permeabilized with 0.5% Triton X-100 (Sigma-Aldrich, T9284) in PB for 10 min at RT. Next, the sections were incubated for one h (at RT with gentle shaking) in a blocking solution containing 5% normal donkey serum (NDS, Jackson ImmunoResearch, 017-000-121), 0.4% Triton X-100 and 0.1% glycine in PB. Afterward, sections were incubated for 48 h (at 4ºC with gentle shaking) with the primary antibodies (see Table 3.1) in blocking solution.

The slices were then washed 3x 10 min at RT in PB and incubated on a shaker for 3 hours at RT with the secondary antibodies (see Table 3.1). Afterward, the sections were washed 3x 10 min at RT with washing buffer and 1x 10 min at RT with PB and mounted on SuperFrost glasses (Thermo SCIENTIFIC, J1800AMNZ) with Fluoromount medium (Sigma-Aldrich, F4680). Images were acquired using a confocal laser-scanning microscope (LSM 700, Carl Zeiss, Germany) and Zen software (Carl Zeiss, Germany). Images were processed using ImageJ software.

Primary antibodies	Catalogue # and supplier	Dilution, incubation time
Chicken polyclonal anti GFP	ab13970, abcam	1:500, 48h at 4ºC
Goat polyclonal anti mCherry	AB0040-200, SICGEN	1:200, 48h at 4ºC
Mouse monoclonal anti NeuN	MAB377, Merck Millipore	1:500, 48h at 4ºC
Secondary antibodies	**Catalogue # and supplier**	**Dilution, incubation time**
Alexa Fluor 488 Donkey anti chicken	703-545-155, Jackson ImmunoResearch	1:500, 3h at RT
Alexa Fluor 568 Donkey anti goat	Ab175704, abcam	1:500, 3h at RT
Alexa Fluor 647 Donkey anti mouse	A31571, ThermoFisher	1:500, 3h at RT

Table 3.1 | Primary and secondary antibodies used for histology.

3.7. Data analysis

3.7.1. Two-photon calcium imaging

Two-photon imaging data sets were acquired during days 1 (baseline), 4 (after learning), and 7 (after relearning) for control experiments, where 200 to 300 neurons from 5 mice were analyzed. Motion artifacts were corrected for by a technique based on nonlinear optimization and discrete Fourier transform (DFT) in low noise imaging (Guizar-Sicairos et al., 2008) for the case of uniform motion artifacts, where the quality of image registration was assessed using normalized root-mean-square (NRMS) between reconstructed and reference images (Fienup, 1997) using the first image frame as the reference. Alternatively, we used a template matching method that split the field-of-view into spatially overlapping patches according to user-determined

dimensions, registered corresponding patches of the template separately and then merged the registered sub-patches to each other (Pnevmatikakis and Giovannucci, 2017) for the case of non-uniform motion artifacts. Image registration quality was measured by the image crispness defined as the Frobenius norm of image gradient vector and image magnitude (Figure 3.6).

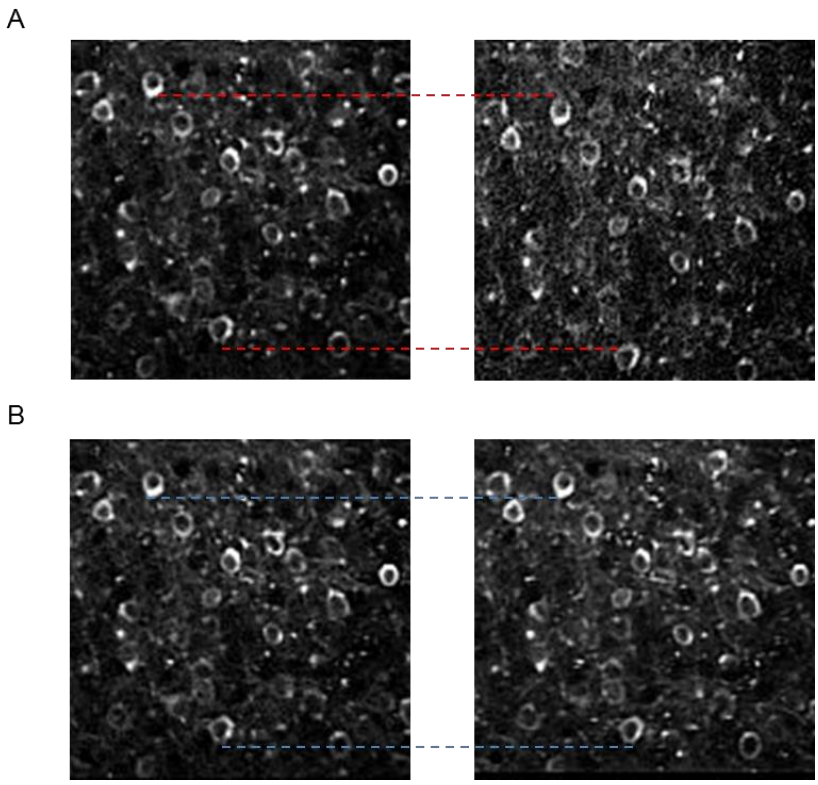

Figure 3.6 | Motion correction of the recorded images.

A. Raw images without motion correction. On the left panel is the average projection of the first 200 images from one recorded session, whereas the right panel is the average projection of the last 200 images from the same session. As is shown, the imaged position moved. **B.** The same set of images after motion correction. On the left panel is the average projection of the first 200 images from one recorded session, whereas the right panel is the average projection of the last 200 images from the same session. After motion correction, all cells keep in the same position as the images required at the beginning of the same session.

To measure the neuronal changes in fluorescence, I used a method that automatically identifies somatic ROIs (including spatially overlapped ones), de-noises, and de-convolves spiking activity (Pnevmatikakis et al., 2016) with open source and adapted MATLAB code (MathWorks, MA, USA). Briefly, this method uses constrained non-negative matrix factorization (cNMF) to isolate spatially and temporally independent fluorescent signals, approximating a parametric model for continuous time-series calcium transients as the impulse

response of an autoregressive process, and then estimates the spiking signal from the sparsest non-negative neural activity signal. This method can de-noise the spatiotemporal imaging set and model the background activity in each image frame by averaging the spatiotemporal background over ROIs. The temporal trace of each ROI was expressed as ΔF/F, raw fluorescence trace divided by background activity. The default parameters were used with few exceptions (the order of AR process *p* was set to 2, temporal downsampling factor "tsub" was set to 4, spatial downsampling "ssub" was set to 2). Between 50 and 70 ROIs corresponding to the somata of neurons were identified per animal per session using this approach after manual confirmation (Figure 3.7).

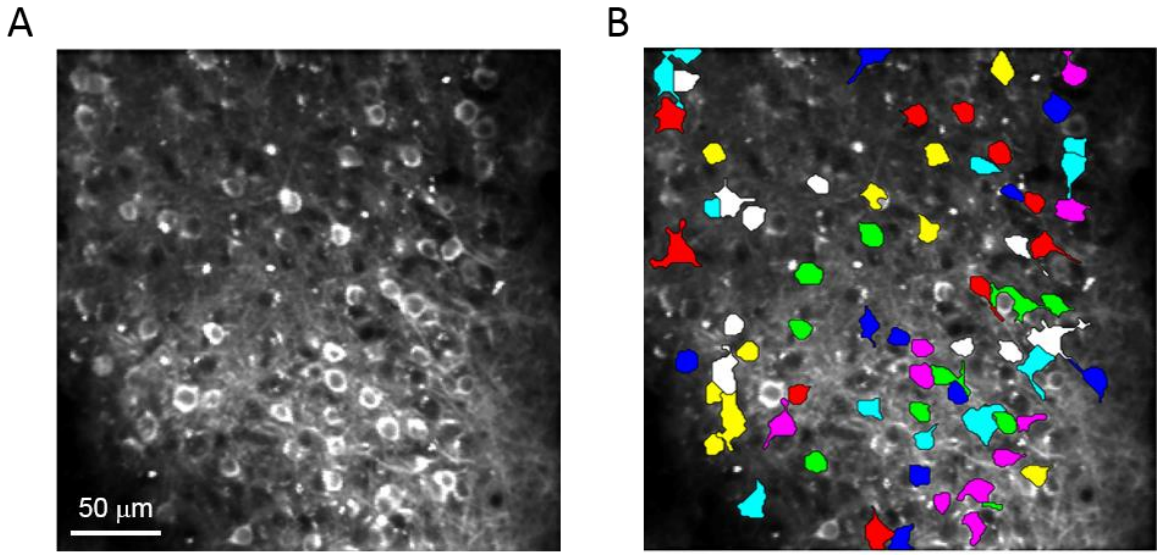

Figure 3.7 | Automatic detection of neurons.
Constrained non-negative matrix factorization (cNMF) was used to isolate spatially and temporally independent fluorescent signals to detect ROIs. **A**. Mean projection of images from one recording session after motion correction. **B**. Detected cells are color-coded.

3.7.2. Position and speed decoding

To analyze the position and speed decoding, changes in fluorescence (ΔF/F) signals were synchronized with recordings of position and speed in the virtual environment (Figure 3.8). A linear regression model with backward stepwise method selection of neurons (XLSTAT, Addinsoft) was used for decoding of the relationship between neuronal activities (ΔF/F values) and the animal's position in a defined virtual context, i.e., the position was predicted by a linear

combination of ΔF/F values with weights that were optimized using the least-squares fitting. In the backward stepwise method, initially, all cells are included in the regression model, and then cells contributing the least to the position prediction are removed one-by-one until the reduction in residual variance was significant ($P<0.05$). To unify analysis for different trials, the position was represented by 18 consecutive position bins, 10cm-long each, and ΔF/F values within one position bin were averaged. Corrected R^2, which corresponds to the fraction of the dependent variable (i.e., distance) variance that is explained by the linear model, was used as a standard measure to report the fitting quality.

Further, the contributions of each neuron to the prediction of position were estimated by type III sum of squares analysis, and neurons with $P<0.05$ were identified as position-encoding cells. Similarly, we performed decoding of the animal's speed after averaging of ΔF/F for speed bins of 10 cm/s using the same procedures. The position and speed decoding analyses were performed separately for each context and experimental day and the outcomes were combined for the analysis of individual cell properties, i.e. to determine if a cell was significantly contributing to encoding of position or speed or both, and if it was contributing to encoding of position or speed in none, 1, 2, or 3 contexts. To validate the quality of the linear regression model, we performed regression analysis after randomly shuffling position and speed bins in each data set.

To categorize speed encoding cells, the averaged preferred speed for all trials was first calculated as below:

$$\overline{V_j} = \frac{\sum_{i=1}^{40} Speed_i * Activity_i}{\sum_{i=1}^{40} Activity_i}$$

Where *i* is *i-th* speed bin and *j* is *j-th* trial in a cell. Speed cell categorization was then set based on the distribution of speed cells and the cumulative probability as a function of mean speed (30% of cells with the slowest speeds were classified as "slow speed"; 30% of cells with the fastest speeds were classified as "fast speed"; the rest 40% was "medium speed" cell).

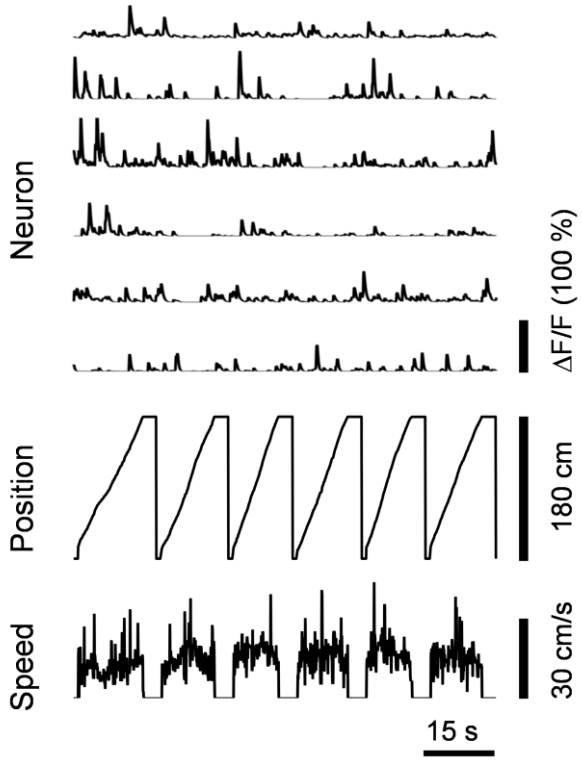

Figure 3.8 | Changes in fluorescence (ΔF/F) signals were synchronized with recordings of position and speed in the virtual environment.

3.7.3. Place cell analysis

Place cells were identified using a previously published approach (Mao et al., 2017; Mao et al., 2018). Briefly, ΔF/F per spatial bin was first averaged, and then the data was filtered with a Gaussian smoothing window of 1 spatial bin width to create position activity maps. Maps of the position activity were then averaged across all trials per day per context to estimate position-tuning-curves and to find the position bin containing the global maximum. The initial threshold was set to 30% of the gap between the highest and lowest activities of the position-tuning-curve. To be included, place fields had to be a continuous area with a minimum of 10 cm and a maximum of 120 cm width. Finally, the mean in-field activity had to be at least three times higher than the mean out-of-field activity, and the position of the global maximum was required to be the same in >30% trials.

3.7.4. Context decoding

Discriminant analysis with backward stepwise cell selection was used for context decoding and categorization of context-encoding neurons (the type III sum of squares analysis, $P<0.05$). A cross-validation method was used to estimate the accuracy of context decoding. The context information in the neuronal activity data set was also randomly shuffled, analogously to that done for the evaluation of results provided by linear regression analysis. Also, two context modulation indices were computed to compare neuronal activities (ΔF/F) of context-encoding cells in contexts 1 and 2 ($context_i$), or to relate these activities to the neutral context (context 3):

$I)$ $\left|Signal_{context_1} - Signal_{context_2}\right| / \left(Signal_{context_1} + Signal_{context_2}\right)$,

II) $\left|Signal_{context_i} - Signal_{context_3}\right| / \left(Signal_{context_i} + Signal_{context_3}\right)$.

3.7.5. Visual encoding cell analysis

To search for visual feature-encoding neurons in the RSC, we described the VR environments by the simple dark-to-light transition (DLT) functions having the value 1 at the spatial bins in which there was a dark-to-light transition in the VR environment and value 0 at other spatial bins. Then a cross-correlation function was computed between the DLT functions and activities of single neurons (averaged ΔF/F values across all trials per day per context). Considering that our VR environments were composed of repeated elements, resulting in periodic DLT functions, the cross-correlation functions were computed for time lags in the range between -3 to +3 bins (corresponding to the period of the slow-changing DLT function in the context 3). The maximal value of the Pearson coefficient of cross-correlation was used to determine at which lag the best fit between neuronal activity and the DLT function is achieved, and the ΔF/F signal was accordingly aligned (Figure 3.9). A cell was classified to be visually responsive if it has the maximal coefficient of cross-correlation significantly different from 0 with $p<0.05$ (after Bonferroni correction for multiple comparisons) and at least two peaks aligned with one of 3 DLT functions.

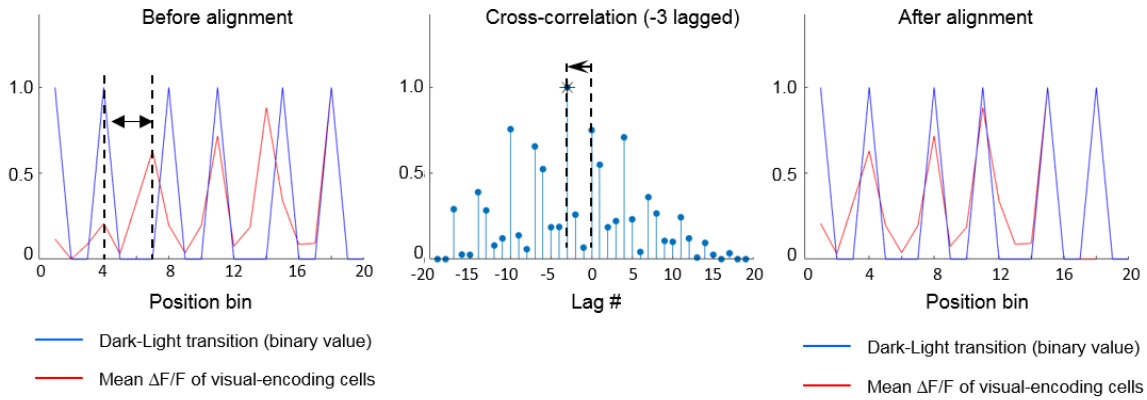

Figure 3.9 | Alignment of ΔF/F signal with DLT function.

The maximal value of the Pearson coefficient of cross-correlation was used to determine at which lag the best fit between neuronal activity and the DLT function is achieved, and the ΔF/F signal was accordingly aligned.

3.7.6. Statistics

In this study, unless indicated otherwise, all values reported represent mean + SEM with n indicating the number of animals. All statistical comparisons were performed using SigmaPlot (version 13; Systat Software, USA) and described in the corresponding figure legends. In figures, "*" and "#" were used to indicate statistical significance (P presents the level of statistical significance, $^{*}P < 0.05$, $^{**}P < 0.01$, $^{***}P < 0.001$; $^{\#}P < 0.05$, $^{\#\#}P < 0.01$, $^{\#\#\#}P < 0.001$) and "+" indicates high tendency for statistical significance with exact P-value provided in figure legends.

4. RESULTS

4.1. Context discrimination in a virtual environment

To study the specific role of the RSC in different phases of learning and memory as well as reversal learning, I established a context discrimination paradigm in virtual reality where mice learned to associate a water reward with a specific location in a particular context. The paradigm provided the possibility to examine the contribution of the RSC to the formation of memory as well as the retrieval of recent memory.

To investigate neuronal activity in the RSC during context discrimination, Thy1-GCaMP6f transgenic mice were implanted with cranial windows, head-fixed, and pre-trained to run on an air-cushioned spherical treadmill reliably. I then performed two-photon Ca^{2+} imaging in the dysgranular retrosplenial cortex in layer 2/3, while mice performed a contextual discrimination task in a VR environment. Three contexts, with identical geometry (2-meter long linear maze/corridor) but unique visual patterns on the virtual corridor walls, were presented to the animals in a random sequence for several days. In the rewarded context for that day, a water reward was given at a fixed location (180 cm from the beginning of the corridor).

Via the cranial window, changes in fluorescence ($\Delta F/F$) were imaged using the genetically encoded calcium indicator GCaMP6f, and signals were analyzed as a function of context, position, and speed during the sessions in the VR environment.

First, I validated that mice can learn to discriminate between the different VR contexts. When a context was rewarded, animals decreased their speed in the anticipation zone (10 cm before the water reward is given) in preparation to consume the water reward (Figure 4.1).

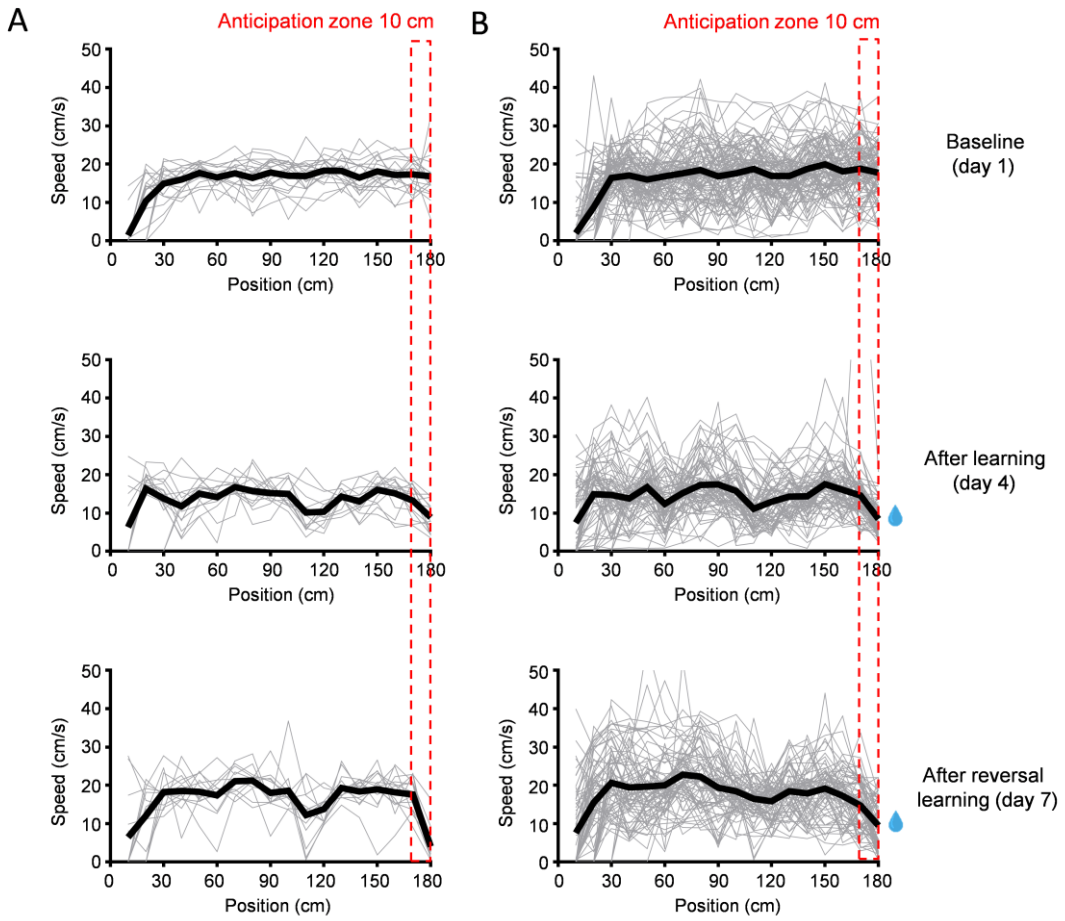

Figure 4.1 | Running speed as a function of position in the VR environment.
A. The speed of each trial (grey lines) and the mean speed of all trials (black) from one animal in the control group are shown. Top: speed on baseline day for all contexts; middle: speed in rewarded context (context 1) during learning [day 4]; bottom: speed in rewarded context (context 2) after reversal learning [day 7]. Blue water drop indicates reward and the anticipation zone before the potential reward is outlined in red. **B**. The speed of each trial (grey lines) and the mean speed of all trials (black) from all five animals in the control group are shown.

This was reproduced in two experimental groups, one in mice with no additional AAV injections (Figure 4.2A, 4.2B) and another with a control AAV injected bilaterally in the RSC and clozapine-N-oxide (CNO) systemically injected (i.p.) on days except on day 1 (Figures 4.2C, 4.2D).

In both groups, on the baseline day, which is the first day of exposure to the VR environment (day 1), when no rewards were given, we found that mice moved through the anticipation zone with approximately the same speed across all three contexts. Conversely, even on the first day of training with a single rewarded context (day 2), mice started to slow down in the anticipation

zone of the rewarded context (i.e., context 1) when compared to the non-rewarded context (i.e., context 2; Figures 4.2B, 4.2D). This reduction became significant in the next training day (day 3). On test day (day 4), when the neutral context never paired with a water reward (context 3) was presented again as on baseline recording day (as it was not shown during the formation of the context-reward association), mice discriminated this context and the non-rewarded context equally well from the rewarded context during learning (Figures 4.2B, 4.2D). On days 5 to day 7, I probed reversal learning by giving the reward in context 2 rather than context 1 and mice again showed a reduction in speed to the rewarded context in anticipation zone, but not the others (Figures 4.2B, 4.2D).

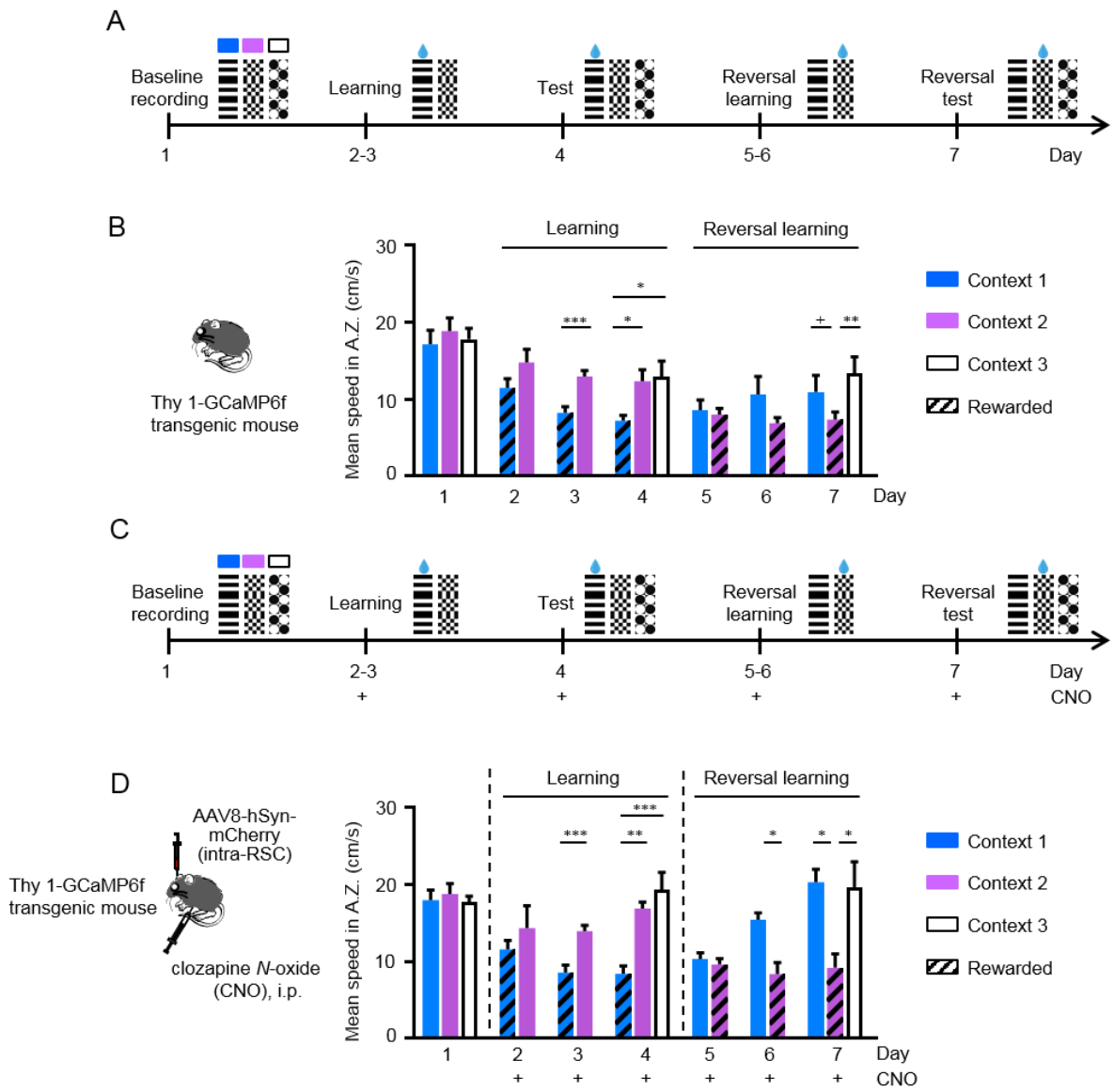

Figure 4.2 | Mice learned to associate the water reward at a specific position in a particular context by a significant reduction of speed in anticipation zone of rewarded context.

A. Timeline for baseline experiments. Contexts 1-3 (C1-3) are indicated by visual pattern, and blue drop indicates the water reward. **B**. Mean running speed in the anticipation zone in the basal experimental group, in which no AAV or drug was applied. Stripe pattern indicates the context that was paired with a water reward. n=6 mice. One-way RM ANOVA and post hoc Holm-Sidak test were used for days 1, 4, and 7. Paired t-test was used for days 2, 3, 5, and 6. *P<0.05, **P<0.01, ***P<0.001; $^{+}$P=0.052. **C**. Timeline for control experiments. CNO application is indicated by "+". **D**. Mean running speed in the anticipation zone for the control experiment where mice were injected with AAV8-hSyn-mCherry and CNO (10mg/kg) was administrated from day 2 to day 7 (indicated by +). Stripe pattern indicates the context that was paired with a water reward. One-way RM ANOVA and post hoc Holm-Sidak test were applied for days 1, 4, and 7; paired t-test was used for days 2, 3, 5, and 6; n=5 mice.

The reward-related reduction in speed was specific for the anticipation zone and not observed when I computed mean speed for the entire virtual corridor (Figures 4.3). These behavioural data demonstrate that mice could initially learn to discriminate between contexts and then flexibly relearn the context values in our VR paradigm.

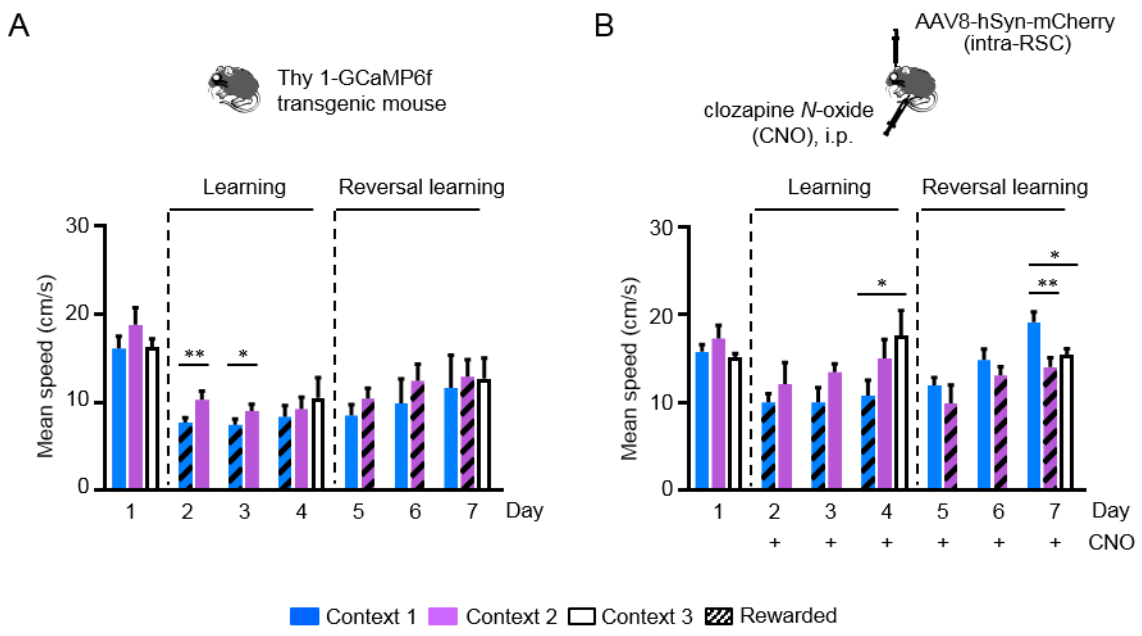

Figure 4.3 | Mean running speed in the corridor is not modulated by context or reward. **A**. Mean running speed along the entire virtual corridor (0-180 cm) in the basal experimental group; n=6 mice. **B.** Mean running speed along the entire virtual corridor (0-180 cm) in the control experimental group, in which mice were injected with AAV8-hSyn-mCherry (mCherry fluorophore control) and CNO (10mg/kg) was administrated on day 2-7 (indicated by +). The

bar graph shows the mean values and SEMs (n=5 mice). For both, the stripe pattern indicates the context that was paired with a water reward. One-way RM ANOVA and post hoc Holm-Sidak test were applied for days when three contexts were presented. Paired t-test was used for days when two contexts were presented. *P<0.05, **P<0.01.

4.2. The role of the RSC in context discrimination acquisition

Next, I used a chemogenetic approach to investigate if the RSC is indeed involved in context discrimination in this paradigm. Furthermore, if the RSC was involved, I wanted to know in which phase of information processing (acquisition, recall, or both) the RSC played a role. Mice were injected with rAAV8/hSyn-hM4Di-mCherry into the RSC to be able to selectively inhibit neuronal activity in this area by systemic administration of CNO (clozapine-N-oxide) (for the viral expression, see Figure 4.4). As previously stated, control animals were injected with rAAV8/hSyn-mCherry (for the viral expression, see Figure 4.4) lacking the inhibitory G-protein-coupled receptor, hM4Di. Note there were no significant differences in the pattern of behavioural responses between animals with no AAV injection (Figure 4.2B) and the control animals that had control AAV injections as well as CNO treatment without DREADD receptor expression (Figure 4.2D); thus, the performance was not affected by rAAV8 transfection or CNO injection alone.

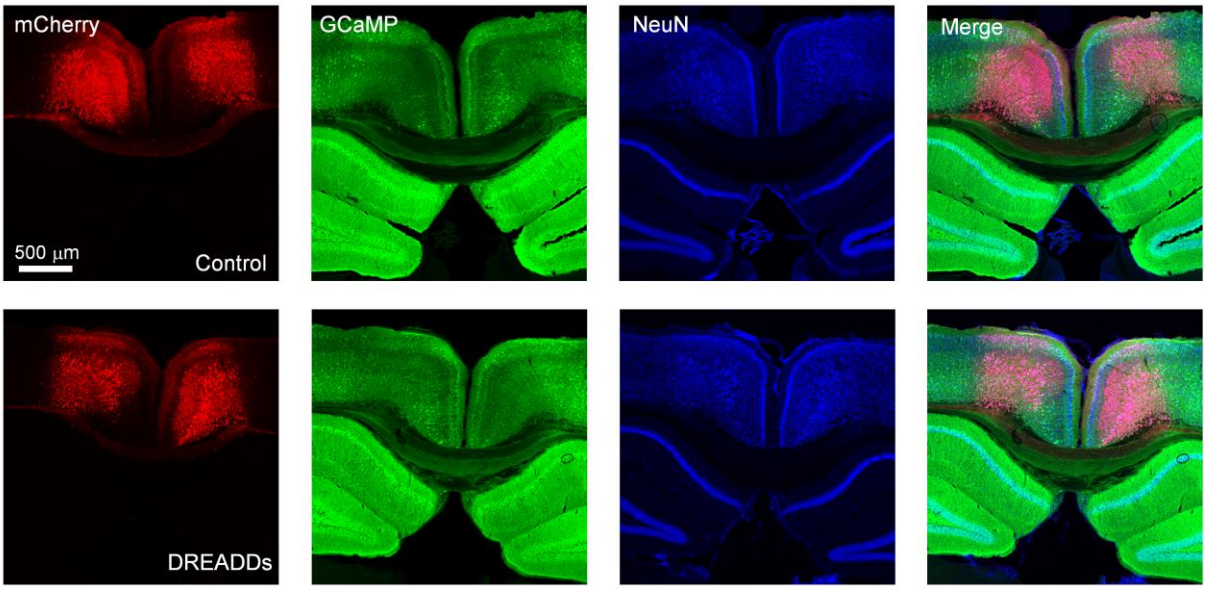

Figure 4.4 | Control and DREADDs viral expression in RSC.

Control virus (rAAV8/hSyn-mCherry) and DREADDs virus (rAAV8/hSyn-hM4Di-mCherry) were expressed throughout the RSC. NeuN (blue), GCaMP6f (green), mCherry (red).

When RSC neuronal activity was inhibited by treating the rAAV8/hSyn-hM4Di-mCherry-infected mice with CNO during learning and initial test days (days 2-4), animals no longer selectively reduced their speed in the rewarded context and, consequently, there were no significant differences in speed between any of the contexts on these initial days (Figures 4.5A, 4.5B). Hence, we found a significant difference in the running speed in anticipation zone for the rewarded vs. the non-rewarded context (context 1/context 2) between the control and DREADDs-expressing experimental groups after CNO treatment on the initial test day (day 4; Figure 4.5C).

Interestingly, although there was no difference in the animal's speed between contexts on this initial test day, we found that mice decreased their speed in the anticipation zone to all contexts after inactivation of the RSC compared to baseline day 1 (Figure 4.5B, 4.5E). This resulted in a significant difference between the control and DREADDs experimental groups when comparing the running speed for the non-rewarded and neutral context, but not the rewarded context (Figure 4.5E). This reward-related reduction in speed was specific in the anticipation zone, as we found no difference between running speed in any context along the length of the entire corridor between the control and DREADD experimental groups (Figure 4.5G).

Thus, with altered RSC activity, mice either failed to discriminate between contexts or failed to associate a particular context with a behaviourally relevant reward, demonstrating instead a positive-value bias, i.e. an inability to specifically assign a negative value to the non-rewarded contexts, instead decreasing their running speed for all contexts (including both rewarded and non-rewarded) as if expecting a positive-value (reward outcome) under all conditions (see Figure 4.5E).

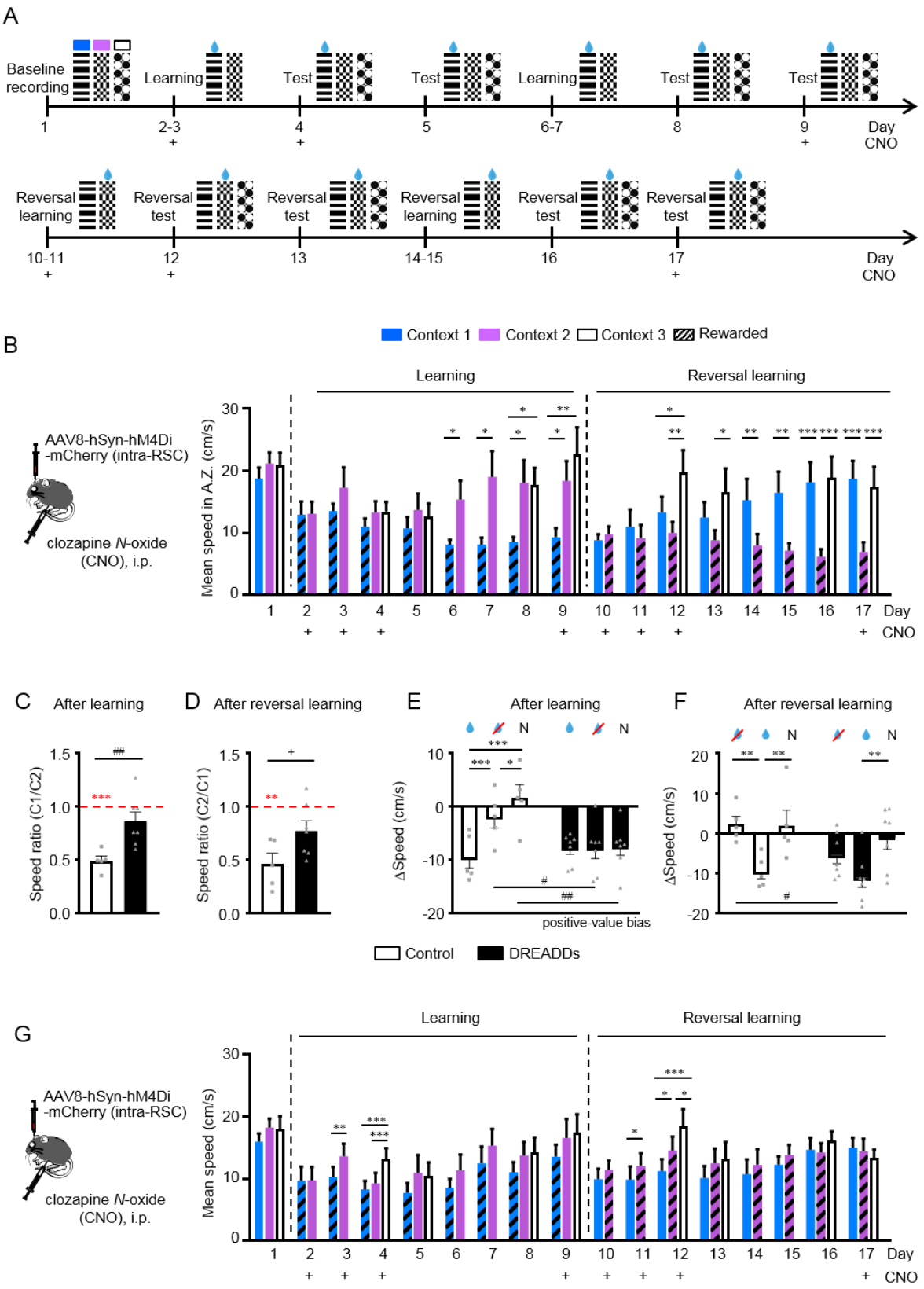

Figure 4.5 | Context discrimination is impaired by the chemogenetic interference in the RSC.

A. Timeline for DREADDs experimental group. **B.** Mean running speed in the anticipation zone is shown for mice injected with AAV8-hSyn-hM4Di-mCherry to express inhibitory DREADDs. CNO (10mg/kg) was applied either during memory formation process (days 2-4 and 10-12) or after the formation of memory (days 9 and 17; indicated by +). One-way RM ANOVA and Holm-Sidak post hoc test were used when three contexts were presented; paired t-test was used for days when two contexts were presented; n=7 mice. **C.** The ratio of speed in anticipation zone between rewarded context (C1) and non-rewarded context (C2) after learning (day 4). **D.** The ratio of speed in anticipation zone between rewarded context (C2) and non-rewarded context (C1) after reversal learning (day 4 for control and day 12 for DREADDs group). (**C-D**) Unpaired t-test was used for comparisons between Control (white; n=5) and DREADDs (black; n=7) groups; one-sample t-test was used to compare to the hypothesized population mean (1.00). **E.** Change in speed normalized to baseline day (day 4-day 1) shows RSC inactivation impairs context discrimination and results in positive-value bias. Rewarded context (blue drop), non-rewarded context (drop with red cross), and neutral context (N). **F.** Change in speed normalized to baseline day (day 7-day 1 for control; day 12-day 1 for DREADDs) shows RSC inactivation impairs the ability to assign a negative value to a previously rewarded context but preserves the ability to assign a negative value to the neutral context (N). (**E-F**) Two-way RM ANOVA and post hoc Holm-Sidak test were used. **G**. Mean running speed along the entire virtual corridor (0-180 cm) for the DREADDs experimental group. In all figures, bar graphs show mean and s.e.m.. For all: *P<0.05, **P<0.01, ***P<0.001; $^{\#\#}$P<0.01; $^{+}$P=0.052.

For the DREADDs experimental group, on day 5, when all three contexts were probed again but now in the absence of CNO, running speed between all contexts continued to remain the same (Figure 4.5B); again, indicating that no effective reward-context association was formed during the previous sessions in the presence of CNO.

I then continued training in the absence of CNO (days 6 and 7), which resulted in significant context discrimination beginning on day 6 and no significant difference between the control (day 4) and DREADDs (day 8) experimental groups by the end of training (Figures 4.5B, 4.6A). These results also confirm the positive-value bias after the inactivation of RSC by within-animal comparison. Specifically, while there was no significant difference in speed within the DREADDs group between any of the contexts on the initial testing day with CNO (day 4; CNO-on), we did find a significant difference in speed between the rewarded and non-rewarded contexts on the testing day without CNO (day 8; CNO-off; Figure 4.6C); indicating that the

animals with DREADD AAV injections could still learn the task if the DREADDs were not activated.

Once this reward-context association was formed, further treatment with CNO during a memory recall probe (on day 9) did not affect the performance of the animals, indicating that altering RSC neuronal activity does not affect context-discrimination performance if an association has already been formed during previous training sessions.

These data clearly demonstrate that these mice can perform the context discrimination if learning was already acquired; hence, DREADDs-mediated inhibition did not affect the ability of the mice to recognize the visual stimuli. Taken together, these data suggest that the RSC is essential for acquisition rather than recall of recent context memories.

Similarly, CNO treatment during reversal learning (days 10-12) also prevented reward-associated context discrimination, which was again reinstated after reversal learning sessions are done in the absence of CNO on days 14-16 (Figures 4.5A, 4.5B). Consequently, similar to the initial learning phase, I found a tendency of difference in the running speed after reversal learning for the rewarded vs the non-rewarded context (context 2/context 1) between the control (day 7) and the DREADDs-expressing (day 12) experimental groups after CNO treatment, however, this did not reach significance (Figure 4.5D). Finally, inactivation of the RSC after reversal learning on the last reversal test day (day 17) did not affect context discrimination (in comparison to day 16; Figure 4.5B), suggesting that the RSC is specifically required for acquisition rather than recall of new values for familiar contexts.

Notably, on the first day of reversal learning while the RSC was inactivated (day 10), mice again reduced their speed in the newly rewarded context 2 to the same level as the previously rewarded context 1. This reward-related reduction of speed was specific to the anticipation zone (Figure 4.5G). Thus, during reversal learning in the presence of CNO mice again demonstrated a positive bias for both rewarded and non-rewarded contexts. However, on the reversal test day during RSC inactivation (day 12) the speed in both the rewarded and non-rewarded contexts were lower than in the neutral context (context 3); indicating that they also recalled that the neutral context was not previously associated with any reward, but they failed to learn that the previously rewarded context 1 was no longer rewarded, i.e., mice failed to update/devalue the previously rewarded context (Figure 4.5F; see also Figure 4.6D for when DREADDs were not activated in these animals and subsequently the previously rewarded context 1 was then devalued).

Considering these results during learning and reversal learning sessions, I suggest that the inactivation of the RSC affects the ability of mice to update the context value to make it negative. This results in a positive bias towards neutral contexts without a previously assigned value and a failure to devalue previously rewarded context while maintaining acquired negative value during reversal learning.

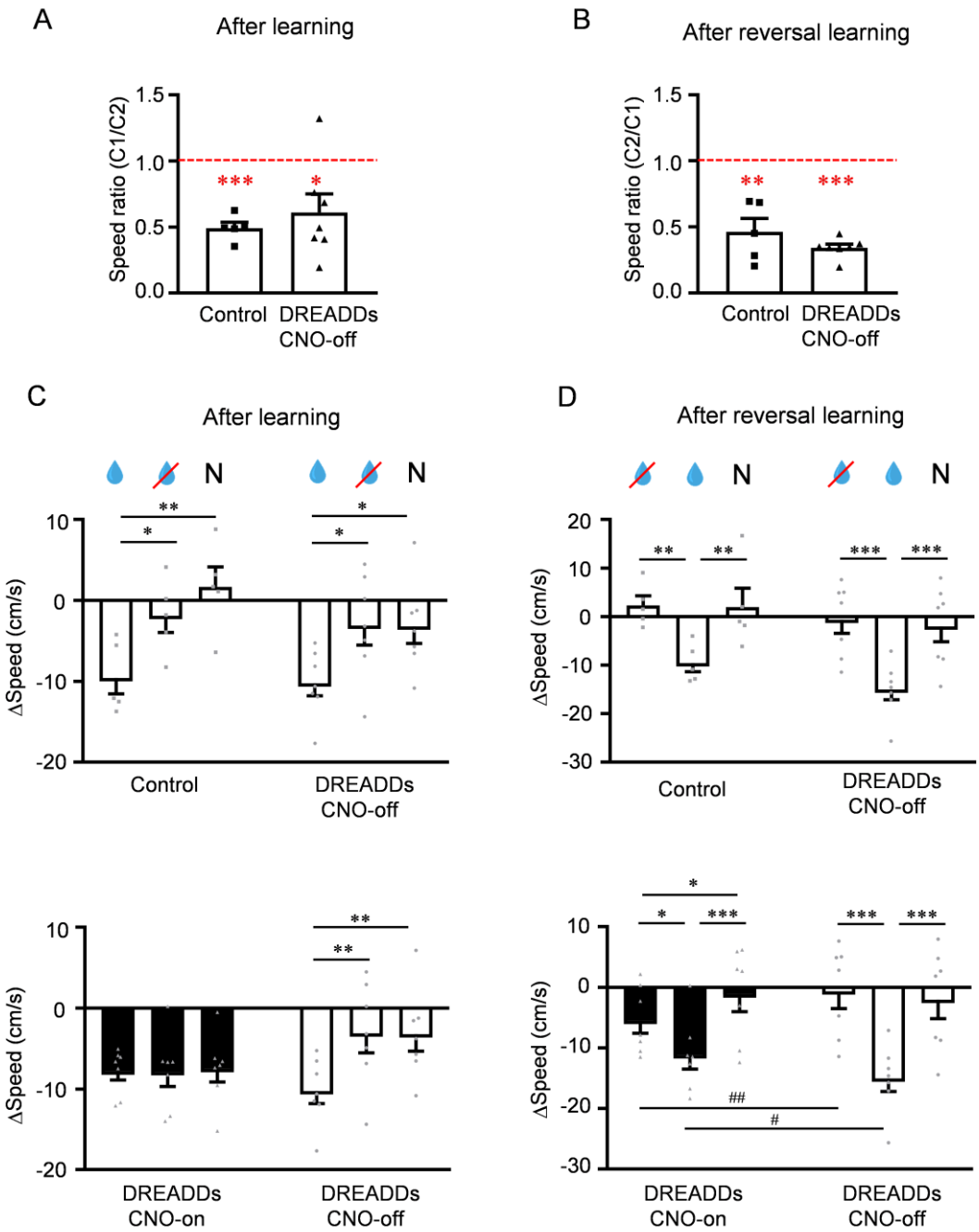

Figure 4.6 | Modulation of speed in chemogenetic experiments.

A. The ratio of speed in the anticipation zone between rewarded context (C1) and non-rewarded context (C2) after learning (day 4 for the control group; day 8 for DREADDs group with CNO-

off). **B.** The ratio of speed in anticipation zone between rewarded context (C2) and non-rewarded context (C1) after reversal learning (day 4 for the control group and day 16 for DREADDs group with CNO-off). Unpaired t-test was used for comparison between groups; one-sample t-test was used to compare to the hypothesized population mean (1.00). **C.** Context discrimination was successfully acquired by the animals injected with the DREADDs AAV once CNO was off as shown by the reduction of mean speed in anticipation zone for the rewarded context only (top: day4-day1 for the control group; day8-day1 for DREADDs group with CNO-off; bottom: day4-day1 for DREAADs group with CNO-on; day8-day1 for DREADDs group with CNO-off). **D.** Reversal learning was achieved by the animals injected with the DREADDs AAV once CNO was off as shown by a reduction of mean speed in the anticipation zone after reversal learning for the newly rewarded context and no change in speed for the non-rewarded and neutral contexts (top: day 7-day1 for the control group; day16-day1 for DREADDs group with CNO-off; bottom: day 12-day1 for DREAADs group with CNO-on; day16-day1 for DREADDs group with CNO-off). For all, control, n= 5 mice; DREADDs, n=7 mice. Two-way RM ANOVA and Holm-Sidak post hoc tests were applied. *P<0.05, **P<0.01, ***P<0.001; $^{\#}$P<0.05, $^{\#\#}$P<0.01.

4.3. Decoding of contextual information

The behavioural data demonstrated that RSC is essential for the acquisition of contextual information related to reward-associated context discrimination. To determine which factors contributed to this function on the single-cell and population level, I examined neuronal activity in the RSC using *in vivo* two-photon calcium imaging. This approach provided the possibility to evaluate how the activities of individual cells and cell ensembles are related to the various contexts during this paradigm in the control group (n = 5; Figure 4.7A).

Indeed, some cells consistently showed specific patterns of activity in only one of the three contexts during repetitive trials (Figure 4.7B). A linear model was used to decode which context the animal was in for each trial from the activity of the imaged RSC neurons before (0-180 cm in VR corridor) and after the time interval when the reward spout was retracted (i.e., during the inter-trial interval, ITI; see Figure 4.7A). Backward stepwise linear discriminant analysis was used to select the model with a minimal number of neurons.

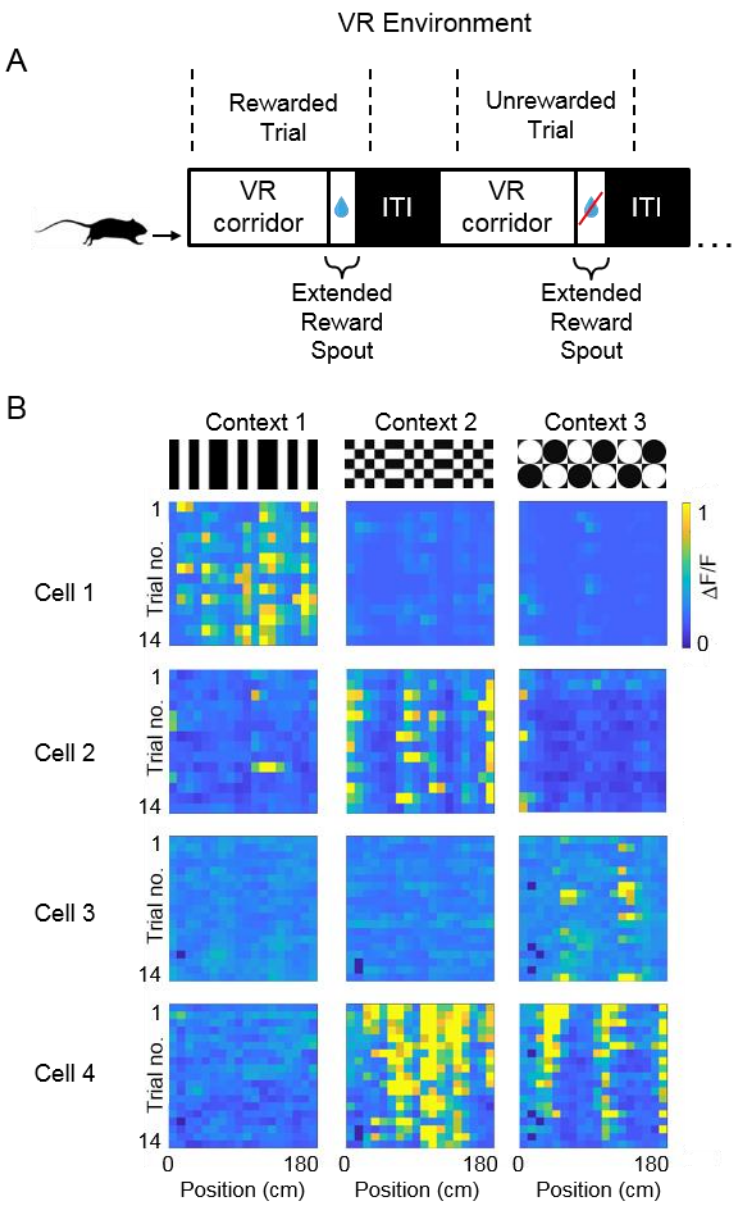

Figure 4.7 | Neurons in the RSC encode context information.

A. Schematic of the trial-by-trial task. Virtual-reality (VR) corridor is presented with a specific context (1-3) followed by a reward (blue drop) or not (drop with red cross) depending on the context, then black screen for 3s-long inter-trial interval (ITI). **B.** Normalized activity (ΔF/F) at positions along the VR corridor (0-180 cm) of four example context-encoding neurons in the RSC across multiple trials.

When taking the average activity across the length of the VR corridor (0-180 cm), I found that the mean accuracy of context decoding was >80%, even before the reward was provided (day 1; Figure 4.8A). This was ≈2-fold higher than the accuracy of decoding for data generated by the random reshuffling of context identity between trials, which was ≈40%, i.e., close to the

chance level (≈33%). There was no difference in the mean accuracy when decoding the context using data along the VR corridor between baseline recordings (day 1) after initial learning (day 4) and after reversal learning (day 7; Figure 4.8A). Additionally, there was no change in the modulation of the neuronal responses between context 1 and 2 (context modulation index; the absolute value of $context_1$-$context_2$/$context_1$+$context_2$) across learning phases (Figure 4.8B), suggesting that the ability of the RSC to discriminate between different contexts is already high in naïve animals and does not change substantially with reward-association (Figure 4.8C).

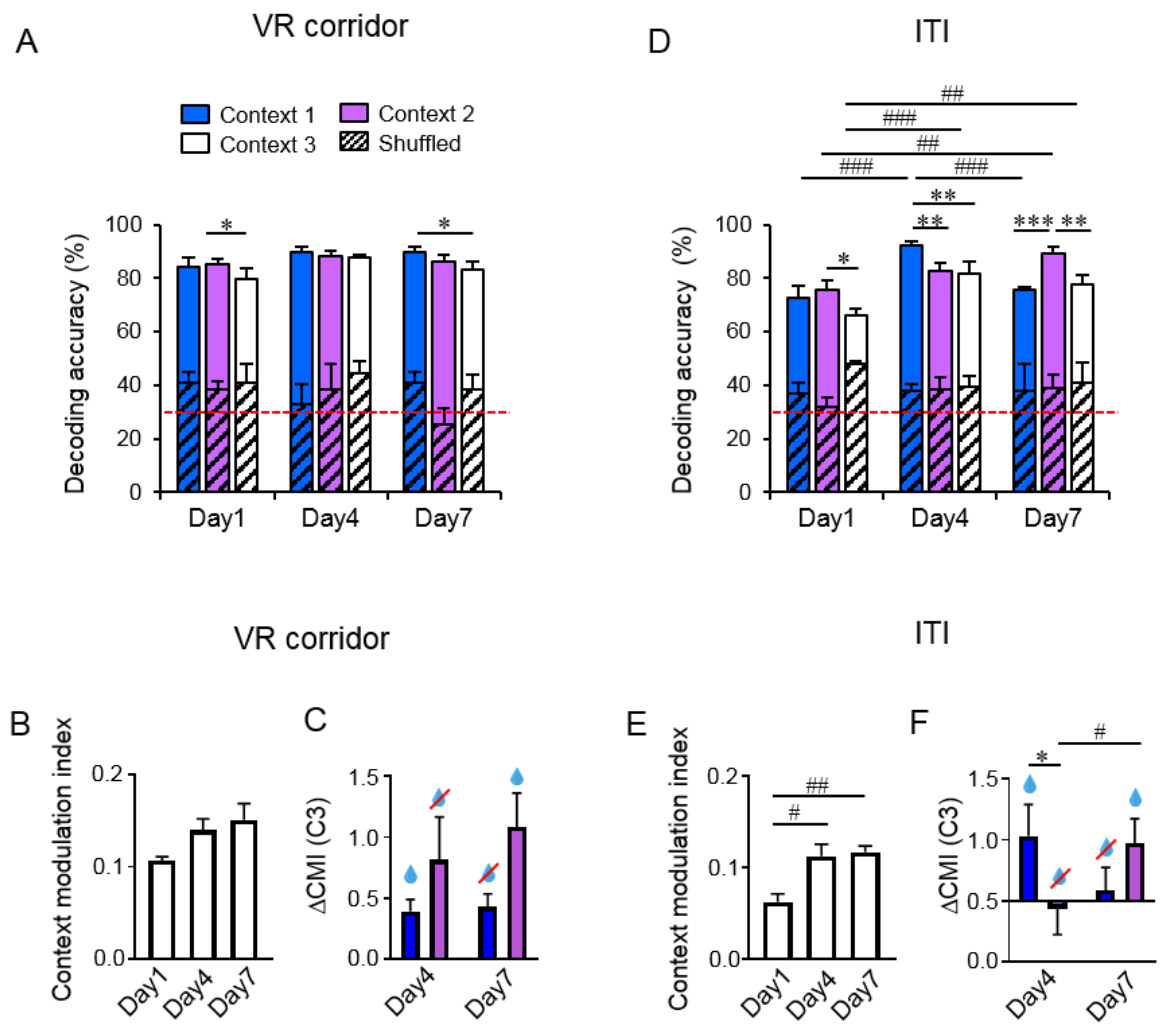

Figure 4.8 | RSC neurons encode context information modulated by learning and reversal learning.

A. Decoding accuracy for each context within the VR corridor (0-180 cm), across days. **B.** Context modulation index (CMI; see methods) between context 1 and 2 of context-encoding cells within the VR corridor. **C.** Change in CMI from baseline day between context 1 (blue) or 2 (purple) in relation to context 3 (neutral context). **D.** Same as in **C** but during ITI. **E.** Same as

in **D** but during ITI. **F.** Same as in **E** but during ITI. For all, n= 5 mice. For **A** and **D,** stripe patterned bars show the results after random shuffling the raw data. For **A**, **D**, **C**, and **F**, two-way RM ANOVA, and post hoc Holm-Sidak test were used. A strong tendency of interaction was detected in **F** (P=0.062) and hence, the post hoc test was applied. For **B** and **E**, one-way RM ANOVA and post hoc Holm-Sidak test were used. *P<0.05, **P<0.01, ***P<0.001; $^{\#}$P<0.05, $^{\#\#}$P<0.01, $^{\#\#\#}$P<0.001.

Previous studies have suggested that RSC receives substantial inputs from the visual cortex, and some neurons in the RSC reliably respond to visual input, e.g., to moving gratings with a specific orientation (Murakami et al., 2015; Wang et al., 2012). Therefore, the high accuracy of context encoding in RSC neurons may result from responses to the visual properties of the VR corridor.

Indeed, when I examined the responses of individual RSC cells to dark-light transitions (DLTs) along the VR corridors, I found reproducible periodic patterns of neuronal activity of RSC neurons (Figure 4.9, 4.11A) with a fixed time lag per neuron and different time lags for different cells. The cross-correlation functions were computed for time lags in the range between -3 to +3 bins and the maximal value of the Pearson coefficient of cross-correlation was used to determine at which lag the best fit between neuronal activity (Figure 4.10). The DLT function is achieved, and the ΔF/F signal was accordingly aligned (Figure 4.9). Using Pearson cross-correlation analysis, a large proportion of RSC neurons (~40% per context) was found to be significantly correlated to the visual pattern in the VR environment (described in a simplified form as DLT functions, see methods) (Figures 4.11B). Furthermore, such visual encoding neurons contribute largely to the encoding of the contexts (Figure 4.13C). I also found that the majority of neurons displaying visual responses were responsive to a specific context (Figure 4.11C), indicating complex context-specific processing of visual information at the RSC rather than generalized responses to light.

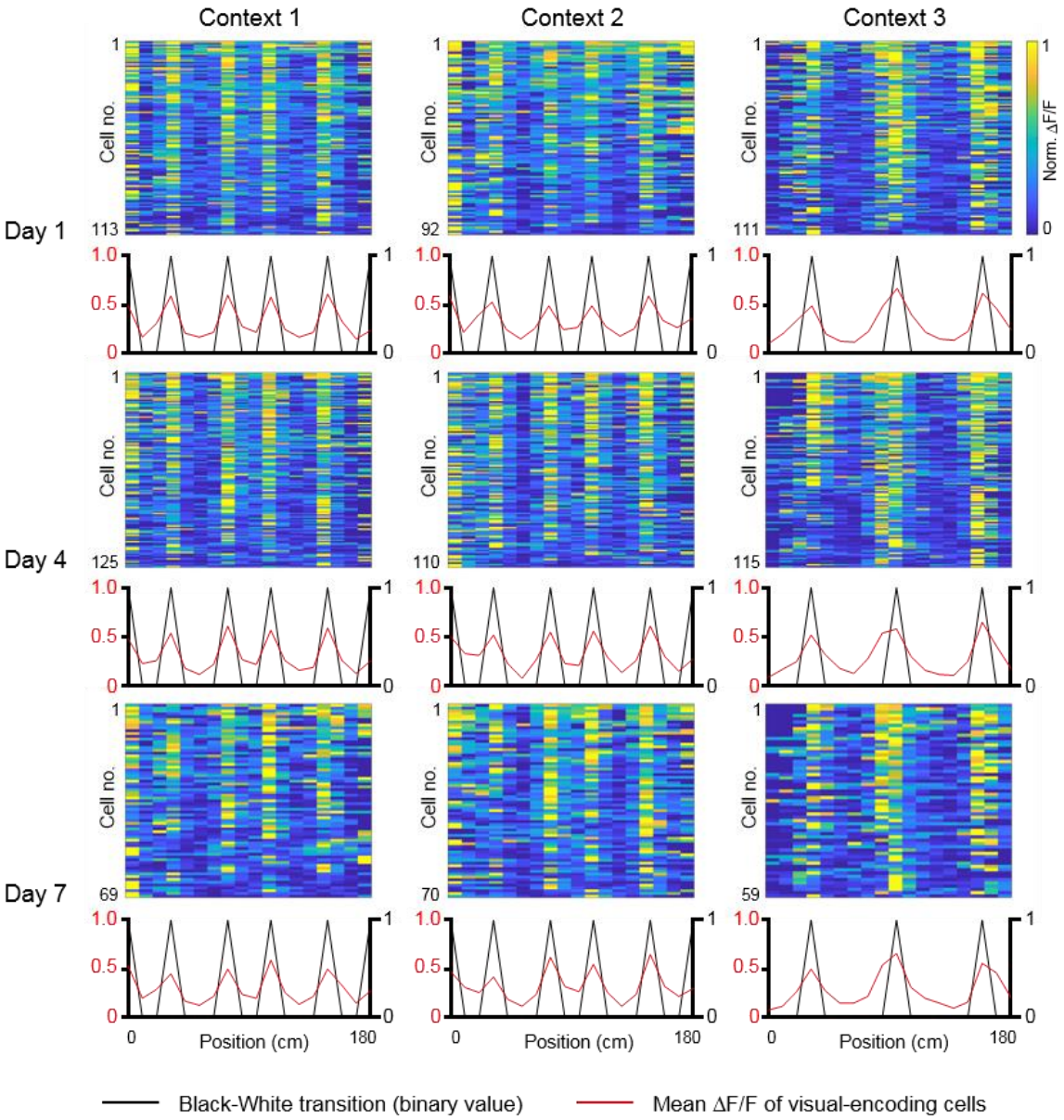

Figure 4.9 | Neurons in the RSC respond to the visual properties of the virtual environment.

Correlation between the ΔF/F of visual encoding cells and visual properties of the VR environment (dark-light transitions). Heatmap shows the normalized ΔF/F of all visual encoding cells from 5 mice, aligned by the time lag calculated using Pearson cross-correlation. Line graphs show the mean ΔF/F of all visual encoding cells (red line) and black-while transitions (black line).

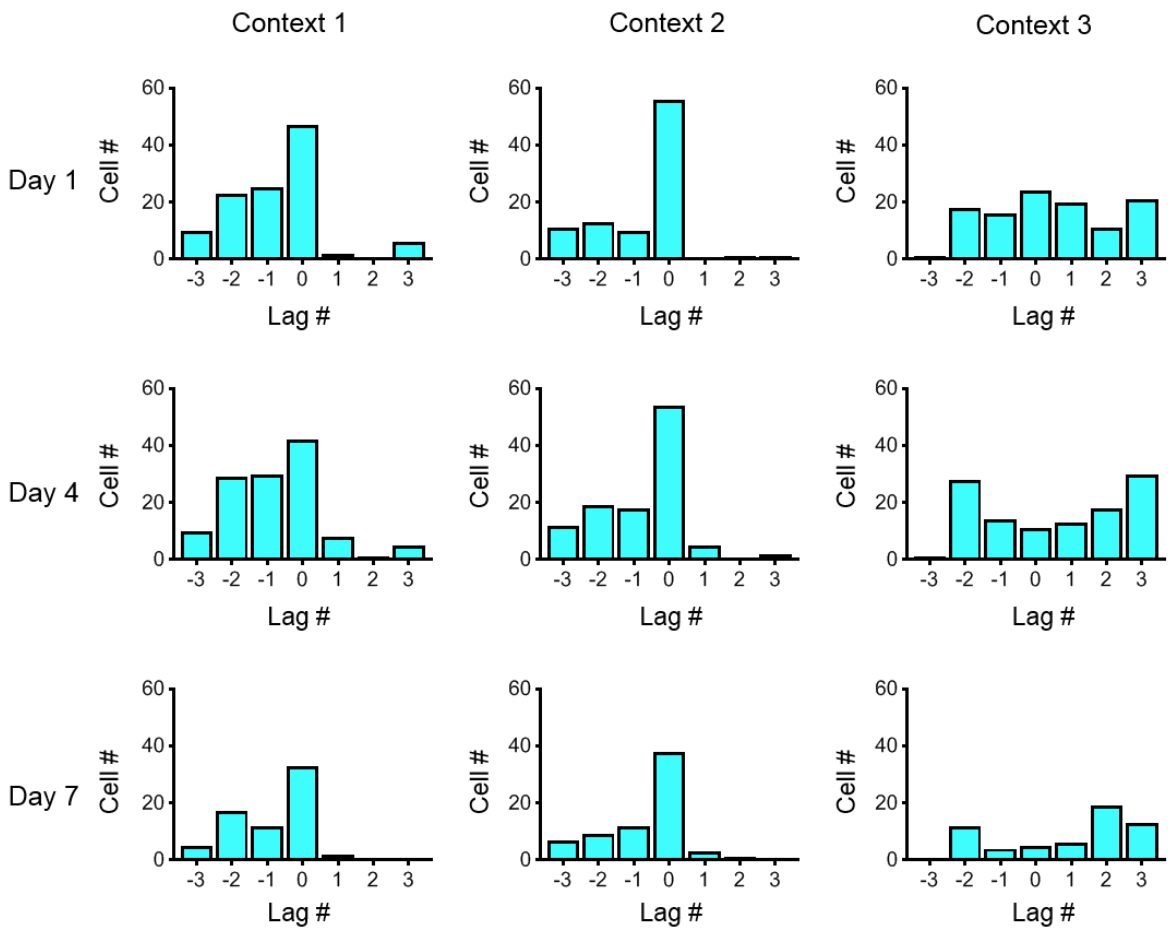

Figure 4.10 | Distribution of lags calculated by cross-correlation.

The cross-correlation functions were computed for time lags in the range between -3 to +3 bins, corresponding to the period of the slow-changing DLT function in context 3.

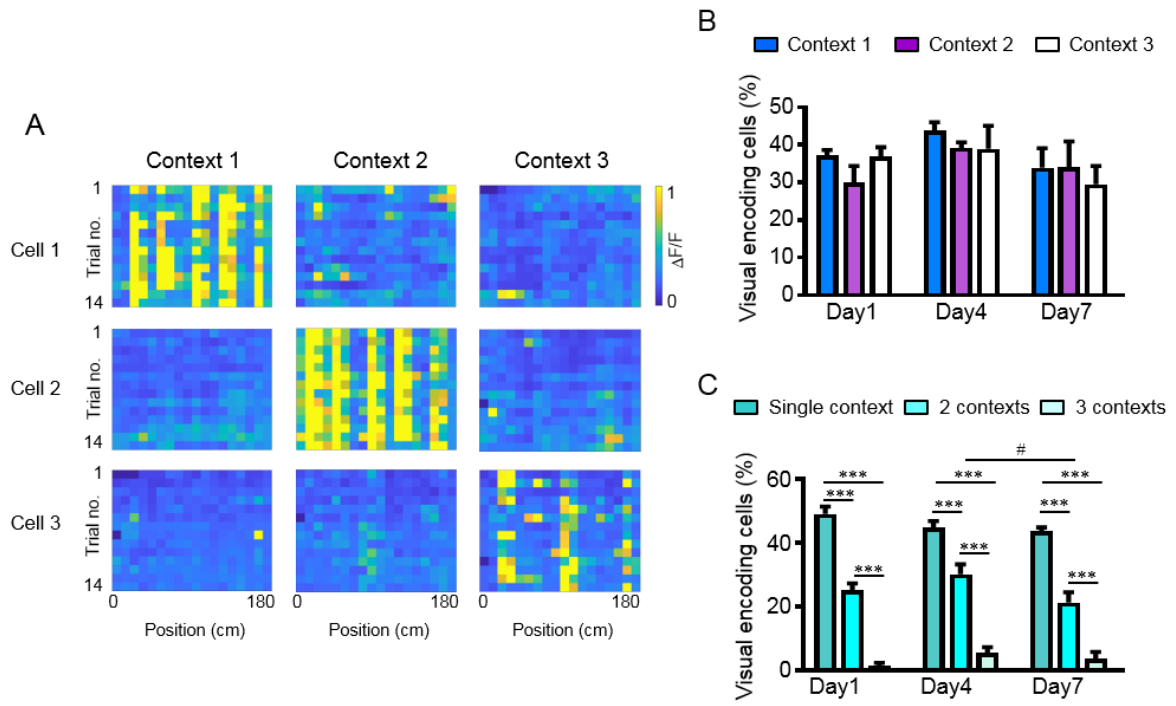

Figure 4.11 | A large proportion of neurons in the RSC respond to the visual properties of the virtual environment in a context-specific manner.

A. Normalized activity (ΔF/F) at positions along the VR corridor (0-180 cm) of three visual-encoding neurons in the RSC across multiple trials. **B.** The proportion of visual encoding cells across contexts and days. C. Context specificity of visual encoding cells on each day. For **B** and **C**, n = 5 mice, Two-way RM ANOVA, and post hoc Holm-Sidak test were used, ***P<0.001, #P<0.05.

Additionally, I observed a minor drop in accuracy for decoding the neutral context (context 3) on days 1 and 7 when compared to contexts 2 and 1, respectively (Figure 4.8A). This may reflect differences in the spatial organization of visual features in context 3, which contains fewer DLTs, again, indicating that the RSC responds strongly to fundamental visual features of the VR environment.

Beyond the visually demarcated context-specific portion of the VR corridor, i.e., after the animal moved 180 cm in VR and the reward was either given/not given, the monitors were switched off for three seconds during the ITI (see Figure 4.7A). Although animals no longer saw the context during this time interval, we examined if there was residual activity reflecting whether the animals received a reward, and hence, could still discriminate between the previously presented contexts. It is possible that during this time interval, the context value-

related information may still be salient and less obscured by activity related to visuospatial information.

Indeed, the identity of the previously presented context was correctly decoded with ≈90% accuracy for the rewarded context (context 1 and 2 on days 4 and 7, respectively), which was significantly higher than for the non-rewarded contexts as well as for day 1 (Figure 4.8D). Furthermore, the context modulation index (for context 1 versus 2, Figure 4.8E; or for contexts 1 and 2 versus the neutral context 3, Figure 4.12B) clearly demonstrated an increase in rewarded context modulation after learning and reversal learning during the ITI period. Notably, context modulation of neuronal activity during the ITI for the rewarded context 1 was higher than that for the non-rewarded context 2 (relative to the neutral context 3) during initial learning and then decreased again during reversal learning when context 1 was no longer rewarded (Figure 4.12B).

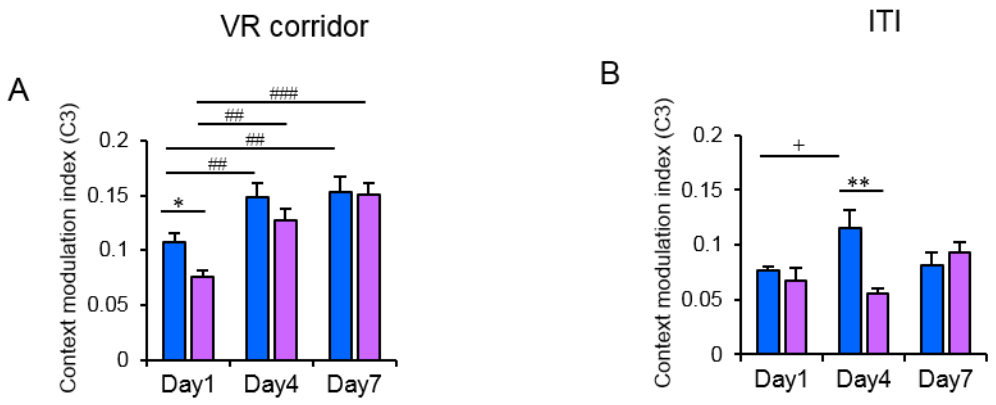

Figure 4.12 | CMI normalized to context 3 (neutral context) across days.
Context modulation index (CMI) analyzed within the VR corridor (0-180 cm). **B**. Same as B, but analyzed during ITI. For both, two way RM ANOVA and post hoc Holm-Sidak test were applied. *P<0.05, **P<0.01, $^{\#\#}$P<0.01, $^{\#\#\#}$P<0.001, $^{+}$P=0.052.

This resulted in the change in neuronal modulation by the context being significantly higher compared to baseline day 1 specifically for the rewarded context, across both initial learning days as well as reversal phases (Figure 4.8F). In other words, the neuronal activity in the ITI period after the rewarded context was always more highly modulated than the non-rewarded context. Taken together, these results suggest that neuronal activity in the RSC can encode reward-associated contextual information and that this information is maintained even immediately after the salient context is presented.

Given the high decoding accuracy of the RSC population, I analyzed the proportion of neurons that could be defined as context-encoding neurons by significantly contributing to the prediction

of which context the animal was in. I found that more than 70% of neurons showed a significant contribution ($P<0.05$) to the encoding of contextual information along the virtual corridor independent of the training day (Figure 4.13A). During the ITI, I found that approximately 60% of neurons contributed to context encoding on the baseline day, and this proportion increased slightly but significantly after learning and reversal learning (Figure 4.13B). The proportions in both the VR corridor and in ITI are in contrast to data after random reshuffling, when only a few cells showed a significant contribution (≈4%, close to the chance level of 5%, corresponding to the threshold $P<0.05$ used for cell selection). Therefore, a large proportion of the RSC neuronal population showed some task-dependent activity that allowed for accurate context discrimination.

Since the modulation of activity by context was generally higher along the VR corridor (Figures 4.8B, 4.8E) and nearly half of the population showed responses phase-locked to at least one of the visual patterns along the VR corridor walls (Figures 4.9, 4.11), one may assume that these responses were due to the contextual visual stimuli alone. However, the results revealed that neuronal responses were also observed when a visual stimulus was no longer present. Therefore, other factors may contribute to contextual discrimination in this paradigm; for instance, the visual patterns along the corridor walls could provide the animal with spatial information. Also, the speed of the animals varied along the VR corridor in a context-specific manner. Hence, I next investigated if these additional factors can evoke specific responses in RSC neurons.

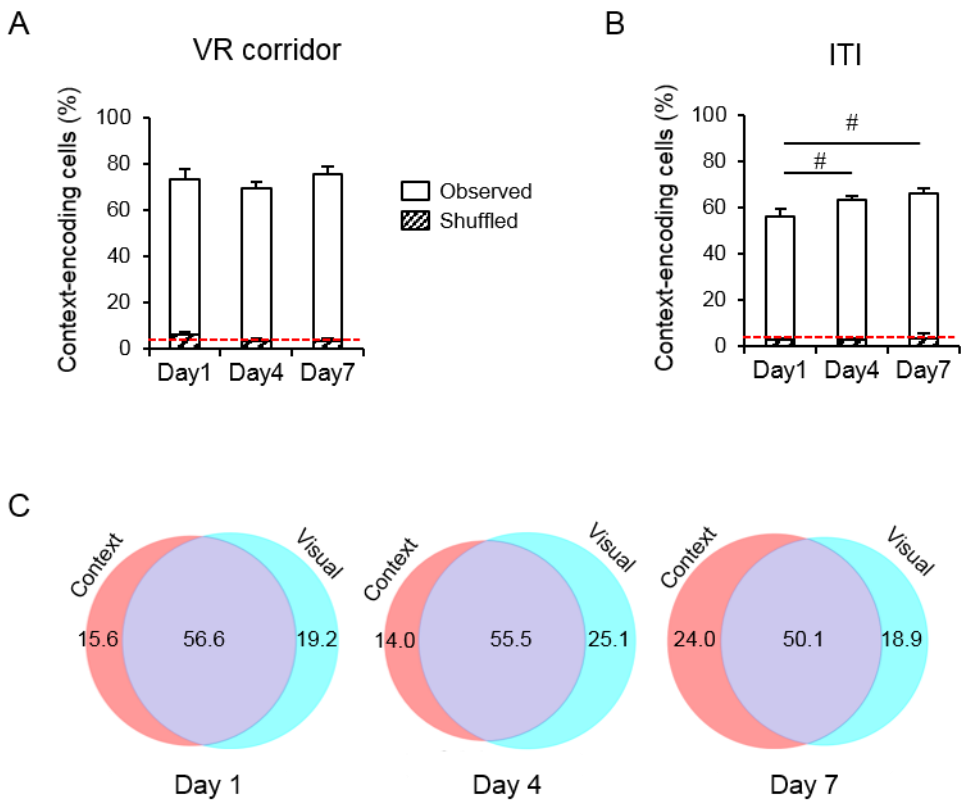

Figure 4.13 | A large proportion of RSC neurons encode context information and visual information.

A. The proportion of context-encoding cells within the VR corridor (0-180cm). **B.** The proportion of context-encoding cells during ITI. **C**. Venn diagrams illustrate the percentage of neurons encoding context and visual properties on each day. For all, n= 5 mice. For **A** and **B,** stripe patterned bars show the results after random shuffling the raw data, one-way RM ANOVA was used.

4.4. Decoding of spatial information

The RSC is known to contain place cells and HD cells. These cells also play a role in spatial navigation (Chen et al., 1994b; Jacob et al., 2016; Mao et al., 2017). Therefore, I examined the relationship between RSC neuronal activity and the animal's position along the virtual corridor in different contexts. It is observed that some neurons were preferentially active at one or multiple specific positions during each trial (Figure 4.14).

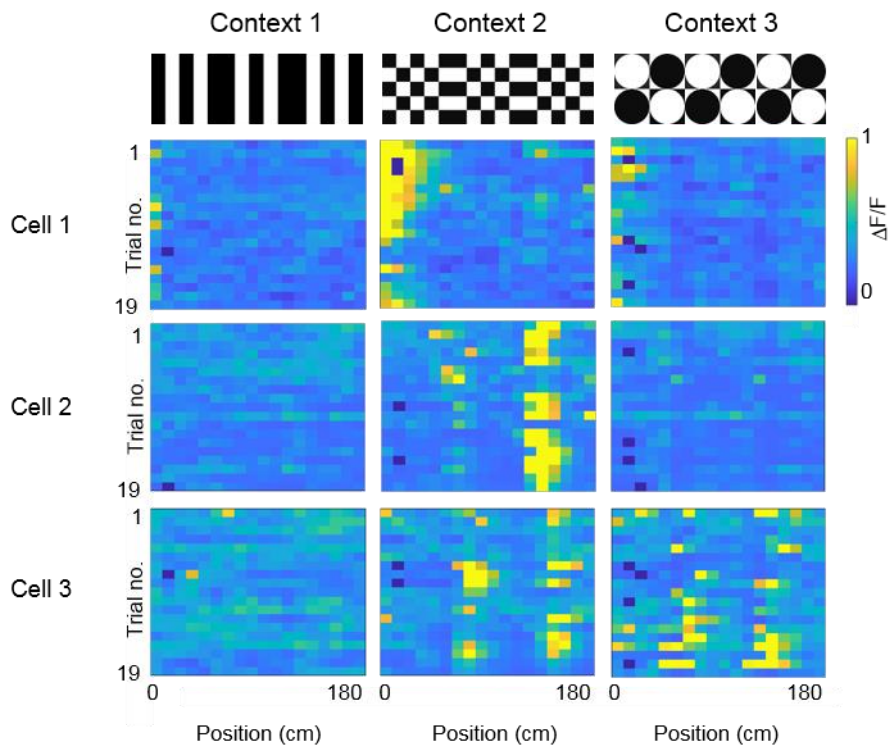

Figure 4.14 | RSC neurons encode position information.
Normalized response (ΔF/F) at positions along the VR corridor (0-180 cm) of three position-encoding neurons in the RSC across multiple trials.

A linear model was then used to decode the animal's position in each of eighteen 10 cm-long spatial bins using the RSC neuronal activity from each animal. Backward stepwise linear regression analysis was used to select the model with a minimal number of cells. The linear model provided accurate decoding of the animal position in a given context, as illustrated by a linear relationship between the predicted and observed values of position (Figure 4.15A).

On average, R^2, which is the measure of model fit (% of position variance explained by neuronal activity), was ≈50% across all contexts (Figure 4.15B). This was much higher than R^2 ≈10% obtained for data generated by the random reshuffling of position values within trials. There was no effect of day on R^2; therefore, position-related responses were not affected by reward-associations and, on the population level, remained consistent across learning.

However, I detected a small reduction in R^2 for the neutral context (context 3) when compared to contexts 1 and 2 on the baseline day (day 1); this may also be due to the less salient edges associated with this visual pattern. Interestingly, R^2 for the neutral context was increased on days 4 and 7, where it then reached the levels observed in other contexts; suggesting that even

though position-encoding in the RSC was not specifically altered with reward, it may still be refined in an experience-dependent manner for less salient spatially defined environments.

Approximately 30% of neurons showed a significant contribution (P<0.05) to the encoding of positional information in each context, independent of day and reward association (Fig. 4.15C). This was significantly higher than after random reshuffling when only ≈10% of cells showed a significant contribution. Although there was no specific change in responses with rewarded/non-rewarded contexts, I did find that a large portion (≈40%) of position-encoding cells only encoded position in a single context, and hence were highly context-specific, while ≈20% contributed to encoding in two contexts, and a small proportion (≈5%) showed position-encoding in all three tested contexts (Figure 4.15D).

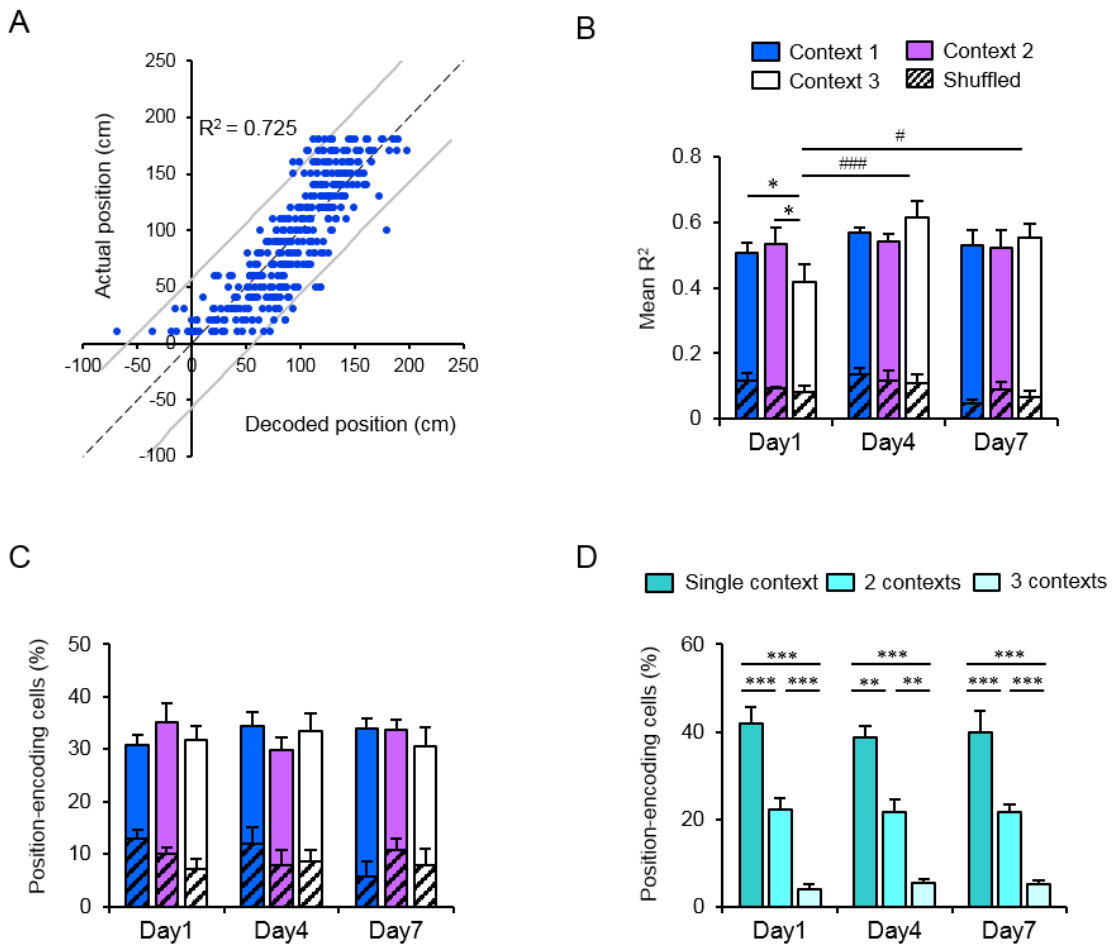

Figure 4.15 | Neurons in the RSC encode position information predominantly in a context-specific manner.

A. Exemplary linear regression plot for the actual position and position decoded from neuronal activities for one animal and one context; a high R^2 value (R^2 = 0.725) indicates a good fit of the linear regression model to the observed data. **B.** Mean R^2 of position decoded in each context

on baseline day (day 1), initial test day (day 4), and after reversal learning (day 7). **C.** The proportion of position-encoding cells across contexts and days. **D.** Context specificity of position-encoding cells on each day. For all, n = 5 mice. For **C** and **D**, stripe patterned bars show results after the random shuffling of the raw data. Two-way RM ANOVA and post hoc Holm-Sidak test were used. *P<0.05, **P<0.01, ***P<0.001; #P<0.05, ###P<0.001.

Interestingly, position encoding was not primarily attributed to classical place cells, since I found only ~5% of neurons with traditional place cell properties in each context, independent of the learning phase; most of these cells were also context-specific (Figure 4.16).

In conclusion, many neurons in the RSC demonstrated the potential for encoding spatial information in a context-specific manner, and these responses were mostly unaffected by the behavioural relevance of the particular context.

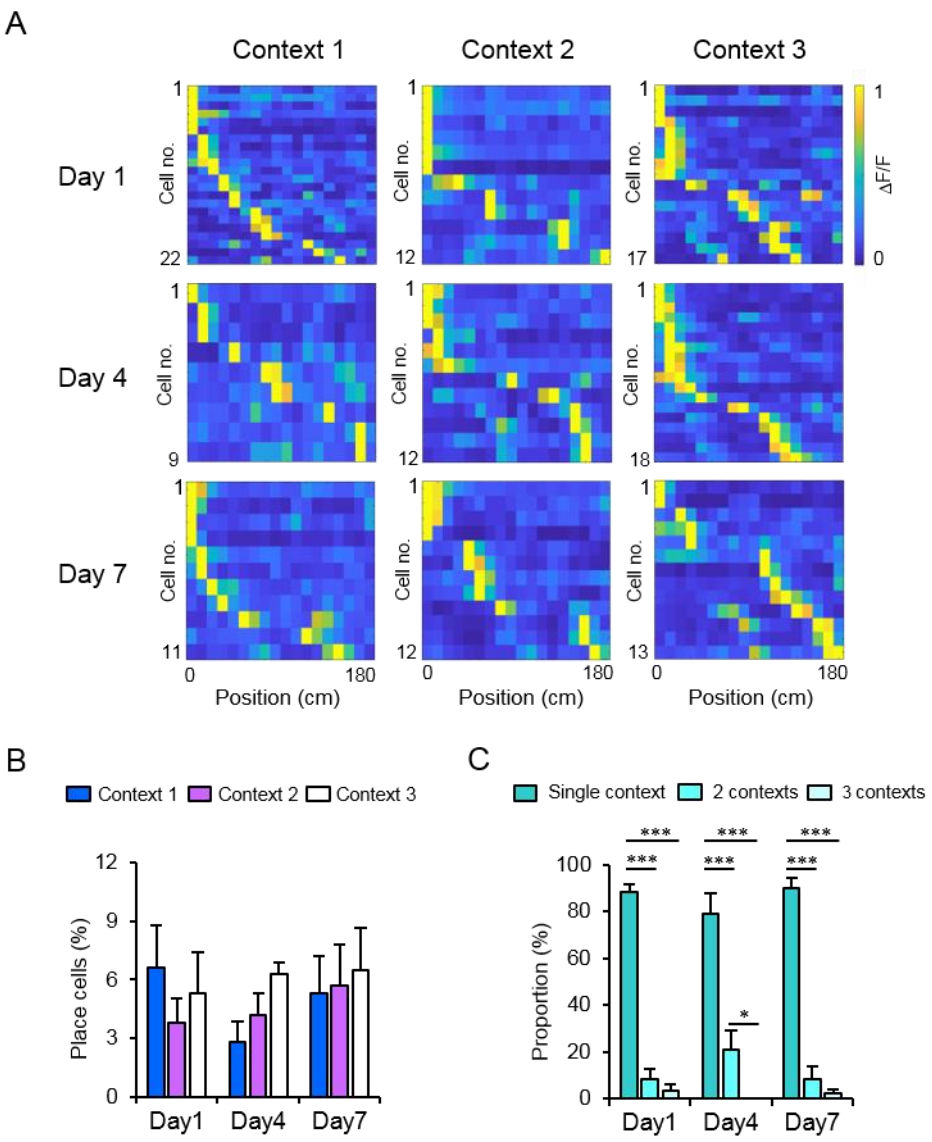

Figure 4.16 | A small proportion of neurons in the RSC show properties of place cells. **A.** Normalized activity (ΔF/F) of place cell-like neurons in each context and day. **B.** The proportion of place cell-like neurons from all imaged neurons in RSC. **C.** The proportion of place cell-like neurons specific to a different number of contexts from all place cell-like neurons. n = 5 mice. Two-way RM ANOVA and post hoc Holm-Sidak test were applied. *P<0.05, ***P<0.001.

4.5. Decoding of speed information

A previous study has suggested that RSC neurons might encode speed selective signals (Cho and Sharp, 2001). Here, I investigated whether the neuronal activity in the RSC is related to the

animal's speed. I observed that some cells were preferentially active during trials when the animal was moving at a slow speed (e.g., cell 1, Figure 4.17), while others responded more when the speed was high (e.g., cells 2,3, Figure 4.17).

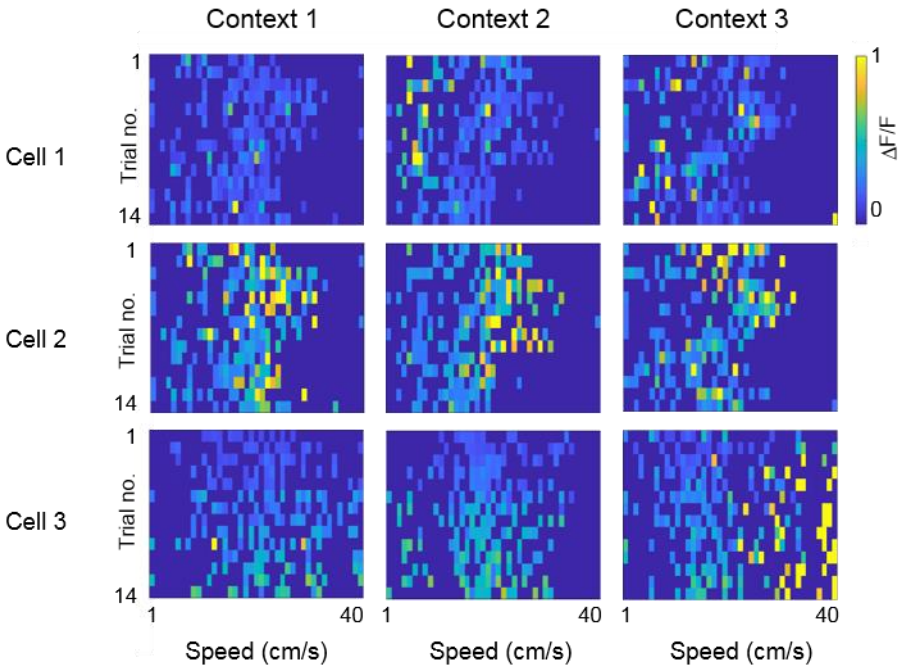

Figure 4.17 | Neurons in the RSC encode speed-related information.
Normalized response (ΔF/F) of three speed-encoding neurons in the RSC across multiple trials as a function of running speed.

When I used a linear model to decode the animal speed based on the neuronal activity, I found that, similar to an animal's position, a linear model provided accurate decoding of an animal's speed in a given context, as illustrated by a linear relationship between predicted and observed values of speed (Figure 4.18A). On average, R^2 was ≈40-50% (Figure 4.18B), which was much higher than R^2 obtained for data generated by the random reshuffling of speed values within trials (≈10-15%). Also, similar to position-encoding in RSC, I found no effect across days or context on R^2 for speed-encoding.

Approximately 30% of cells showed a significant contribution ($P<0.05$) to the encoding of speed information in each of the contexts, independent of training days (Figure 4.18C), which was significantly higher than after random reshuffling. Interestingly, I also found that ≈40% of speed cells were specific to a single context, while ≈20% contributed to decoding in two contexts, and only a small proportion of cells were speed-encoding in all three tested contexts (Figure 4.18D). Notably, there was a moderate but significant increase in the proportion of

neurons encoding speed in two contexts after reversal learning when compared to baseline and initial learning sessions (Figure 4.18D), suggesting that speed encoding may not be entirely unaffected by previous learning.

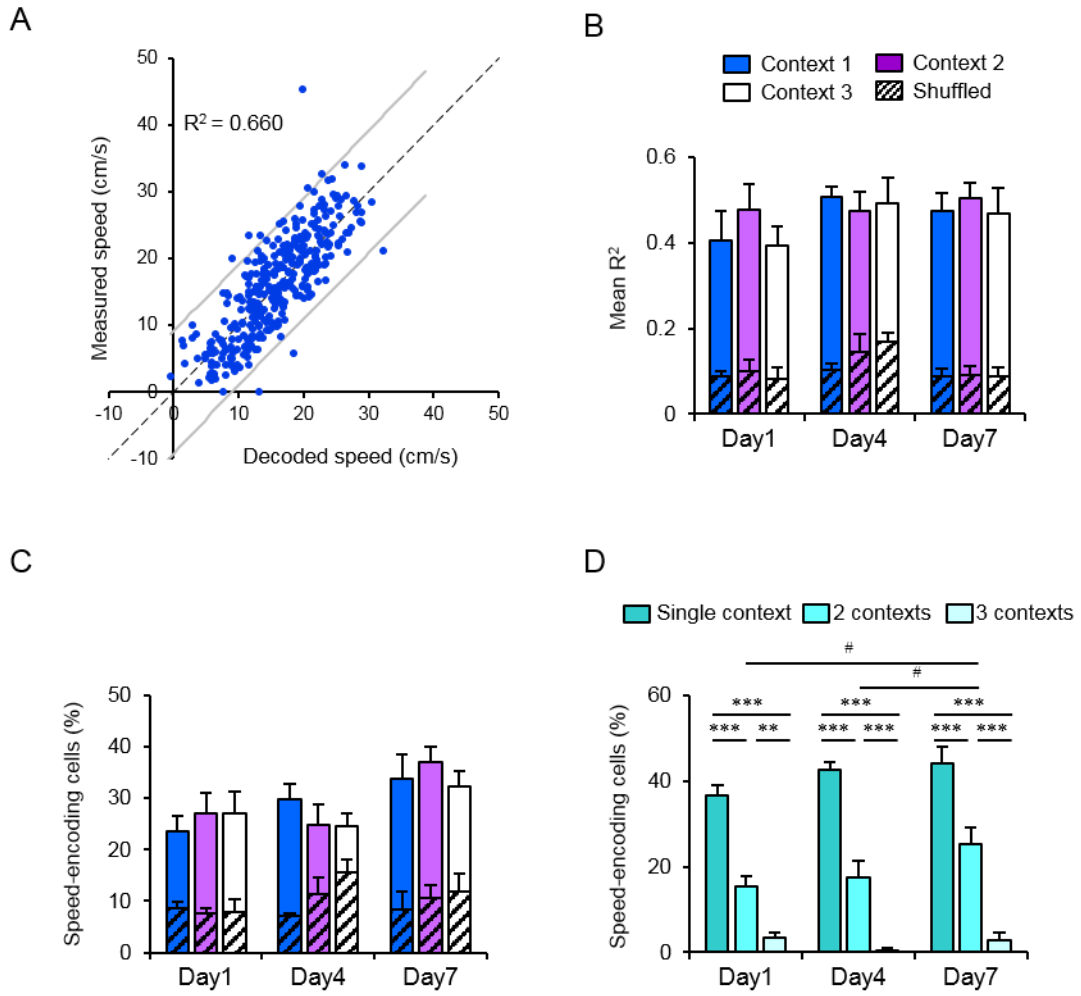

Figure 4.18 | Neurons in the RSC encode speed-related information predominantly in a context-specific manner.

A. Exemplary linear regression plot for actual speed versus speed decoded from neuronal activities for one animal and one context; a high R^2 value ($R^2 = 0.66$) indicates a good fit of the linear regression model to the observed data. **B.** Mean R^2 of actual and decoded speeds in each context on the baseline day (day 1), initial test day (day 4), and after reversal learning (day 7). **C.** Proportion of speed-encoding cells across contexts and days. **D.** Context specificity of speed-encoding cells on each day. For all, n = 5 mice. For **B** and **C**, stripe patterned bars show results after the random shuffling of the raw data. Two-way RM ANOVA and post hoc Holm-Sidak test were applied for **B-D**. **P<0.01, ***P<0.001.

If this was the case, since the animals slowed down in the rewarded context, there may be a bias towards speed-encoding cells for the reward-associated context. To examine this, speed cell categorization was set based on the cumulative distribution of speed cells for all days and contexts as a function of average preferred speed (lower 30% were categorized as slow speed cells; upper 30% were fast speed cells, and the residual 40% were medium speed cells, see Figures 4.19A, 4.19B).

Indeed, I found that the fraction of slow-speed encoding cells was significantly modulated along with the rewarded context across learning (Figure 4.19C). One may predict that speed encoding would be more independent of context and learning and hence show a higher and consistent proportion of neurons encoding in all three contexts, however the fact that most neurons showed context-specific responses and changes according to the value-based association of the context suggests that this may be a fundamental property of spatial and locomotion related encoding in the RSC, i.e., that the activity of most neurons in the RSC are fundamentally affected by contextual cues.

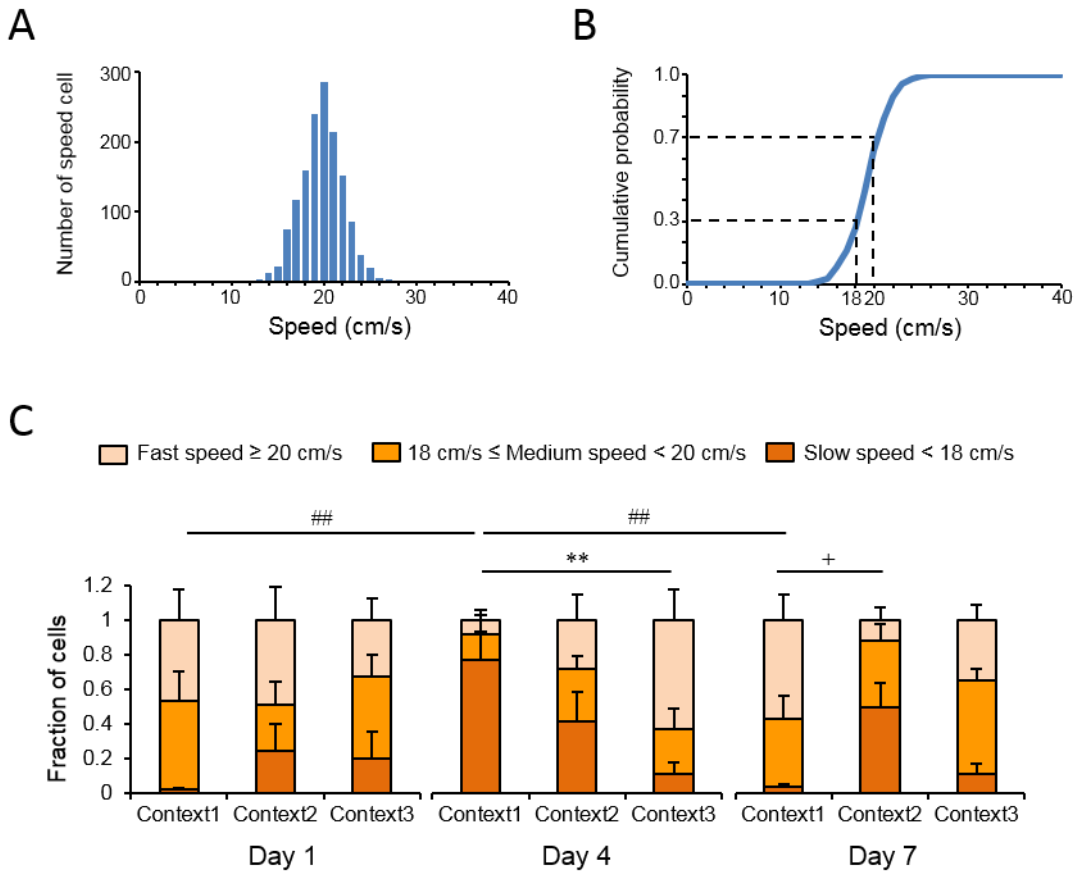

Figure 4.19 | Slow speed encoding correlates with reward.

A. Distribution of speed cells as a function of normalized speed. **B**. Cumulative probability as a function of mean preferred speed to categorize speed cells (lower and upper 30% was categorized as slow and fast speed cells; the rest are medium speed cells). **C**. Fraction of neurons selectively responding to slow speeds is correlated with the rewarded context. n = 5 mice. Two-way RM ANOVA and post hoc Holm-Sidak test were applied. **$P<0.01$; $^{\#\#}P<0.01$; $^{+}P=0.056$.

4.6. Multidimensional encoding nature of RSC neurons

As described above, subsets of neurons in the RSC encode different information, including context, position, and speed. To determine the influence of the various task parameters/dimensions on neuronal activity in the RSC, I analyzed the contribution of all neurons in decoding context, position, and speed, which are the key parameters in the experiments, for each animal (e.g., an animal in Figure 4.20A). Indeed, many neurons in the RSC appeared not only to be involved in a single encoding task but multiple encoding tasks (neurons connected to all parameters: ‘Context’, ‘Position’, and ‘Speed’).

Analysis across all animals (Figure 4.20B) revealed that neurons specifically encoding only ‘Context’, ‘Position’, or ‘Speed’ constituted 10% or less of recorded RSC neurons. Higher proportions (10-20%) were observed for cells encoding for two task parameters: ‘Context + Position’, ‘Context + Speed’, or ‘Position + Speed’. However, the most common class of cells were, what we refer to as multidimensional encoding neurons, encoding for three dimensions ‘Context + Position + Speed’.

Interestingly, the frequency of these multidimensional encoding neurons was not changed after initial learning on day 4 but was significantly increased from ≈30% to ≈40% after reversal learning on day 7 (Figure 4.20C); suggesting that the need for cognitive flexibility leads to an increase in the proportion of multidimensional encoding neurons.

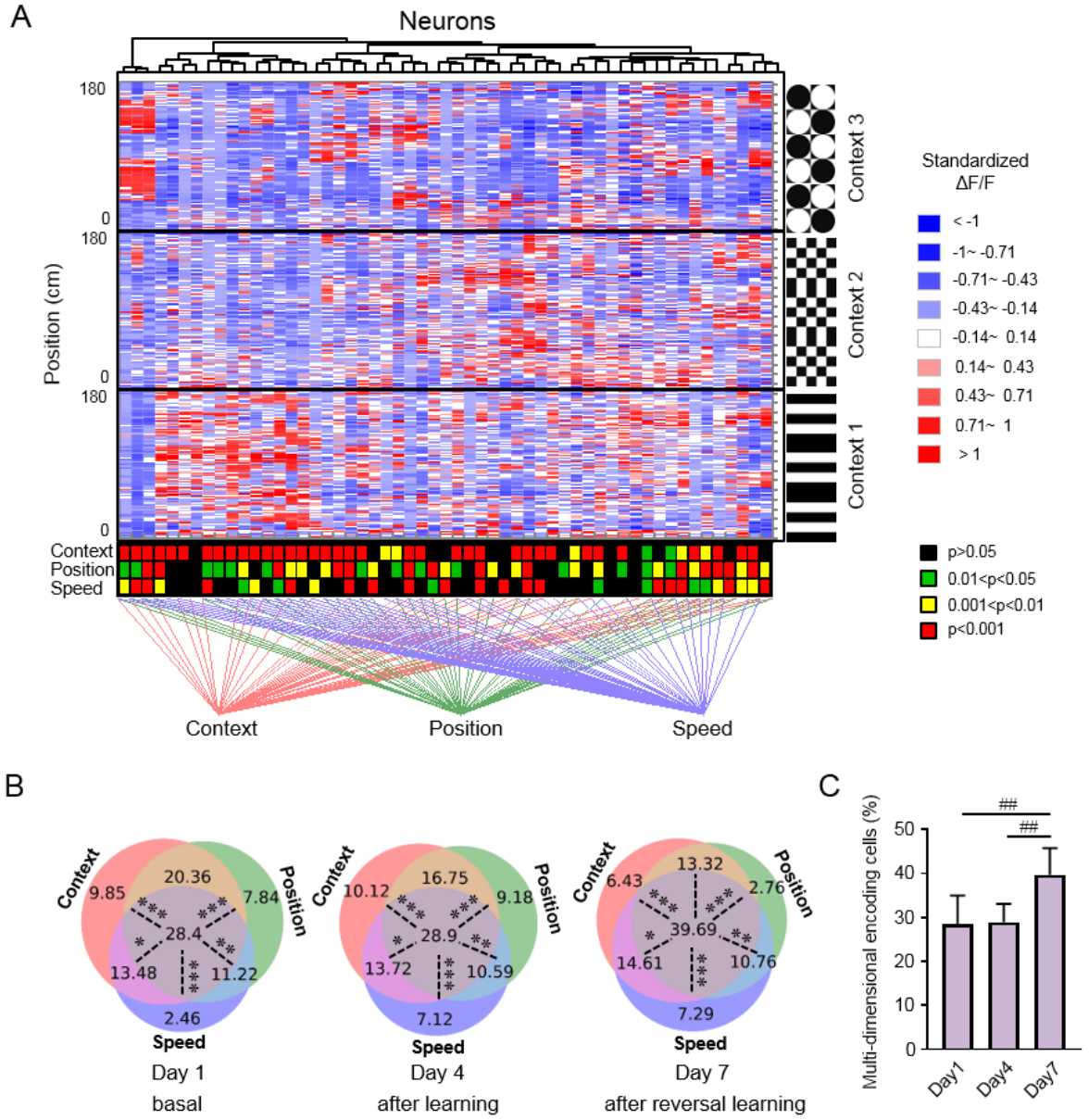

Figure 4.20 | The RSC predominantly contains multidimensional encoding neurons, and this proportion is increased after reversal learning.

A. Normalized response (ΔF/F) of all imaged RSC neurons from one animal in three contexts (neurons in columns, positions in rows). Neurons that encoded specific information were categorized into different aspects using hierarchical cluster analysis. The color-coded significance values of their contributions to the encoding of context, position, and speed are given below the heatmap of neuronal activities. **B.** Percentage of neurons encoding various parameters on each day. **C.** The proportion of multidimensional (context, position, and speed) encoding neurons. For **B** and **C**: n = 5 mice. Two-way RM ANOVA and post hoc Holm-Sidak test were applied. *P<0.05, **P<0.01, ***P<0.00; ##P<0.01.

5. DISCUSSION

As revealed by anatomical studies, the RSC is located at a unique position that connects multiple important brain regions, including the HF, the ATN, parahippocampal formation, and visual and entorhinal cortices, which are involved in a variety of complex cognitive functions. Therefore, it is suggested the role of the RSC in a variety of cognitive functions, including navigation, spatial memory, contextual memory. Indeed, a wide range of studies in both humans and animals have shown the contributions of the RSC in navigation and contextual memory.

Additionally, it has been suggested that the RSC has a crucial integrative function. However, how the integration is implemented at the cellular level is still unclear. The integration may be achieved through interaction between subpopulations of neurons that encode a single stimulus dimension/parameter, or by neurons encoding multiple dimensions, or through mixed mono- and multidimensional encoding.

Also, single-neuron studies have shown specific features of the RSC (Mitchell et al., 2018). For example, it was found that specific subpopulations of RSC neurons process the properties of HD cells (Chen et al., 1994b; Jacob et al., 2016) or hippocampal CA1 place cells (Mao et al., 2017) and furthermore, the RSC encodes spatial information (Alexander and Nitz, 2015; Czajkowski et al., 2014; Mao et al., 2018) and spatial memory engram (Milczarek et al., 2018), trajectories and reward locations (Vedder et al., 2017), history- and value-related information (Hattori et al., 2019). These observations suggest that RSC is involved in the processing of spatial, contextual, and reward-related information. However, these studies were focused on specific cognitive dimensions and did not study the cellular basis of multidimensional integration in the RSC.

In order to address these questions, in this thesis, I established a new methodology to combine a series of state-of-the-art techniques including virtual reality, in vivo two-photon calcium imaging at the cellular level, and an advanced chemogenetic approach (DREADDs). I utilized a context discrimination paradigm in a virtual reality environment to provide a comprehensive account of the specific role of the RSC in various stages of learning and memory including the formation of the memory and the recall of the memory, as well as how neurons in the RSC integrate multiple aspects of information during context discrimination behaviour. This work anvances our understanding of the role of the RSC in the phase of acquisition and recall of contextual memory, and the neuronal encoding underlying such functions. Thus, this work

provides a foundation for further understanding of the role of the RSC in pathological conditions.

5.1. A novel virtual context discrimination paradigm

To relate animal position and neuronal dynamics, a linear track is a simple and highly efficient solution. The development of the VR approach significantly extends the usage of linear tracks in cognitive tasks. More importantly, it allows researchers to redefine the rules that link the subject's actions to changes in its world, which is usually impossible to achieve in the real world (Minderer et al., 2016).

Indeed, some studies have already used a linear track built in the VR environment in combination with two-photon imaging effectively to investigate cognitive functions among a variety of brain regions (Hainmueller and Bartos, 2018; Harvey et al., 2012; Rajasethupathy et al., 2015). To my knowledge, however, the current work is the first to explore the role of the RSC and the neuronal dynamics underlying the function of the RSC using the VR system combined with two-photon calcium imaging.

In this paradigm, mice were presented to different virtual contexts to discriminate and build associations between a particular context and a water reward at a specific spatial location. Thus, this paradigm includes not only context discrimination but also spatial learning, and hence allowed me to study the role of the RSC in the interaction between context discrimination and spatial learning. Combining VR and two-photon calcium imaging facilitated the analysis of neuronal activity as a function of animal position and speed in the VR world.

Since this is not a widely used method, the first step was to validate the paradigm. First of all, I validated the context discrimination paradigm, which was built up in the virtual reality in both the baseline experiment group, in which the mice did not receive any additional manipulations and the control group, in which the mice received m-Cherry control virus and systemic injection of CNO. In both groups, the mice were able to discriminate between the rewarded context and non-rewarded contexts by a significant reduction of speed in the anticipation zone, which is near the reward position only in the rewarded context in preparation co consume the water reward. The reduction of speed in anticipation already showed up on the first learning day and became significant from the second learning day, indicating the context discrimination paradigm established in VR fulfills the aim of the study.

5.2. The RSC supports acquisition rather than recall of recent contextual memories

Using chemogenetic inactivation during a context discrimination paradigm, I found that the RSC is essential for the acquisition phase of reward-context associations to previously neutral contexts but not necessary for recent memory recall. Previous studies have examined the role of the RSC mostly by introducing a permanent lesion (Mitchell et al., 2018; Vann et al., 2009), making it difficult to determine the role of the RSC in a particular phase of learning and memory. Instead of permanent lesions, temporal and repeated inactivation of the RSC is thought to be more advanced regarding investigating the precise role of the RSC and has the potential to determine the contribution of the RSC at different phases of learning and memory. Chemogenetic technologies are potentially good candidates to achieve such temporal and repeated inactivation.

Chemogenetic technologies have been developed as valuable tools to control neuronal signal transduction, cellular signaling, and behaviour, and importantly, it can link the behavioural outputs with neural circuits (Dar et al., 2012; Roth, 2016; Whissell et al., 2016). Among these chemogenetically engineered proteins, Designer Receptors Exclusively Activated by Designer Drugs (DREADDs) is the most popularly used by neuroscientists (Roth, 2016) and is also the one I used in this study. DREADDs can be used to activate or inactivate targeted populations of neurons, depending on the expression of the receptor and timing of designer drug application. DREADDs receptors can be introduced in a particular brain region via different gene transfer strategies, and in this study, the gene delivery of inhibitory receptor hM4Di was done using by AAV. The receptor is only activated after the application of CNO and thus provides the ability to apply temporally-controlled and repeatable interventions (Smith et al., 2016). This is one of the most significant advantages of DREADDs compared to the lesion approach used for investigating the role of the RSC, which generates permanent damage and loses the potential to study the contribution in different phases.

One recent study (Robinson et al., 2014) aimed to investigate the engagement of the RSC in the process of the formation of associations between different sensory cues by applying a chemogenetic approach (DREADDs) similar to what I used in this study. They trained rats in a sensory preconditioning paradigm to form an association between different sensory cues, and

they found that inactivating neurons in the RSC by DREADDs during the phase of preconditioning impaired the formation of an association between the sensory cues. The findings revealed that the RSC is vital for the formation of episodic memory is in line with the results in the present study.

In the current work, successful context discrimination depends on the formation of an association between the particular context and the reward. When the neuronal activity was altered by DREADDs during the acquisition of the memory, the mice failed to discriminate the contexts, which indicate the association between the context and the reward was not formed. At this point, we have similar findings.

However, in this previous study, they only addressed the involvement of the RSC during the phase of memory formation but not the phase of memory retrieval. Here in the present study, I further extended these conclusions by performing inactivation of RSC neurons in the phase of recent memory recall. I found that the performance of context discrimination was not affected when the chemogenetic inactivation was applied during memory retrieval but not during the acquisition of the memory. This indicates that chemogenetic inactivation of RSC after contextual memory formation is not affecting the recall of recently acquired memory in the conditions presented in this thesis.

This finding is supported by another study, in which the authors demonstrated that damage to the RSC did not impair recall of recent fear memories to a visual conditioned stimulus when the lesion was made 1 day following conditioning (Jiang et al., 2018); however, they did find that remote recall, when the lesion was performed 28 days later, was impaired, suggesting the RSC may be involved in more long-term memory storage, which remains to be determined using our paradigm.

Therefore, the results in the current study suggest that the RSC is essential for the acquisition of contextual memory but not necessary for the retrieval of recently formed memories. Still, the role of RSC in the transfer of contextual values from recent to remote memories remains to be investigated, e.g., by long-term inactivation of RSC after memory acquisition.

In the present study, after two days of learning in the VR environment, the mice were able to discriminate the contexts by not only associating the reward with a particular context but also associating the reward with a specific position. However, with chemogenetic inactivation of RSC neurons, the animals failed to form such an association between the reward and the specific

position in a particular context. These results indicate that the RSC not only plays a role in the formation of contextual memory but also contributes to spatial memory and this may be due to the direct connection between the RSC and the hippocampus. A recent study (Patai et al., 2019) applied fMRI scanning while subjects navigated in the familiar virtual environment as well as the newly learned environment. They found that the activity in the posterior hippocampal correlated with the distance to the target in both familiar and newly learned environments. While the RSC only tracked the distance in the familiar environment. This is supporting our result that the inactivation of RSC neurons led to behavioural impairments in the mice when associating the reward with a specific position.

Through iterations of learning and reversal learning with and without RSC inactivation, it was further shown that inactivation of RSC led to a failure for the mice to devalue previously rewarded contexts, while mice maintained the previously acquired negative value of the neutral context which was never paired with a reward during reversal learning. In other words, mice have to devalue the previously rewarded context because of the conflict between the previously established value of the context and new reality. This data complements the reported role of RSC in fear extinction, as in the paradigm used for this work, a positive reinforcement is used for learning. This function of RSC is very close to the role of PFC and might reflect their cross connectivity. It would be highly interesting to perform parallel recordings in both regions to reveal their specific roles with respect to the devaluation of contexts.

It is noteworthy that previous studies revealed that the RSC is engaged in the tasks dealing with conflict information. For instance, damage to the RSC impaired the ability of rats to navigate in a rotated maze, which contains conflict proximal and distal cues (Pothuizen et al., 2008) and impaired the ability of rats to isolate spatial information in place avoidance task (Wesierska et al., 2009). A recent study has also found that RSC encodes history-dependent value and acute optogenetic inactivation of RSC selectively debilitated behavioural dependency on the reward-related choice history, while keeping the choice bias (Hattori et al., 2019).

These findings are in line with our results that chemogenetic inactivation of RSC altered the history-related behaviours. The difference is our history-related information is not trial-based but relatively longer session-based history. Besides, I extended these conclusions in the thesis and suggest that the inactivation of the RSC affects the ability of mice to assign a previously formed negative value rather than the current positive value to a context. This results in a positive-value bias of all contexts presented during learning, as well as more novel contexts

without previously assigned value, and reinforces the notion that the RSC is required for reward-value based behaviours.

5.3. Information processed in the RSC

After revealing the role of the RSC in the context discrimination at behavioural level, I then analyzed the response properties of neurons in the RSC during this contextual discrimination paradigm using two-photon calcium imaging data and found that RSC neurons encode for task-dependent features, including context-specificity, visual features of the environment, the context-associated reward value as well as the spatial position and speed of the animal.

The RSC in humans and rodents is subdivided into granular and dysgranular subregions. Although granular and dysgranular retrosplenial cortices prominently share similar connectivity and functions, several studies have shown different properties and contributions to cognitive functions between them. In this study, the dysgranular RSC was selected as the exact region of interest for two-photon calcium imaging.

The first reason to select the dysgranular RSC as the region for two-photon imaging is due to its relatively easier access since the dysgranular RSC is mostly reaching the surface of the mouse brain. Additionally, based on the evidence provided from previous studies, the dysgranular RSC is more suitable for the aim of this work. For example, earlier studies have found that dysgranular RSC is essential for using visual cues to successfully perform working memory related task (Vann and Aggleton, 2005) or to discriminate between two spatial locations (Hindley et al., 2014c).

Also, immediate-early gene imaging in rats (Pothuizen et al., 2009) provided evidence that the dysgranular subregion plays a selective role in the task that requires visual information, while the granular subregion is mainly involved with navigation based on internal cues. In addition, anatomical data reveal the dysgranular RSC is densely connected with dorsal stream visual areas (Wang et al., 2012), and visual information first reaching the RSC preferentially targets the dysgranular subregion (van Groen and Wyss, 1992a). In the paradigm used in this thesis, the visual inputs from the virtual environment are the most critical inputs to the mice, by which the mice could perceive different contexts and navigate within them. Based on these important facts, I performed two-photon calcium imaging in the dysgranular RSC.

By examining the relationship between RSC neuronal activity and the animal's position along the virtual corridor in different contexts, I found that some neurons were preferentially active at one or multiple specific positions during each trial. Further analysis revealed that many neurons in the RSC demonstrated the potential for encoding spatial information in a context-specific manner. Previous studies support this finding. For example, (Mao et al., 2017) revealed a population of neurons predominantly in the superficial layers of the RSC whose ensemble neuronal activity showed highly similar properties to the place cells in hippocampal CA1 recorded within the same task. In the present study, I found a relatively larger proposition of RSC neurons contributing to the encoding of positional information than the previous study. However, position encoding was not largely attributed to classical place cells. These differences may be due to the paradigm established in virtual reality rather than the typical physical treadmill.

In addition, other studies also showed that the RSC encodes spatial information (Alexander and Nitz, 2015, 2017). The RSC encodes spatial information may be due to the important fact that the RSC receives direct inputs from CA1 area (Cenquizca and Swanson, 2007; Mitchell et al., 2018; Miyashita and Rockland, 2007), which is well known to encode spatial information (O'Keefe and Dostrovsky, 1971). In addition to the evidence from anatomical data, another study (Mao et al., 2018) showed the place cell-like activity in the RSC is severely attenuated by hippocampal lesion, which further supports this the notion at the functional level.

Previous studies have suggested that RSC neurons might encode speed selective signals. For instance, in one early study, (Cho and Sharp, 2001) used single-cell electrophysiological recording and found that the activity of some cells in the RSC correlated with the spatial-movement variables that were examined and suggested the RSC contains movement-related signals. Another recent study (Chinzorig et al., 2019) also found the activity of some neurons in the RSC correlated with the speed of the rat running on the treadmill. However, they have not further analyzed the property of encoding speed information in the RSC.

In the present study, I investigated whether the neuronal activity in the RSC is related to the animal's speed using the virtual treadmill and indeed I observed that some cells were preferentially active during trials when the animal was moving at a slow speed, while others responded more when the speed was high. Further analysis revealed that a large proportion of RSC neurons encode speed information in a context-specific manner. Moreover, the more in-depth analysis showed that the fraction of slow-speed encoding cells was significantly

modulated along with the rewarded context across learning. The findings that most neurons showed context-specific responses and changes according to the value-based association of the context suggest that this may be a fundamental property of spatial and locomotion related encoding in the RSC, i.e., that the activity of most neurons in the RSC are fundamentally affected by contextual cues.

As is shown by the behaviour results that the mice could discriminate between different contexts, it is interesting to detect the relationship between the contextual information and the neuronal activity in the RSC.

It has been shown that the neurons in the hippocampus have unique activity patterns for different contexts that can be considered as encoding for the context (Anderson and Jeffery, 2003; Smith and Mizumori, 2006). Based on the fact that the hippocampus and the RSC are anatomically connected and both regions contribute to learning a memory, another study (Smith et al., 2012) aimed to explore the roles of the hippocampus and the RSC in behavioural context discrimination. It was found in this previous study that neurons in the hippocampus showed context-specific responses to a range of task stimuli and events, whereas neurons in the RSC only responded to the reward location context-specifically.

However, in the current study, in contrast to the previous study, it is observed that some cells in the RSC consistently showed specific patterns of activity in only one of the three contexts during repetitive trials, and further analysis revealed that the neuronal activity in the RSC could be used to predict which context the animal is in even the context was not paired with a reward. Besides, there was no difference in the mean accuracy when decoding the context using data along the VR corridor between baseline recordings (day 1) after initial learning (day 4) and after reversal learning (day 7). Additionally, there was no change in the modulation of the neuronal responses between context 1 and 2 across learning phases, suggesting that the ability of the RSC to discriminate between different contexts is already high and does not change substantially with reward-association. These results indicate that RSC neurons can encode contextual information even without reward.

Visual features of contexts likely allow efficient context discrimination irrelevant to its value. However, during ITI when VR was off, decoding accuracy for rewarded contexts on day 4 and 7 were significantly higher than for non-rewarded contexts and the accuracy for corresponding context decoding on day 1. This observation may be explained by the important fact that the RSC is uniquely situated at the intermediate layer within the DMN, which was known to be

more active during inter-trial rest periods than during goal-directed behaviour (Buckner et al., 2008; Raichle et al., 2001). Recent studies showed the DMN is active during multiple processes relevant to episodic memory and suggested DMN activity reflects internally driven memory processing (Buckner et al., 2008; Mason et al., 2007; Spreng et al., 2009). Coupled with previous findings, my results suggest a role of the RSC in internally driven memory processing, which involves contextual values, and thus allows a better accuracy of context discrimination after learning/relearning as compared to baseline session.

5.4. Multidimensional encoding neurons in the RSC

This thesis demonstrates that the majority of individual RSC neurons encode multiple parameters, integrating different aspects of information to support reward-value contextual associations. It is highlighted in this study that RSC neurons encode information regarding context, position, speed, and visual regularities within the virtual environment. Previous studies have separately shown that subsets of RSC neurons can generate speed selective signals (Cho and Sharp, 2001), have properties of hippocampal place cells (Mao et al., 2017), respond to visual stimulation (Murakami et al., 2015), as well as encode contexts (Cowansage et al., 2014; Hattori et al., 2019; Robinson et al., 2014), indicating that the RSC is involved in the processing of various information related to the spatial and contextual properties of the environment. Importantly, I found that the majority of RSC neurons are multidimensional encoding, i.e., predominantly integrate multiple aspects of information, rather than just one or two.

In the present study, I observed visual semi-periodic patterns of neuronal activity which corresponded (with a variable lag) to dark-light horizontal transitions in the visual pattern of the virtual corridor. Approximately 70% of RSC neurons showed these response patterns, and 70% of all neurons were found to contribute to the context discrimination, with >50% overlap. Thus, the contexts used here were primarily, but not exclusively, represented in the RSC by the pattern of dark-light transitions. These data substantially extend the understanding of how complex contexts are encoded by the RSC and add to mounting evidence that the RSC plays an active role in both visual and spatial processing.

This study also highlights the potential functional importance of reciprocal connections between the RSC and visual cortex, with supportive evidence of orientation-selective visual responses within the RSC (Murakami et al., 2015) as well as spatial information represented in

the visual cortex (Pakan et al., 2018; Saleem et al., 2018). In the current study, the visual contextual patterns themselves also contained strong spatial cues and as the movement in the virtual environment was controlled by the animal's locomotion, mice could use the information from visual self-motion cues (optic flow) as well as physical self-motion cues (speed) to determine their distance traveled (Harvey et al., 2012; Hindley et al., 2014c).

Thus, this semi-periodic pattern observed in this study may be not merely due to the responses to the visual information but also due to the RSC encoding of the speed and distance traveled (see also (Alexander and Nitz, 2017)). This notion is supported by recent fMRI work in humans, which revealed strong RSC correlates with virtual distance integration (Chrastil et al., 2015; Sherrill et al., 2013; Wiener et al., 2016). Therefore, further studies are needed to separate the visual and spatial components of neuronal activity in the RSC and, as such, better understand the exact information encoded by the semi-periodic patterns observed in this study.

As the RSC is densely interconnected with a wide range of brain regions and involved in an array of cognitive functions, previous studies have proposed a critical 'translational' function of the RSC in the integration and transformation of information. This proposed translational function is supported by multiple behavioural studies showing that the RSC is involved in integrating different kinds of navigational information (Vann et al., 2009), forming associations between multiple sensory stimuli (Robinson et al., 2011), and processing the conjunction between allocentric and egocentric spatial frames (Alexander and Nitz, 2015). This functional role for the RSC is in line with the direct demonstration that RSC neurons predominantly and concurrently encode multiple aspects of information; thus, the finding here demonstrates the potential cellular basis for the integrative function of the RSC.

Furthermore, I show that the proportion of multidimensional encoding cells increased after reversal learning but not after initial learning phases. A possible explanation for this may be that during the initial learning phase mice only need to associate the reward with one particular context, whereas the reversal learning phase requires that mice not only establish a new association between the previous non-rewarded context and the reward but also to disassociate the previously formed associations. This task is more complicated than initial learning and hence, may require more neural resources to support it. The increase in the fraction of multidimensional cells after reversal learning may represent the recruitment of such additional resources for cognitive flexibility. The use of multiple parameters in the environment indeed provides a strategy to resolve conflicting value-based information. This is a role previously

assigned to the RSC on the behavioural level (Nelson et al., 2015; Wesierska et al., 2009), and here I have now demonstrated this on the neuronal level.

5.5. Limitations and outlook

In this study, I utilized a virtual environment to enable precise control over the contextual surroundings and to relate the animal's context, position, and speed to neuronal dynamics in the RSC. However, using this technique, animals are head-fixed, which imposes some limitations on examining spatial processing. Since it has been reported that some RSC cells demonstrate properties of HD cells (Chen et al., 1994b; Jacob et al., 2016), head-fixation precludes analysis of HD cells and may impact the dynamics of spatial processing in the RSC during this type of spatial navigation task. On the other hand, the proportion of HD cells found in previous studies has been only around 10%, while the majority of neurons show more complex activity during spatial navigation; a result that is supported by the multi-parametric encoding of RSC neurons found in the current study.

Although it is found in this study that the majority of RSC neurons showed multitasking responses, it is possible that these responses may not be homogeneous across the entire RSC. For instance, in the current study, data were collected from the dysgranular subregion, and as described above, differences in both contextual/spatial processing, as well as memory function, may exist between RSC divisions. Additionally, since Thy1-GCaMP6 transgenic mice were used in the current study, where GCaMP6f is expressed in a subset of excitatory projection neurons (Chen et al., 2012; Dana et al., 2014), I cannot exclude the possibility that the properties of our imaged RSC neurons may not be representative of all RSC neurons.

From the behaviour data, by using a chemogenetic temporal and repeated inactivation approach, it is shown that the RSC is essential for the acquisition of contextual memory but not necessary for the recent recall of the already formed memory. However, in order not to express DREADDs outside of the RSC, especially not to the visual cortex, the DREADDs virus was only injected in the center of the RSC. Therefore, it is not guaranteed that all neurons in the RSC were inactivated, so I cannot exclude the possibility that some neurons in the RSC remained unaffected and contributed to the recall of the recent memory.

In this work, I demonstrated that a reduction in the running speed of the animal within the anticipation zone can be used as a reliable measure of learning and memory. The use of this

behavioural read-out would be interesting in combination with other behavioural parameters, such as timing and frequency of licking, which may further characterize the precision of learning and be orthogonal in terms of motor response.

Besides, it is known that the ability to form and recall contextual memory depends on the complex network of various brain regions, including neocortex, thalamus, and the hippocampus (Frankland and Bontempi, 2005; Pergola and Suchan, 2013; Rugg and Vilberg, 2013). The hippocampus is believed to be involved preferentially during learning and recent retrieval, while neocortical regions are more engaged in remote memory retrieval (Bontempi et al., 1999; Frankland et al., 2004; Piefke et al., 2003). The RSC has been suggested to contribute to the process of systems memory consolidation due to its unique location that connects to both the hippocampus and neocortical areas.

In the current work, it is shown that the RSC is essential for the formation of contextual memory, which requires synaptic consolidation but not necessary for recent memory retrieval. However, it has not been shown in this study whether the RSC is essential for the retrieval of remote memory. A recent study (de Sousa et al., 2019) used an optogenetic approach to test the hypothesis that post-learning reactivation of RSC engram neurons mediates systems consolidation. Interestingly, the authors found that artificial high-frequency stimulation of the RSC neurons that activated during the memory formation generated a recent memory that has the properties of remote memory, including less dependence on the hippocampus, higher engagement of neocortex and contextual generalization. These findings support the hypothesis that the post-learning reactivation of RSC engram neurons is a mechanism of systems consolidation. Therefore, it will be interesting to further study the role of the RSC in remote memory retrieval and the contribution to both synaptic consolidation and systems consolidation.

Last but not least, considering the RSC is an early-onset region for dysfunction in neurodegenerative disorders such as Alzheimer’s disease (Nestor et al., 2003; Pengas et al., 2010; Tan et al., 2013), further studies investigating the specific changes in encoding properties of RSC neurons, especially the multidimensional encoding properties of the RSC may provide a useful marker for neurodegenerative progression in both human and animal studies.

6. CONCLUSIONS

- The context discrimination paradigm established for virtual reality in this study is validated to be effective for addressing the specific roles of the RSC in various stages of learning and memory.

- Naïve mice and mice injected with a control virus can associate a water reward with a specific location in a particular context after learning and reversal learning.

- CNO per se does not affect the context discrimination.

- Context discrimination is impaired when the RSC is chemogenetically perturbed during acquisition and reversal learning, indicating the RSC is essential for the formation of contextual memory.

- Contextual discrimination is not affected by chemogenetic inactivation of the RSC, indicating the RSC is not/less crucial for the recall of recent contextual memory.

- The RSC contributes to the contextual-value associations and thus allows a better accuracy of context discrimination across learning during goal-directed behaviours.

- RSC neurons encode contextual information as well as visual information.

- RSC neurons encode position- and speed-related information predominantly in a context-specific manner.

- The same RSC neurons predominantly encode context, position, and speed, and the proportion of these multidimensional encoding neurons increases after reversal learning.

7. REFERENCES

Aggleton, J.P. (2010). Understanding retrosplenial amnesia: Insights from animal studies. Neuropsychologia *48*, 2328-2338.

Aggleton, J.P., Saunders, R.C., Wright, N.F., and Vann, S.D. (2014). The origin of projections from the posterior cingulate and retrosplenial cortices to the anterior, medial dorsal and laterodorsal thalamic nuclei of macaque monkeys. The European journal of neuroscience *39*, 107-123.

Agster, K.L., and Burwell, R.D. (2009). Cortical efferents of the perirhinal, postrhinal, and entorhinal cortices of the rat. Hippocampus *19*, 1159-1186.

Albasser, M.M., Poirier, G.L., Warburton, E.C., and Aggleton, J.P. (2007). Hippocampal lesions halve immediate-early gene protein counts in retrosplenial cortex: distal dysfunctions in a spatial memory system. The European journal of neuroscience *26*, 1254-1266.

Alexander, A.S., and Nitz, D.A. (2015). Retrosplenial cortex maps the conjunction of internal and external spaces. Nat Neurosci *18*, 1143.

Alexander, A.S., and Nitz, D.A. (2017). Spatially Periodic Activation Patterns of Retrosplenial Cortex Encode Route Sub-spaces and Distance Traveled. Current Biology *27*, 1551-1560.e1554.

Alsaadi, T., Binder, J.R., Lazar, R.M., Doorani, T., and Mohr, J.P. (2000). Pure topographic disorientation: A distinctive syndrome with varied localization. Neurology *54*, 1864-1866.

Anderson, M.I., and Jeffery, K.J. (2003). Heterogeneous Modulation of Place Cell Firing by Changes in Context. The Journal of Neuroscience *23*, 8827.

Archer, J.S., Abbott, D.F., Waites, A.B., and Jackson, G.D. (2003). fMRI "deactivation" of the posterior cingulate during generalized spike and wave. NeuroImage *20*, 1915-1922.

Auger, S.D., and Maguire, E.A. (2018). Retrosplenial Cortex Indexes Stability beyond the Spatial Domain. The Journal of Neuroscience *38*, 1472.

Auger, S.D., Mullally, S.L., and Maguire, E.A. (2012). Retrosplenial cortex codes for permanent landmarks. PloS one *7*, e43620.

Auger, S.D., Zeidman, P., and Maguire, E.A. (2015). A central role for the retrosplenial cortex in de novo environmental learning. eLife *4*, e09031.

Aupée, A.M., Desgranges, B., Eustache, F., Lalevée, C., de la Sayette, V., Viader, F., and Baron, J.C. (2001). Voxel-Based Mapping of Brain Hypometabolism in Permanent Amnesia with PET. NeuroImage *13*, 1164-1173.

Bakker, R., Tiesinga, P., and Kotter, R. (2015). The Scalable Brain Atlas: Instant Web-Based Access to Public Brain Atlases and Related Content. Neuroinformatics *13*, 353-366.

Bar, M., and Aminoff, E. (2003). Cortical Analysis of Visual Context. Neuron *38*, 347-358.

Baumann, O., and Mattingley, J.B. (2010). Medial parietal cortex encodes perceived heading direction in humans. J Neurosci *30*, 12897-12901.

Bluhm, R.L., Miller, J., Lanius, R.A., Osuch, E.A., Boksman, K., Neufeld, R.W., Theberge, J., Schaefer, B., and Williamson, P.C. (2009). Retrosplenial cortex connectivity in schizophrenia. Psychiatry research *174*, 17-23.

Bontempi, B., Laurent-Demir, C., Destrade, C., and Jaffard, R. (1999). Time-dependent reorganization of brain circuitry underlying long-term memory storage. Nature *400*, 671-675.

Buckner, R.L., Andrews-Hanna, J.R., and Schacter, D.L. (2008). The brain's default network: anatomy, function, and relevance to disease. Annals of the New York Academy of Sciences *1124*, 1-38.

Burgess, N., Becker, S., King, J.A., and O'Keefe, J. (2001). Memory for events and their spatial context: models and experiments. Philosophical transactions of the Royal Society of London Series B, Biological sciences *356*, 1493-1503.

Byrne, P., Becker, S., and Burgess, N. (2007). Remembering the past and imagining the future: a neural model of spatial memory and imagery. Psychological review *114*, 340-375.

Cain, D.P., Humpartzoomian, R., and Boon, F. (2006). Retrosplenial cortex lesions impair water maze strategies learning or spatial place learning depending on prior experience of the rat. Behav Brain Res *170*, 316-325.

Cenquizca, L.A., and Swanson, L.W. (2007). Spatial organization of direct hippocampal field CA1 axonal projections to the rest of the cerebral cortex. Brain Res Rev *56*, 1-26.

Chen, L.L., Lin, L.H., Barnes, C.A., and McNaughton, B.L. (1994a). Head-direction cells in the rat posterior cortex. II. Contributions of visual and ideothetic information to the directional firing. Exp Brain Res *101*, 24-34.

Chen, L.L., Lin Lh Fau - Green, E.J., Green Ej Fau - Barnes, C.A., Barnes Ca Fau - McNaughton, B.L., and McNaughton, B.L. (1994b). Head-direction cells in the rat posterior cortex. I. Anatomical distribution and behavioral modulation. Exp Brain Res *101:8*.

Chen, T.-W., Wardill, T.J., Sun, Y., Pulver, S.R., Renninger, S.L., Baohan, A., Schreiter, E.R., Kerr, R.A., Orger, M.B., Jayaraman, V., *et al.* (2013). Ultrasensitive fluorescent proteins for imaging neuronal activity. Nature *499*, 295.

Chetelat, G., Desgranges, B., Landeau, B., Mezenge, F., Poline, J.B., de la Sayette, V., Viader, F., Eustache, F., and Baron, J.C. (2008). Direct voxel-based comparison between grey matter hypometabolism and atrophy in Alzheimer's disease. Brain *131*, 60-71.

Chinzorig, C., Nishimaru, H., Matsumoto, J., Takamura, Y., Berthoz, A., Ono, T., and Nishijo, H. (2019). Rat Retrosplenial Cortical Involvement in Wayfinding Using Visual and Locomotor Cues. Cerebral Cortex.

Cho, J., and Sharp, P.E. (2001). Head direction, place, and movement correlates for cells in the rat retrosplenial cortex. Behav Neurosci *115*, 3-25.

Chrastil, E.R., Sherrill, K.R., Hasselmo, M.E., and Stern, C.E. (2015). There and Back Again: Hippocampus and Retrosplenial Cortex Track Homing Distance during Human Path Integration. The Journal of Neuroscience *35*, 15442.

Clark, B.J., Bassett, J.P., Wang, S.S., and Taube, J.S. (2010). Impaired head direction cell representation in the anterodorsal thalamus after lesions of the retrosplenial cortex. J Neurosci *30*, 5289-5302.

Clark, B.J., Brown, J.E., and Taube, J.S. (2012). Head direction cell activity in the anterodorsal thalamus requires intact supragenual nuclei. Journal of neurophysiology *108*, 2767-2784.

Clark, B.J., Simmons, C.M., Berkowitz, L.E., and Wilber, A.A. (2018). The retrosplenial-parietal network and reference frame coordination for spatial navigation. Behav Neurosci *132*, 416-429.

Cooper, B.G., Manka, T.F., and Mizumori, S.J. (2001). Finding your way in the dark: the retrosplenial cortex contributes to spatial memory and navigation without visual cues. Behav Neurosci *115*, 1012-1028.

Cooper, B.G., and Mizumori, S.J. (1999). Retrosplenial cortex inactivation selectively impairs navigation in darkness. Neuroreport *10*, 625-630.

Cooper, B.G., and Mizumori, S.J. (2001). Temporary inactivation of the retrosplenial cortex causes a transient reorganization of spatial coding in the hippocampus. J Neurosci *21*, 3986-4001.

Cowansage, Kiriana K., Shuman, T., Dillingham, Blythe C., Chang, A., Golshani, P., and Mayford, M. (2014). Direct Reactivation of a Coherent Neocortical Memory of Context. Neuron *84*, 432-441.

Czajkowski, R., Jayaprakash, B., Wiltgen, B., Rogerson, T., Guzman-Karlsson, M.C., Barth, A.L., Trachtenberg, J.T., and Silva, A.J. (2014). Encoding and storage of spatial information in the retrosplenial cortex. Proceedings of the National Academy of Sciences *111*, 8661.

Dar, A.C., Das, T.K., Shokat, K.M., and Cagan, R.L. (2012). Chemical genetic discovery of targets and anti-targets for cancer polypharmacology. Nature *486*, 80-84.

de Sousa, A.F., Cowansage, K.K., Zutshi, I., Cardozo, L.M., Yoo, E.J., Leutgeb, S., and Mayford, M. (2019). Optogenetic reactivation of memory ensembles in the retrosplenial cortex induces systems consolidation. Proceedings of the National Academy of Sciences *116*, 8576.

Donnelly, J.F., Thompson, S.M., and Robertson, R.T. (1983). Organization of projections from the superior colliculus to the thalamic lateral posterior nucleus in the rat. Brain Res *288*, 315-319.

Drexel, M., Romanov, R.A., Wood, J., Weger, S., Heilbronn, R., Wulff, P., Tasan, R.O., Harkany, T., and Sperk, G. (2017). Selective Silencing of Hippocampal Parvalbumin

Interneurons Induces Development of Recurrent Spontaneous Limbic Seizures in Mice. The Journal of Neuroscience *37*, 8166.

Elduayen, C., and Save, E. (2014). The retrosplenial cortex is necessary for path integration in the dark. Behav Brain Res *272*, 303-307.

Epstein, R.A. (2008). Parahippocampal and retrosplenial contributions to human spatial navigation. Trends in Cognitive Sciences *12*, 388-396.

Epstein, R.A., Higgins, J.S., Jablonski, K., and Feiler, A.M. (2007a). Visual Scene Processing in Familiar and Unfamiliar Environments. Journal of Neurophysiology *97*, 3670-3683.

Epstein, R.A., Parker, W.E., and Feiler, A.M. (2007b). Where Am I Now? Distinct Roles for Parahippocampal and Retrosplenial Cortices in Place Recognition. The Journal of Neuroscience *27*, 6141.

Epstein, R.A., and Vass, L.K. (2013). Neural systems for landmark-based wayfinding in humans. Philosophical transactions of the Royal Society of London Series B, Biological sciences *369*, 20120533-20120533.

Fienup, J.R. (1997). Invariant error metrics for image reconstruction. Appl Opt *36*, 8352-8357.

Finch, D.M., Derian, E.L., and Babb, T.L. (1984). Excitatory projection of the rat subicular complex to the cingulate cortex and synaptic integration with thalamic afferents. Brain Research *301*, 25-37.

Fournier, D.I., Eddy, M.C., DeAngeli, N.E., Huszár, R., and Bucci, D.J. (2019). Retrosplenial cortex damage produces retrograde and anterograde context amnesia using strong fear conditioning procedures. Behavioural Brain Research *369*, 111920.

Frankland, P.W., and Bontempi, B. (2005). The organization of recent and remote memories. Nature reviews Neuroscience *6*, 119-130.

Frankland, P.W., Bontempi, B., Talton, L.E., Kaczmarek, L., and Silva, A.J. (2004). The involvement of the anterior cingulate cortex in remote contextual fear memory. Science *304*, 881-883.

Fuhrmann, F., Justus, D., Sosulina, L., Kaneko, H., Beutel, T., Friedrichs, D., Schoch, S., Schwarz, Martin K., Fuhrmann, M., and Remy, S. (2015). Locomotion, Theta Oscillations, and the Speed-Correlated Firing of Hippocampal Neurons Are Controlled by a Medial Septal Glutamatergic Circuit. Neuron *86*, 1253-1264.

Garden, D.L., Massey, P.V., Caruana, D.A., Johnson, B., Warburton, E.C., Aggleton, J.P., and Bashir, Z.I. (2009). Anterior thalamic lesions stop synaptic plasticity in retrosplenial cortex slices: expanding the pathology of diencephalic amnesia. Brain *132*, 1847-1857.

Greicius, M.D., Supekar, K., Menon, V., and Dougherty, R.F. (2009). Resting-state functional connectivity reflects structural connectivity in the default mode network. Cereb Cortex *19*, 72-78.

Guizar-Sicairos, M., Thurman, S.T., and Fienup, J.R. (2008). Efficient subpixel image registration algorithms. Opt Lett *33*, 156-158.

Haijima, A., and Ichitani, Y. (2008). Anterograde and retrograde amnesia of place discrimination in retrosplenial cortex and hippocampal lesioned rats. Learning & memory (Cold Spring Harbor, NY) *15*, 477-482.

Haijima, A., and Ichitani, Y. (2012). Dissociable anterograde amnesic effects of retrosplenial cortex and hippocampal lesions on spontaneous object recognition memory in rats. Hippocampus *22*, 1868-1875.

Hainmueller, T., and Bartos, M. (2018). Parallel emergence of stable and dynamic memory engrams in the hippocampus. Nature *558*, 292-296.

Harker, K.T., and Whishaw, I.Q. (2002). Impaired Spatial Performance in Rats with Retrosplenial Lesions: Importance of the Spatial Problem and the Rat Strain in Identifying Lesion Effects in a Swimming Pool. The Journal of Neuroscience *22*, 1155.

Harvey, C.D., Coen, P., and Tank, D.W. (2012). Choice-specific sequences in parietal cortex during a virtual-navigation decision task. Nature *484*, 62.

Hashimoto, R., and Nakano, I. (2014). The Card Placing Test: a new test for evaluating the function of the retrosplenial and posterior cingulate cortices. European neurology *72*, 38-44.

Hattori, R., Danskin, B., Babic, Z., Mlynaryk, N., and Komiyama, T. (2019). Area-Specificity and Plasticity of History-Dependent Value Coding During Learning. Cell *177*, 1858-1872.e1815.

Haugland, K.G., Sugar, J., and Witter, M.P. (2019). Development and topographical organization of projections from the hippocampus and parahippocampus to the retrosplenial cortex. European Journal of Neuroscience *50*, 1799-1819.

Hindley, E.L., Nelson, A.J., Aggleton, J.P., and Vann, S.D. (2014a). The rat retrosplenial cortex is required when visual cues are used flexibly to determine location. Behav Brain Res *263*, 98-107.

Hindley, E.L., Nelson, A.J.D., Aggleton, J.P., and Vann, S.D. (2014b). Dysgranular retrosplenial cortex lesions in rats disrupt cross-modal object recognition. Learning & memory (Cold Spring Harbor, NY) *21*, 171-179.

Hindley, E.L., Nelson, A.J.D., Aggleton, J.P., and Vann, S.D. (2014c). The rat retrosplenial cortex is required when visual cues are used flexibly to determine location. Behavioural Brain Research *263*, 98-107.

Holtmaat, A., Bonhoeffer, T., Chow, D.K., Chuckowree, J., De Paola, V., Hofer, S.B., Hübener, M., Keck, T., Knott, G., Lee, W.-C.A., *et al.* (2009). Long-term, high-resolution imaging in the mouse neocortex through a chronic cranial window. Nature Protocols *4*, 1128.

Honda, Y., Furuta, T., Kaneko, T., Shibata, H., and Sasaki, H. (2011). Patterns of axonal collateralization of single layer V cortical projection neurons in the rat presubiculum. The Journal of comparative neurology *519*, 1395-1412.

Honda, Y., and Ishizuka, N. (2015). Topographic distribution of cortical projection cells in the rat subiculum. Neuroscience Research *92*, 1-20.

Huang, C., Wahlund, L.-O., Svensson, L., Winblad, B., and Julin, P. (2002). Cingulate cortex hypoperfusion predicts Alzheimer's disease in mild cognitive impairment. BMC Neurol *2*, 9-9.

Iaria, G., Chen, J.K., Guariglia, C., Ptito, A., and Petrides, M. (2007). Retrosplenial and hippocampal brain regions in human navigation: complementary functional contributions to the formation and use of cognitive maps. The European journal of neuroscience *25*, 890-899.

Ino, T., Doi, T., Hirose, S., Kimura, T., Ito, J., and Fukuyama, H. (2007). Directional Disorientation Following Left Retrosplenial Hemorrhage: a Case Report with FMRI Studies. Cortex *43*, 248-254.

Jacob, P.-Y., Casali, G., Spieser, L., Page, H., Overington, D., and Jeffery, K. (2016). An independent, landmark-dominated head-direction signal in dysgranular retrosplenial cortex. Nat Neurosci *20*, 173.

Jenkins, T.A., Vann, S.D., Amin, E., and Aggleton, J.P. (2004). Anterior thalamic lesions stop immediate early gene activation in selective laminae of the retrosplenial cortex: evidence of covert pathology in rats? The European journal of neuroscience *19*, 3291-3304.

Jiang, M.Y., DeAngeli, N.E., Bucci, D.J., and Todd, T.P. (2018). Retrosplenial cortex has a time-dependent role in memory for visual stimuli. Behav Neurosci *132*, 396-402.

Johnson, K.A., Jones, K., Holman, B.L., Becker, J.A., Spiers, P.A., Satlin, A., and Albert, M.S. (1998). Preclinical prediction of Alzheimer's disease using SPECT. Neurology *50*, 1563-1571.

Kaushik, R., Morkovin, E., Schneeberg, J., Confettura, A.D., Kreutz, M.R., Senkov, O., and Dityatev, A. (2018). Traditional Japanese Herbal Medicine Yokukansan Targets Distinct but Overlapping Mechanisms in Aged Mice and in the 5xFAD Mouse Model of Alzheimer's Disease. Front Aging Neurosci *10*, 411.

Keene, C.S., and Bucci, D.J. (2008a). Contributions of the retrosplenial and posterior parietal cortices to cue-specific and contextual fear conditioning (American Psychological Association), pp. 89-97.

Keene, C.S., and Bucci, D.J. (2008b). Neurotoxic lesions of retrosplenial cortex disrupt signaled and unsignaled contextual fear conditioning (American Psychological Association), pp. 1070-1077.

Keene, C.S., and Bucci, D.J. (2009). Damage to the retrosplenial cortex produces specific impairments in spatial working memory. Neurobiology of Learning and Memory *91*, 408-414.

Kobayashi, Y., and Amaral, D.G. (2007). Macaque monkey retrosplenial cortex: III. Cortical efferents. Journal of Comparative Neurology *502*, 810-833.

Kveraga, K., Ghuman, A.S., Kassam, K.S., Aminoff, E.A., Hämäläinen, M.S., Chaumon, M., and Bar, M. (2011). Early onset of neural synchronization in the contextual associations network. Proc Natl Acad Sci U S A *108*, 3389-3394.

Laurens, K.R., Kiehl, K.A., Ngan, E.T., and Liddle, P.F. (2005). Attention orienting dysfunction during salient novel stimulus processing in schizophrenia. Schizophr Res *75*, 159-171.

Lee, S.-J., An, Y.-S., Lim, T.S., and Moon, S.Y. (2014). Card-placing test in amnestic mild cognitive impairment and its neural correlates. BMC Neurol *14*, 123-123.

Liberzon, I., Taylor, S.F., Amdur, R., Jung, T.D., Chamberlain, K.R., Minoshima, S., Koeppe, R.A., and Fig, L.M. (1999). Brain activation in PTSD in response to trauma-related stimuli. Biological psychiatry *45*, 817-826.

Lukoyanov, N.V., Lukoyanova, E.A., Andrade, J.P., and Paula-Barbosa, M.M. (2005). Impaired water maze navigation of Wistar rats with retrosplenial cortex lesions: effect of nonspatial pretraining. Behav Brain Res *158*, 175-182.

Maeshima, S., Ozaki, F., Masuo, O., Yamaga, H., Okita, R., and Moriwaki, H. (2001). Memory impairment and spatial disorientation following a left retrosplenial lesion. Journal of clinical neuroscience : official journal of the Neurosurgical Society of Australasia *8*, 450-451.

Maguire, E. (2001). The retrosplenial contribution to human navigation: A review of lesion and neuroimaging findings. Scandinavian Journal of Psychology *42*, 225-238.

Maguire, E.A., Nannery, R., and Spiers, H.J. (2006). Navigation around London by a taxi driver with bilateral hippocampal lesions. Brain *129*, 2894-2907.

Mao, D., Kandler, S., McNaughton, B.L., and Bonin, V. (2017). Sparse orthogonal population representation of spatial context in the retrosplenial cortex. Nature Communications *8*, 243.

Mao, D., Neumann, A.R., Sun, J., Bonin, V., Mohajerani, M.H., and McNaughton, B.L. (2018). Hippocampus-dependent emergence of spatial sequence coding in retrosplenial cortex. Proceedings of the National Academy of Sciences *115*, 8015.

Marchette, S.A., Vass, L.K., Ryan, J., and Epstein, R.A. (2014). Anchoring the neural compass: coding of local spatial reference frames in human medial parietal lobe. Nat Neurosci *17*, 1598-1606.

Martinez-Bisbal, M.C., Arana, E., Marti-Bonmati, L., Molla, E., and Celda, B. (2004). Cognitive impairment: classification by 1H magnetic resonance spectroscopy. European journal of neurology *11*, 187-193.

Mason, M.F., Norton, M.I., Van Horn, J.D., Wegner, D.M., Grafton, S.T., and Macrae, C.N. (2007). Wandering minds: the default network and stimulus-independent thought. Science *315*, 393-395.

Matuszko, G., Curreli, S., Kaushik, R., Becker, A., and Dityatev, A. (2017). Extracellular matrix alterations in the ketamine model of schizophrenia. Neuroscience *350*, 13-22.

McDonald, C.R., Crosson, B., Valenstein, E., and Bowers, D. (2001). Verbal encoding deficits in a patient with a left retrosplenial lesion. Neurocase *7*, 407-417.

Milczarek, M.M., Vann, S.D., and Sengpiel, F. (2018). Spatial Memory Engram in the Mouse Retrosplenial Cortex. Current Biology *28*, 1975-1980.e1976.

Miller, A.M.P., Mau, W., and Smith, D.M. (2019). Retrosplenial Cortical Representations of Space and Future Goal Locations Develop with Learning. Current Biology *29*, 2083-2090.e2084.

Miller, A.M.P., Vedder, L.C., Law, L.M., and Smith, D.M. (2014). Cues, context, and long-term memory: the role of the retrosplenial cortex in spatial cognition. Front Hum Neurosci *8*, 586-586.

Minderer, M., Harvey, C.D., Donato, F., and Moser, E.I. (2016). Virtual reality explored. Nature *533*, 324.

Minoshima, S., Giordani, B., Berent, S., Frey, K.A., Foster, N.L., and Kuhl, D.E. (1997). Metabolic reduction in the posterior cingulate cortex in very early Alzheimer's disease. Annals of neurology *42*, 85-94.

Mitchell, A.S., Czajkowski, R., Zhang, N., Jeffery, K., and Nelson, A.J.D. (2018). Retrosplenial cortex and its role in spatial cognition. Brain and Neuroscience Advances *2*, 2398212818757098.

Mitelman, S.A., Shihabuddin, L., Brickman, A.M., Hazlett, E.A., and Buchsbaum, M.S. (2005). Volume of the cingulate and outcome in schizophrenia. Schizophrenia Research *72*, 91-108.

Miyashita, T., and Rockland, K.S. (2007). GABAergic projections from the hippocampus to the retrosplenial cortex in the rat. European Journal of Neuroscience *26*, 1193-1204.

Murakami, T., Yoshida, T., Matsui, T., and Ohki, K. (2015). Wide-field Ca2+ imaging reveals visually evoked activity in the retrosplenial area. Frontiers in Molecular Neuroscience *8*, 20.

Nelson, A.J., Powell, A.L., Holmes, J.D., Vann, S.D., and Aggleton, J.P. (2015). What does spatial alternation tell us about retrosplenial cortex function? Frontiers in behavioral neuroscience *9*, 126.

Nestor, P.J., Fryer, T.D., Ikeda, M., and Hodges, J.R. (2003). Retrosplenial cortex (BA 29/30) hypometabolism in mild cognitive impairment (prodromal Alzheimer's disease). The European journal of neuroscience *18*, 2663-2667.

Newell, K.A., Zavitsanou, K., and Huang, X.F. (2005). Ionotropic glutamate receptor binding in the posterior cingulate cortex in schizophrenia patients. Neuroreport *16*, 1363-1367.

Nugent, A.C., Milham, M.P., Bain, E.E., Mah, L., Cannon, D.M., Marrett, S., Zarate, C.A., Pine, D.S., Price, J.L., and Drevets, W.C. (2006). Cortical abnormalities in bipolar disorder investigated with MRI and voxel-based morphometry. NeuroImage *30*, 485-497.

O'Keefe, J., and Dostrovsky, J. (1971). The hippocampus as a spatial map. Preliminary evidence from unit activity in the freely-moving rat. Brain Research *34*, 171-175.

O‘Mara, S. (2013). The anterior thalamus provides a subcortical circuit supporting memory and spatial navigation. Frontiers in Systems Neuroscience *7*, 45.

Osawa, A., Maeshima, S., and Kunishio, K. (2008). Topographic disorientation and amnesia due to cerebral hemorrhage in the left retrosplenial region. European neurology *59*, 79-82.

Pakan, J.M.P., Currie, S.P., Fischer, L., and Rochefort, N.L. (2018). The Impact of Visual Cues, Reward, and Motor Feedback on the Representation of Behaviorally Relevant Spatial Locations in Primary Visual Cortex. Cell Reports *24*, 2521-2528.

Pakan, J.M.P., Lowe, S.C., Dylda, E., Keemink, S.W., Currie, S.P., Coutts, C.A., and Rochefort, N.L. (2016). Behavioral-state modulation of inhibition is context-dependent and cell type specific in mouse visual cortex. eLife *5*, e14985.

Parron, C., and Save, E. (2004). Comparison of the effects of entorhinal and retrosplenial cortical lesions on habituation, reaction to spatial and non-spatial changes during object exploration in the rat. Neurobiology of Learning and Memory *82*, 1-11.

Patai, E.Z., Javadi, A.H., Ozubko, J.D., O'Callaghan, A., Ji, S., Robin, J., Grady, C., Winocur, G., Rosenbaum, R.S., Moscovitch, M., *et al.* (2019). Hippocampal and Retrosplenial Goal Distance Coding After Long-term Consolidation of a Real-World Environment. Cereb Cortex *29*, 2748-2758.

Pengas, G., Hodges, J.R., Watson, P., and Nestor, P.J. (2010). Focal posterior cingulate atrophy in incipient Alzheimer's disease. Neurobiology of aging *31*, 25-33.

Pergola, G., and Suchan, B. (2013). Associative learning beyond the medial temporal lobe: many actors on the memory stage. Frontiers in behavioral neuroscience *7*, 162.

Piefke, M., Pestinger, M., Arin, T., Kohl, B., Kastrau, F., Schnitker, R., Vohn, R., Weber, J., Ohnhaus, M., Erli, H.J., *et al.* (2007). The neurofunctional mechanisms of traumatic and non-traumatic memory in patients with acute PTSD following accident trauma. Neurocase *13*, 342-357.

Piefke, M., Weiss, P.H., Zilles, K., Markowitsch, H.J., and Fink, G.R. (2003). Differential remoteness and emotional tone modulate the neural correlates of autobiographical memory. Brain *126*, 650-668.

Pnevmatikakis, E.A., and Giovannucci, A. (2017). NoRMCorre: An online algorithm for piecewise rigid motion correction of calcium imaging data. Journal of Neuroscience Methods *291*, 83-94.

Pnevmatikakis, Eftychios A., Soudry, D., Gao, Y., Machado, T.A., Merel, J., Pfau, D., Reardon, T., Mu, Y., Lacefield, C., Yang, W., *et al.* (2016). Simultaneous Denoising, Deconvolution, and Demixing of Calcium Imaging Data. Neuron *89*, 285-299.

Pothuizen, H.H., Aggleton, J.P., and Vann, S.D. (2008). Do rats with retrosplenial cortex lesions lack direction? The European journal of neuroscience *28*, 2486-2498.

Pothuizen, H.H.J., Davies, M., Albasser, M.M., Aggleton, J.P., and Vann, S.D. (2009). Granular and dysgranular retrosplenial cortices provide qualitatively different contributions to spatial working memory: evidence from immediate-early gene imaging in rats. European Journal of Neuroscience *30*, 877-888.

Powell, A.L., Vann, S.D., Olarte-Sanchez, C.M., Kinnavane, L., Davies, M., Amin, E., Aggleton, J.P., and Nelson, A.J.D. (2017). The retrosplenial cortex and object recency memory in the rat. The European journal of neuroscience *45*, 1451-1464.

Raichle, M.E., MacLeod, A.M., Snyder, A.Z., Powers, W.J., Gusnard, D.A., and Shulman, G.L. (2001). A default mode of brain function. Proceedings of the National Academy of Sciences *98*, 676.

Rajasethupathy, P., Sankaran, S., Marshel, J.H., Kim, C.K., Ferenczi, E., Lee, S.Y., Berndt, A., Ramakrishnan, C., Jaffe, A., Lo, M., *et al.* (2015). Projections from neocortex mediate top-down control of memory retrieval. Nature *526*, 653.

Reed, L.J., Lasserson, D., Marsden, P., Stanhope, N., Stevens, T., Bello, F., Kingsley, D., Colchester, A., and Kopelman, M.D. (2003). FDG-PET findings in the Wernicke-Korsakoff syndrome. Cortex *39*, 1027-1045.

Ries, M.L., Wichmann, A., Bendlin, B.B., and Johnson, S.C. (2009). Posterior Cingulate and Lateral Parietal Gray Matter Volume in Older Adults with Depressive Symptoms. Brain imaging and behavior *3*, 233-239.

Robinson, S., Keene, C.S., Iaccarino, H.F., Duan, D., and Bucci, D.J. (2011). Involvement of retrosplenial cortex in forming associations between multiple sensory stimuli. Behav Neurosci *125*, 578-587.

Robinson, S., Todd, T.P., Pasternak, A.R., Luikart, B.W., Skelton, P.D., Urban, D.J., and Bucci, D.J. (2014). Chemogenetic Silencing of Neurons in Retrosplenial Cortex Disrupts Sensory Preconditioning. The Journal of Neuroscience *34*, 10982.

Roth, B.L. (2016). DREADDs for Neuroscientists. Neuron *89*, 683-694.

Rugg, M.D., and Vilberg, K.L. (2013). Brain networks underlying episodic memory retrieval. Current opinion in neurobiology *23*, 255-260.

Saleem, A.B., Diamanti, E.M., Fournier, J., Harris, K.D., and Carandini, M. (2018). Coherent encoding of subjective spatial position in visual cortex and hippocampus. Nature *562*, 124-127.

Sherrill, K.R., Erdem, U.M., Ross, R.S., Brown, T.I., Hasselmo, M.E., and Stern, C.E. (2013). Hippocampus and retrosplenial cortex combine path integration signals for successful navigation. J Neurosci *33*, 19304-19313.

Shine, J.P., Valdes-Herrera, J.P., Hegarty, M., and Wolbers, T. (2016). The Human Retrosplenial Cortex and Thalamus Code Head Direction in a Global Reference Frame. J Neurosci *36*, 6371-6381.

Smith, D.M., Barredo, J., and Mizumori, S.J.Y. (2012). Complimentary roles of the hippocampus and retrosplenial cortex in behavioral context discrimination. Hippocampus *22*, 1121-1133.

Smith, D.M., and Mizumori, S.J.Y. (2006). Hippocampal place cells, context, and episodic memory. Hippocampus *16*, 716-729.

Smith, K.S., Bucci, D.J., Luikart, B.W., and Mahler, S.V. (2016). DREADDS: Use and application in behavioral neuroscience. Behav Neurosci *130*, 137-155.

Spiers, H.J., and Maguire, E.A. (2007). The neuroscience of remote spatial memory: a tale of two cities. Neuroscience *149*, 7-27.

Spreng, R.N., Mar, R.A., and Kim, A.S. (2009). The common neural basis of autobiographical memory, prospection, navigation, theory of mind, and the default mode: a quantitative meta-analysis. Journal of cognitive neuroscience *21*, 489-510.

Squire, L.R. (1992). Memory and the hippocampus: A synthesis from findings with rats, monkeys, and humans. *99*, 195-231.

Starck, T., Nikkinen, J., Rahko, J., Remes, J., Hurtig, T., Haapsamo, H., Jussila, K., Kuusikko-Gauffin, S., Mattila, M.L., Jansson-Verkasalo, E., *et al.* (2013). Resting state fMRI reveals a default mode dissociation between retrosplenial and medial prefrontal subnetworks in ASD despite motion scrubbing. Front Hum Neurosci *7*, 802.

Sugar, J., Witter, M., van Strien, N., and Cappaert, N. (2011). The Retrosplenial Cortex: Intrinsic Connectivity and Connections with the (Para)Hippocampal Region in the Rat. An Interactive Connectome. Frontiers in Neuroinformatics *5*, 7.

Sugiura, M., Shah, N.J., Zilles, K., and Fink, G.R. (2005). Cortical Representations of Personally Familiar Objects and Places: Functional Organization of the Human Posterior Cingulate Cortex. Journal of cognitive neuroscience *17*, 183-198.

Sun, W., Suzuki, K., Toptunov, D., Stoyanov, S., Yuzaki, M., Khiroug, L., and Dityatev, A. (2019). In vivo Two-Photon Imaging of Anesthesia-Specific Alterations in Microglial Surveillance and Photodamage-Directed Motility in Mouse Cortex. Frontiers in Neuroscience *13*, 421.

Sutherland, R.J., Whishaw, I.Q., and Kolb, B. (1988). Contributions of cingulate cortex to two forms of spatial learning and memory. J Neurosci *8*, 1863-1872.

Takahashi, N., Kawamura, M., Shiota, J., Kasahata, N., and Hirayama, K. (1997). Pure topographic disorientation due to right retrosplenial lesion. Neurology *49*, 464.

Tan, R.H., Wong, S., Hodges, J.R., Halliday, G.M., and Hornberger, M. (2013). Retrosplenial cortex (BA 29) volumes in behavioral variant frontotemporal dementia and Alzheimer's disease. Dementia and geriatric cognitive disorders *35*, 177-182.

Taube, J.S. (1995). Head direction cells recorded in the anterior thalamic nuclei of freely moving rats. J Neurosci *15*, 70-86.

Taube, J.S. (2007). The head direction signal: origins and sensory-motor integration. Annual review of neuroscience *30*, 181-207.

Thompson, S.M., and Robertson, R.T. (1987). Organization of subcortical pathways for sensory projections to the limbic cortex. II. Afferent projections to the thalamic lateral dorsal nucleus in the rat. The Journal of comparative neurology *265*, 189-202.

Todd, T.P., and Bucci, D.J. (2015). Retrosplenial Cortex and Long-Term Memory: Molecules to Behavior. Neural plasticity *2015*, 414173.

Todd, T.P., Mehlman, M.L., Keene, C.S., DeAngeli, N.E., and Bucci, D.J. (2016). Retrosplenial cortex is required for the retrieval of remote memory for auditory cues. Learning & memory (Cold Spring Harbor, NY) *23*, 278-288.

Troiani, V., Stigliani, A., Smith, M.E., and Epstein, R.A. (2014). Multiple Object Properties Drive Scene-Selective Regions. Cerebral Cortex *24*, 883-897.

Tulving, E., and Markowitsch, H.J. (1998). Episodic and declarative memory: Role of the hippocampus. Hippocampus *8*, 198-204.

van Groen, T., Kadish, I., and Wyss, J.M. (2004). Retrosplenial cortex lesions of area Rgb (but not of area Rga) impair spatial learning and memory in the rat. Behav Brain Res *154*, 483-491.

Van Groen, T., and Wyss, J.M. (1990). Connections of the retrosplenial granular a cortex in the rat. Journal of Comparative Neurology *300*, 593-606.

van Groen, T., and Wyss, J.M. (1992a). Connections of the retrosplenial dysgranular cortex in the rat. Journal of Comparative Neurology *315*, 200-216.

Van Groen, T., and Wyss, J.M. (1992b). Projections from the laterodorsal nucleus of the thalamus to the limbic and visual cortices in the rat. Journal of Comparative Neurology *324*, 427-448.

Van Groen, T., and Wyss, J.M. (1995). Projections from the anterodorsal and anteroventral nucleus of the thalamus to the limbic cortex in the rat. The Journal of comparative neurology *358*, 584-604.

Van Groen, T., and Wyss, J.M. (2003). Connections of the retrosplenial granular b cortex in the rat. Journal of Comparative Neurology *463*, 249-263.

Vann, S.D., and Aggleton, J.P. (2002). Extensive cytotoxic lesions of the rat retrosplenial cortex reveal consistent deficits on tasks that tax allocentric spatial memory. Behavioral Neuroscience *116*, 85-94.

Vann, S.D., and Aggleton, J.P. (2004). Testing the importance of the retrosplenial guidance system: effects of different sized retrosplenial cortex lesions on heading direction and spatial working memory. Behav Brain Res *155*, 97-108.

Vann, S.D., and Aggleton, J.P. (2005). Selective dysgranular retrosplenial cortex lesions in rats disrupt allocentric performance of the radial-arm maze task. Behav Neurosci *119*, 1682-1686.

Vann, S.D., Aggleton, J.P., and Maguire, E.A. (2009). What does the retrosplenial cortex do? Nature Reviews Neuroscience *10*, 792.

Vann, S.D., Kristina Wilton, L.A., Muir, J.L., and Aggleton, J.P. (2003). Testing the importance of the caudal retrosplenial cortex for spatial memory in rats. Behav Brain Res *140*, 107-118.

Vedder, L.C., Miller, A.M.P., Harrison, M.B., and Smith, D.M. (2017). Retrosplenial Cortical Neurons Encode Navigational Cues, Trajectories and Reward Locations During Goal Directed Navigation. Cereb Cortex *27*, 3713-3723.

Vogt, B.A., and Miller, M.W. (1983). Cortical connections between rat cingulate cortex and visual, motor, and postsubicular cortices. The Journal of comparative neurology *216*, 192-210.

Vogt, B.A., Pandya, D.N., and Rosene, D.L. (1987). Cingulate cortex of the rhesus monkey: I. Cytoarchitecture and thalamic afferents. Journal of Comparative Neurology *262*, 256-270.

Vogt, B.A., and Paxinos, G. (2014). Cytoarchitecture of mouse and rat cingulate cortex with human homologies. Brain Struct Funct *219*, 185-192.

Vogt, B.A., and Peters, A. (1981). Form and distribution of neurons in rat cingulate cortex: areas 32, 24, and 29. The Journal of comparative neurology *195*, 603-625.

Wang, G., Xie, H., Wang, L., Luo, W., Wang, Y., Jiang, J., Xiao, C., Xing, F., and Guan, J.-S. (2019). Switching From Fear to No Fear by Different Neural Ensembles in Mouse Retrosplenial Cortex. Cerebral Cortex.

Wang, Q., Sporns, O., and Burkhalter, A. (2012). Network Analysis of Corticocortical Connections Reveals Ventral and Dorsal Processing Streams in Mouse Visual Cortex. The Journal of Neuroscience *32*, 4386.

Weng, S.J., Wiggins, J.L., Peltier, S.J., Carrasco, M., Risi, S., Lord, C., and Monk, C.S. (2010). Alterations of resting state functional connectivity in the default network in adolescents with autism spectrum disorders. Brain Res *1313*, 202-214.

Wesierska, M., Adamska, I., and Malinowska, M. (2009). Retrosplenial cortex lesion affected segregation of spatial information in place avoidance task in the rat. Neurobiol Learn Mem *91*, 41-49.

Whissell, P.D., Tohyama, S., and Martin, L.J. (2016). The Use of DREADDs to Deconstruct Behavior. Frontiers in Genetics *7*, 70.

Wiener, M., Michaelis, K., and Thompson, J.C. (2016). Functional correlates of likelihood and prior representations in a virtual distance task. Human Brain Mapping *37*, 3172-3187.

Wik, G., Fischer, H., Finer, B., Bragee, B., Kristianson, M., and Fredrikson, M. (2006). Retrospenial cortical deactivation during painful stimulation of fibromyalgic patients. The International journal of neuroscience *116*, 1-8.

Wiltgen, B.J., Sanders, M.J., Anagnostaras, S.G., Sage, J.R., and Fanselow, M.S. (2006). Context Fear Learning in the Absence of the Hippocampus. The Journal of Neuroscience *26*, 5484.

Wyass, J.M., and Van Groen, T. (1992). Connections between the retrosplenial cortex and the hippocampal formation in the rat: A review. Hippocampus *2*, 1-11.

Yamawaki, N., Radulovic, J., and Shepherd, G.M.G. (2016). A Corticocortical Circuit Directly Links Retrosplenial Cortex to M2 in the Mouse. The Journal of Neuroscience *36*, 9365.

Zola-Morgan, S.M., and Squire, L.R. (1990). The primate hippocampal formation: evidence for a time-limited role in memory storage. Science *250*, 288.